MULTIMEDIA EXPOSURE ASSESSMENT MODEL (MULTIMED) FOR EVALUATING THE LAND DISPOSAL OF WASTES-- MODEL THEORY

by

Atul M. Salhotra[1]
Phil Mineart[1]
Susan Sharp-Hansen[2]
Terry Allison[3]

Woodward-Clyde Consultants[1]
Oakland, CA 94607

AQUA TERRA Consultants[2]
Mountain View, CA 94043

Computer Sciences Corporation[3]
Athens, GA 30605-2720

DISCLAIMER

FOREWORD

As environmental controls become more costly to implement and the penalties of judgment errors become more severe, environmental quality management requires more efficient management tools based on greater knowledge of the environmental phenomena to be managed. As part of this Laboratory's research on the occurrence, movement, transformation, impact and control of environmental contaminants, the Assessment Branch develops management or engineering tools to help pollution control officials assess the risk to human health and the environment posed by land disposal of hazardous wastes.

This report describes a computer model for simulating the transport and transformation of contaminants released from a hazardous waste disposal facility into the multimedia environment. The MULTIMED model simulates release to air and soil, including the unsaturated and saturated zones, and possible interception of the subsurface contaminant plume by a surface stream. It further simulates movement through the air, soil, groundwater and surface water media to humans and other potentially affected species. MULTIMED is intended for general exposure and risk assessments of waste facilities and for analyses of the impacts of engineering and management controls.

                                        Rosemarie C. Russo, Ph.D.
                                        Director
                                        Environmental Research Laboratory
                                        Athens, GA

ABSTRACT

The Environmental Protection Agency's Multimedia Exposure Assessment Model (MULTIMED) simulates the movement of contaminants leaching from a waste disposal facility. The model includes two options for simulating leachate flux. Either the infiltration rate to the unsaturated or saturated zone can be specified directly or a landfill module can be used to estimate the infiltration rate. The landfill module is one-dimensional and steady-state, and simulates the effect of precipitation, runoff, infiltration, evapotranspiration, barrier layers (which can include flexible membrane liners), and lateral drainage. A steady-state, one-dimensional, semi-analytical module simulates flow in the unsaturated zone. The output from this module, water saturation as a function of depth, is used as input to the unsaturated zone transport module. The latter simulates transient, one-dimensional (vertical) transport in the unsaturated zone and includes the effects of longitudinal dispersion, linear adsorption, and first-order decay. Output from the unsaturated zone modules--i.e., steady-state or time series contaminant concentrations at the water table--is used to couple the unsaturated zone transport module with the steady-state or transient, semi-analytical saturated zone transport module. The latter includes one-dimensional uniform flow, three-dimensional dispersion, linear adsorption, first-order decay, and dilution due to direct infiltration into the groundwater plume. Contamination of a surface stream due to the complete interception of a steady-state saturated zone plume is simulated by the surface water module. Finally, the air emissions and the atmosphere dispersion modules simulate the movement of chemicals into the atmosphere.

The fate of contaminants in the various media depends on the chemical properties of the contaminants as well as a number of media- and environment-specific parameters. The uncertainty in these parameters is quantified using the Monte Carlo simulation technique.

To enhance the user-friendly nature of the model, separate interactive pre- and postprocessing software have been developed for use in creating and editing input and in plotting model output.

This report provides the conceptual and theoretical details of the various modules and the Monte Carlo simulation technique. A user's manual for implementing MULTIMED is currently in progress. In addition, an application manual describes the use of MULTIMED in modeling Subtitle D land disposal facilities.

TABLE OF CONTENTS

FIGURES

TABLES

ACKNOWLEDGEMENTS

Introduction

1.1 Overview of the Model

This chapter provides an overview of the U.S. Environmental Protection
Agency's Multimedia Exposure Assessment Model (MULTIMED). The model simulates
the fate and transport of contaminants released from a waste disposal facility
into the multimedia environment. Release to either air or soil, including the
unsaturated and the saturated zone, and possible interception of the
subsurface contaminant plume by a surface stream are included in the model.
Thus, the model can be used as a technical and quantitative management tool to
address the problem of the land disposal of chemicals. At this time, the air
modules of the model are not linked to the other model modules. As a result,
the estimated release of contaminants to the air is independent of the
estimated contaminant release to the subsurface and surface water.

MULTIMED utilizes analytical and semi-analytical solution techniques to solve
the mathematical equations describing flow and transport. The simplifying
assumptions required to obtain the analytical solutions limit the complexity
of the systems which can be represented by MULTIMED. The model does not
account for site-specific spatial variability, the shape of the land disposal
facility, site-specific boundary conditions, multiple aquifers, or pumping
wells. Nor can MULTIMED simulate processes, such as flow in fractures and
chemical reactions between contaminants, which can have a significant affect
on the concentration of contaminants at a site. In more complex systems, it
may be beneficial to use MULTIMED as a "screening level" model which would
allow a user to obtain an understanding of the system. A numerical model
could then be used if there are sufficient data and necessity to justify the
use of a more complex model.

1.2 The Physical Scenario

The physical scenario simulated by the model is a land disposal facility that
releases pollutants into the air, soil, and/or groundwater. In response to a
number of complex physical, chemical, and biological fate and transport
processes, the pollutants move in the multimedia environment (air, water, and
soil), resulting in potential toxic exposure to humans and other receptors.
Note that the processes affecting air emissions are not linked in the model to
the processes affecting subsurface transport. In other words, the
concentration calculated in the one medium is not affected by the release of
the contaminant to the other medium.

The sources of pollutants considered in the current version are either the
leachate from a waste disposal facility or air emissions during the post-
closure period. Inadequate long-term functioning or failure of the facility's
engineering controls (i.e., the caps and liners) are assumed to occur after
closure and result in the release of leachate to soil or groundwater beneath
the facility and emission of vapor to the atmosphere. Note that the use of
the air-emissions module is most appropriate for high concentrations of waste
in the facility. Also, the model does not include fate processes, such as
complexation and solids precipitation, that affect the transport of metals.

1.3 MODEL CAPABILITIES

During the development of this model, emphasis has been placed on the creation of a unified, user-friendly, software framework, with the capability to perform uncertainty analysis, that can be easily enhanced by adding modules and/or modifying existing modules.

The major functions currently performed by this model include:

- Allocation of default values to some input parameters/variables.

- Reading of the input data files.

- Echo of input data to output files.

- Derivation of some parameters, if specified by the user.

- Depending on user-selected options:
  - simulation of leachate flux emanating from the source
  - simulation of unsaturated zone flow and transport
  - simulation of saturated zone transport only
  - computation of in-stream concentrations due to contaminant loading assuming complete interception of a plume in the saturated zone
  - computation of the rate of contaminant emission from the waste disposal unit into the atmosphere
  - simulation of dispersion of the contaminants into the atmosphere

- Generation of random numbers for Monte Carlo simulations.

- Performance of statistical analyses of Monte Carlo simulations.

- Writing the concentrations at specified receptors to output for deterministic runs. In the Monte Carlo mode, writing the cumulative frequency distribution and selected percentiles of concentrations at receptors to output.

- Printing the values of randomly generated input parameters and the computed concentration values for each Monte Carlo run.

The fate and transport of contaminants critically depends on a number of media-specific parameters. Typically many of these parameters exhibit spatial and temporal variability as well as variability due to measurement errors. MULTIMED has the capability to analyze the impact of uncertainty and variability in the model inputs on the model outputs (concentrations at specified points in the multimedia environment), using the Monte Carlo simulation technique.

To enhance the user-friendly nature of the model, separate interactive preprocessing and postprocessing software has been developed, using the ANNIE Interaction Development Environment (AIDE) (Kittle et al., 1989), for use in creating and editing input and in plotting model output. The pre- and postprocessors have not been integrated with MULTIMED because of the size limitations of desktop computers. Therefore, after using the preprocessor to create or modify input, the model is run in batch mode. Afterwards, the postprocessor can be used to produce plots of the Monte Carlo output or concentration versus time.

Finally, model results can be used to manually 'back-calculate' the maximum source concentration (for a steady-state, infinite contaminant source) of a chemical which ensures protection of human health and/or the environment at a

down-gradient point of exposure (see Section 9.6). Details of the back-calculation procedure for an unsteady-state (finite contaminant source) case have been discussed by Mulkey and Allison (1988).

1.4 Report Generation

This report includes the theoretical background and other information necessary to understand MULTIMED. Chapter 2 describes the landfill source module, which can be used to estimate leachate rates from a waste disposal facility. Chapter 3 contains a description of the steady-state, one-dimensional, unsaturated zone flow module, which computes saturation as a function of depth. This information is used by the landfill module and the unsaturated zone transport module, which is described in Chapter 4. The saturated zone transport module and its coupling with the unsaturated zone is described in Chapter 5. Chapter 6 discusses the surface water module, which computes in-stream concentrations of a contaminant based on the assumption of complete interception of a steady-state saturated zone plume. The emission of contaminants from the facility into the atmosphere and their transport and dispersion are described in Chapters 7 and 8, respectively. Chapter 9 contains a discussion of the Monte Carlo simulation technique that is incorporated into the model. Each of these chapters presents the necessary mathematical equations and relationships, limitations, and major assumptions of the modules and details of the required input parameters.

A user's manual for implementing MULTIMED is in progress at this time. In addition, a MULTIMED Subtitle D application manual has been written (Sharp-Hansen et al., 1990). The manual explains how to use the unsaturated and saturated zone modules of MULTIMED to study and design Subtitle D land disposal facilities. Installation of the code, the use of the pre- and postprocessors, the format of the input and output, parameter estimation, and example problems are addressed in the Subtitle D application manual.

SECTION 2

The Landfill Module

2.1 Introduction

This section presents the details of the landfill module included in MULTIMED. The landfill module provides a physically-based estimate of the amount of leachate that may be generated at a RCRA Subtitle C or D landfill. The module is one-dimensional and steady-state. It uses a water balance approach to simulate the effects of hydrologic processes including precipitation, evapotranspiration, runoff, infiltration, and lateral drainage. A schematic diagram of a typical hazardous waste landfill is shown in Figure 2.1. The design components shown in this figure have been used to develop the conceptual basis of the landfill module. The user can adapt these components to his specific problem by assigning varying layer thicknesses and hydraulic properties, by rearranging layers, and by omitting or adding layers. Thus, a variety of climatic conditions and typical landfill designs may be specified by the user. Note that the landfill module was initially developed as a "stand-alone" code and was later integrated into MULTIMED. Details of the stand alone code are presented in Meeks et al. (1988).

In general, two options are available in the code for the simulation of leachate flux from the source. Under option 1, the landfill module is not used and the user specifies an infiltration rate and chemical concentration. The unsaturated zone flow module (described in Section 3) then simulates the movement of the leachate to the water table. Under option 2, the infiltration rate is not specified. Instead, the leachate flux is calculated by the landfill module described in this section. Because the leachate flux depends strongly on underlying soil moisture conditions, the landfill module must be coupled with the unsaturated zone flow module. These two modules are solved iteratively in a sequential manner until the percolation rates estimated by the two modules agree. The landfill module does not estimate the chemical concentration in the leachate. Thus, a chemical concentration must be specified by the user for either option.

This chapter is organized into four sections. Section 2.2 describes the governing equations and the iterative solution technique used to estimate a leachate flux that satisfies both the surface water balance and the unsaturated zone flow module. The major assumptions and limitations inherent in the module are identified in Section 2.3

●   *The data required in the landfill module are described in Section 2.4.*

2.2 GOVERNING EQUATIONS AND SOLUTION TECHNIQUES

The volume of leachate generated from a landfill is governed by:

- ● The availability of water

- ● Underlying soil and refuse conditions

The amount of water available for leachate generation from a landfill is controlled by climatic conditions, surface conditions (e.g., soil and vegetation type, soil moisture conditions), groundwater influx, and liquids

inherently associated with the waste. In this module the contributions to leachate from groundwater influx and liquids inherent in the waste are considered negligible. The amount of water available from other sources is estimated using an event-based surface water balance technique described in Section 2.2.1.

The underlying soil and refuse conditions include 1) the hydraulic properties of subsurface materials, and 2) the design and functioning of engineering controls. These conditions affect the amount of infiltration that can percolate through the landfill layers and the unsaturated zone. The unsaturated zone flow module described in Section 3 calculates percolation based on a semi-analytical solution to the Richard's Equation. The coupling of the unsaturated zone flow module with the landfill module for the leachate calculation is discussed in Section 2.2.2. Effects of engineering controls (i.e., synthetic liners and lateral drains) are described in Section 2.2.3.

Under steady-state conditions, the water available for infiltration must equal the lateral drainage flux plus the percolation rate through the unsaturated zone below the drainage layer. That is, the water made available for leaching must pass through each of the landfill layers and out of the lateral drains or through the bottom of the landfill. This is necessitated by the fact that no change in storage of water within the landfill can occur in the steady-state formulation of the problem. Section 2.2.4 describes how the landfill module uses the prescribed equality of these fluxes to calculate the steady-state leachate rate.

The landfill module solves for the steady-state leachate rate based on representative steady-state climatic data, which must be estimated from actual data for precipitation, storm interval, etc. Because climatic variables, such as evapotranspiration rates and precipitation characteristics, may have strong seasonal variability, the code includes the option to consider seasonal variability in precipitation events and evapotranspiration while retaining the assumption of steady-state (see Section 2.2.1.2). This option should not be used to estimate transient leaching rates because information is not passed from one season to the following season.

2.2.1 Surface Water Balance

A surface water balance is used to estimate the water available for infiltration into the landfill. The water balance is based on an event approach. That is, the water balance is evaluated for the period of time from the beginning of a precipitation event, and through the period of no precipitation which follows. The calculation period ends at the onset of the next precipitation event. Figure 2.2 depicts the event approach. The algorithm used in the landfill module partitions precipitation into runoff, evapotranspiration, and infiltration. Changes in surface water storage (e.g., snow melt) are not included. Because the module is steady-state, changes in soil moisture are precluded and do not need to be considered in the water balance. Infiltration (volume per unit area) into the soil during a precipitation event can then be expressed by (Dass et al., 1977):

$$INFIL = PRECIP - RO - ET \tag{2.1}$$

where

      INFIL = water available for infiltration during an event [cm]
      PRECIP = storm precipitation [cm]
      RO   = runoff during an event [cm]
      ET   = evapotranspiration during the event interval [cm]

The procedures used to estimate the volume of runoff and of actual evapotranspiration are described individually in the following sections. Based on the calculated infiltration volume, the average steady-state infiltration rate is given by:

$$I = INFIL/DEVENT \qquad (2.2)$$

where

    I   = infiltration rate [cm/d]
    DEVENT = event duration [d]

2.2.1.1 Calculation of Runoff

Some fraction of the incident precipitation runs off the landfill and is lost to overland flow before it has a chance to infiltrate. The landfill module computes runoff by the SCS runoff curve number method in the manner described in the HELP model documentation (Schroeder et al., 1984b). The SCS procedures were developed from observed runoff-rainfall relationships for large storms on small watersheds.

The relation between precipitation, runoff, and retention for a particular set of environmental conditions was found to be:

$$RO = \frac{(PRECIP - 0.2S)^2}{(PRECIP + 0.8S)} \qquad (2.3)$$

where

    RO   = runoff during an event [cm]
    PRECIP = storm precipitation [cm]
    S   = retention parameter [cm]

The retention parameter, S, for a given soil varies as a function of the soil moisture in the underlying soil (Schroeder et al., 1984b):

$$S = S_{mx}[1 - \frac{SM - WP}{UL - WP}] \qquad (2.4)$$

where

    S_{mx} = maximum value of the retention parameter [cm]
    SM   = soil water content in the upper soil layer [dimensionless fraction]
    UL   = upper limit moisture content in the upper soil layer [dimensionless fraction]
    WP   = wilting point moisture content in the upper soil layer [dimensionless fraction]

8

The upper limit of soil moisture content is the moisture content at saturation and is numerically equal to the effective porosity. The wilting point moisture content is the lowest naturally occurring soil water content and is equal to the effective porosity multiplied by the residual saturation. Since soil water is not distributed uniformly throughout the soil profile and since the soil moisture near the surface influences infiltration more strongly than that located elsewhere, the retention parameter is depth-weighted in the landfill module (Meeks et al., 1988). The soil profile in the uppermost soil layer is divided into seven segments. The thickness of the top segment is set equal to one thirty-sixth of the total upper layer thickness and the thickness of the second segment is five thirty-sixths of the layer's thickness. The thickness of each of the bottom five segments in the uppermost soil layer is defined as one-sixth of the total layer thickness. The depth-weighted retention parameter is computed with the following equation (Knisel, 1980):

$$S = S_{mx} [1 - \sum_{j=1}^{7} W_j (\frac{SM_j - WP}{UL - WP})] \tag{2.5}$$

where

SM_j = soil moisture content of segment j [fraction]
W_j = weighting factor for segment j [dimensionless]

The weighting factors decrease with the depth of the segment. In accordance with the development of CREAMS (Knisel, 1980), the weighting factors for segments 1, 2, 3, 4, 5, 6 and 7 are 0.111, 0.397, 0.254, 0.127, 0.063, 0.032, and 0.016, respectively.

The maximum value of the retention parameter, S_{mx}, is the value of S at the lowest soil moisture content and is calculated from the SCS curve number for average moisture conditions (CN_{II}).

2.2.1.2 Calculation of Evapotranspiration

Evapotranspiration from a landfill is a function of climatic conditions, vegetation, soil moisture, and the ability of the soil to transmit water and water vapor. A two-step approach is taken to calculate actual evapotranspiration.

First, the potential evapotranspiration during the interval between storms is calculated from the seasonal potential evapotranspiration input by the user. This calculation takes the form:

where

$$EPET = PET (\frac{DEVENT}{365/ISEA}) \tag{2.6}$$

EPET = event potential evapotranspiration [cm]
PET = seasonal potential evapotranspiration [cm]
DEVENT = event duration [d]
ISEA = number of seasons in a year [dimensionless]

The second step involves estimating the availability of water, stored as soil moisture in the shallow subsurface, to meet the evapotranspiration demand. The available soil moisture is estimated as a function of the moisture content above the wilting point in the upper soil layer. The user must take care in defining the thickness of this layer so that its depth accurately reflects the depth over which evapotranspiration takes place. In general, the zone of evapotranspiration extends only a few feet or less from the surface. If the top of the landfill is vegetated, it is suggested that the uppermost layer thickness correspond to the root zone depth. The module assumes that at the top of the uppermost layer the soil moisture can be depleted to the wilting point and that at the bottom of the uppermost layer the soil moisture is not affected by evapotranspiration. The soil moisture level above which soil moisture is available is linearly interpolated between these two depths as shown in Figure 2.3. That is, a triangular distribution is assumed from the surface to the bottom of the uppermost layer with the maximum soil moisture taken from near the surface. This approach is similar to that taken in the PRZM model (Carsel et al., 1984). The available moisture for evapotranspiration can be expressed as:

$$AW = 100 \sum_{j=1}^{7} (SM_j - [WP + \frac{z_j}{THICK} (SM-WP)]) \Delta z_j \qquad (2.7)$$

where

AW = water available for evapotranspiration [cm]
$THICK$ = the thickness of the uppermost layer [m]
WP = wilting point moisture content in the upper soil layer [dimensionless fraction]
SM = soil water content in the upper soil layer [dimensionless fraction]
Δz_j = thickness of segment j [m]
SM_j = soil water content in segment j [fraction]
z_j = depth to the center of segment j [m]

The potential evapotranspiration and the available soil moisture are compared and the lesser of the two amounts is assigned as the actual evapotranspiration. Thus, the actual evapotranspiration for an event during a specific season is:

where

$$ET = \min (EPET, AW) \qquad (2.8)$$

ET = evapotranspiration during an event in a specific season [cm]

Finally, the evapotranspiration rates for all of the seasons are aggregated to estimate a representative steady-state value.

2.2.2 Percolation through the Landfill

Percolation rates through the landfill are determined by treating the landfill layers and the unsaturated soil layers as one continuous system and applying the one-dimensional Richard's Equation for unsaturated flow. The governing equations and solution procedure are described in Section 3.2. The results of the unsaturated flow module calculations are the soil moisture and pressure head profiles in the landfill and the unsaturated zone for a given percolation rate. The soil moisture values are used as input into the runoff and evapotranspiration calculations, described in Section 2.2.1. Thus, the soil moisture values impact the surface water balance and the leaching rate predicted by the landfill module. Section 2.2.4 provides a step-by-step description of how the unsaturated zone module and the landfill module are coupled.

2.2.3 Landfill Control Features

Engineering controls can be used in landfill design to reduce the amount of leachate emanating from the base of the landfill. The two important types of engineering controls that may be simulated using this module are:

- Low-permeability synthetic liners

- Lateral drainage systems

The user may indicate the presence of synthetic liners and a drainage layer at any location within the landfill as shown in Figure 2.1. One synthetic liner per landfill layer may be included; however, only one lateral drainage layer can be simulated. In addition, the user can elect to specify failure of the synthetic liners. The techniques used to implement the effects of liners and drains are discussed in the following paragraphs.

2.2.3.1 Low-permeability Liners

Low-permeability liners are thin sheets of rubber or plastic material used as barriers to vertical flow. Liners are generally installed immediately above or within barrier soil layers and together with the barrier soil layer reduce vertical flow. Because the liner itself is too thin to treat numerically as a separate layer, its hydraulic properties are combined with those of the soil layer below it and both units are treated as one layer by the module. That is, the effective hydraulic conductivity of the soil layer below is reduced when using a synthetic liner. According to Freeze and Cherry (1979), the effective hydraulic conductivity of the liner and adjacent soil layer is:

$$K_{LS} = \frac{(T_L + T_S)}{\dfrac{T_L}{K_L} + \dfrac{T_S}{K_S}}$$

(2.9)

where

K_{LS} = effective conductivity of the liner and soil layer [m/yr]
K_L = hydraulic conductivity of the liner [m/yr]
K_S = hydraulic conductivity of the soil layer [m/yr]
T_L = thickness of the liner [m]
T_S = thickness of the soil layer [m]

The user can elect to specify the degree of failure of the synthetic liner
system. To implement a liner failure, the user selects a percent failure (0
to 100 percent). The hydraulic conductivity of the liner/soil system is
increased by the selected failure percentage. That is:

$$K_F = K_{LS} - \frac{FPERC}{100.0} \; (K_{LS} - K_S)$$
(2.10)

where

        FPERC = percent liner failure [dimensionless]
        K_F = hydraulic conductivity of failed liner and soil layer [m/yr]

Note that the maximum hydraulic conductivity (at 100 percent failure) is the
hydraulic conductivity of the soil layer alone.

2.2.3.2 The Drainage System

Lateral drains are commonly utilized in landfill design to remove excess water
which may accumulate above barrier soil layers. Therefore, they serve to
reduce percolation through the landfill. The landfill module is capable of
simulating the effect of one drainage system placed anywhere in the landfill
profile. Generally, such a drainage system would be placed immediately above
or below the refuse layer.

The presence of lateral drains affects the surface infiltration rate, the
percolation rate to the water table, and the rate of lateral drainage. These
three effects are simulated by an algorithm which is based on the assumption
that the steady-state pressure head at the drain is less than or equal to
zero. That is, the drains operate at full efficiency and remove all ponded
infiltration above the drainage layer.

The first step in the lateral drainage algorithm is the simulation of the
moisture distribution within the landfill and unsaturated zone without
considering the effect of the drainage system. The pressure head at the
intended drain location is checked. If the pressure head indicates
unsaturated conditions, the module assigns zero as a lateral drainage rate.
If the pressure head value indicates saturated conditions at the drain
location, the pressure head at the drain is reduced to zero, and the system is
resimulated. The zero pressure head at the drainage layer serves as a
boundary condition, that is:

$$\psi(LD) = 0.0$$
(2.11)

where

        LD = location of the lateral drain [cm].

This boundary condition allows the landfill and the unsaturated zone to be
broken into two independent unsaturated flow systems--one above the drainage
layer and the other below the drainage layer.

The system above the drain is solved in the same manner as the unsaturated
flow system which was described in Sections 2.2.1 and 2.2.2. The only change
in the solution procedure is that the location of the bottom boundary
condition is changed from the water table to the drainage layer. The result
of this calculation is the infiltration rate into the top of the landfill.

This rate is generally larger than it would be in the absence of the drainage system.

The system below the drain is solved in a similar manner, but Equation 2.11 is used as a top boundary condition. Therefore, the surface water balance calculation described in Section 2.2.1 is not used in the calculation. That is, the percolation rate under the drainage layer is not significantly impacted by surface water hydraulics and the unsaturated flow equations in Section 3 are solved directly. The calculated percolation rate underlying the drainage system is less than or equal to what it would be in the absence of the drainage system.

The rate of lateral drainage is calculated based on a mass balance approach. The lateral drainage rate plus the rate at which percolation reaches the water table (Q_f) must be equal to the infiltration (I) rate into the top of the landfill. Solving for the lateral drainage results in:

$$QLAT = I - Q_f \qquad\qquad (2.12)$$

where

$$
\begin{aligned}
QLAT \quad &= \text{lateral drainage rate [cm/d]} \\
I \quad &= \text{infiltration rate [cm/d]} \\
Q_f \quad &= \text{percolation rate [cm/d]}
\end{aligned}
$$

2.2.4 Solution Method for Identifying Steady-State Leaching Rate

Section 2.2.1 describes the estimation of the infiltration rate (I) into the landfill, based on a water balance method. Section 2.2.2 describes the estimation of the percolation rate (Q) through the landfill, using the unsaturated zone module described in Section 3. Section 2.2.3 explains how landfill control features (liners and drains) affect the surface infiltration rate and percolation rates from the bottom of the landfill. At steady-state the percolation rate from the bottom of the landfill plus the lateral drainage rate must be exactly equal to the infiltration rate into the landfill as there can be no net change in moisture storage within the landfill.

The infiltration and percolation rates are coupled through the soil moisture content of the upper portion of the landfill. This section describes the iterative procedure used to estimate the steady-state leachate rate (and the soil moisture profile) starting with an initial estimate of percolation. If the calculated infiltration rate is different than the estimated percolation, the estimate of percolation is adjusted, and the moisture content profile and infiltration rate are recalculated. This procedure is repeated until sufficient agreement between the percolation and infiltration rates is attained and a solution which satisfies the surface water budget and the unsaturated flow equations is found.

The procedure to calculate leachate rates consists of 10 iterative steps:

   1. Calculate the effective hydraulic conductivity of the synthetic liner/soil layers. Find the layer with the smallest hydraulic conductivity in the landfill profile. Estimate an initial percolation rate (Q) which is equal to the saturated vertical hydraulic conductivity of this layer. This initial estimate is not critical to the final solution, but simply allows the module to start computations with a reasonable value.

2. Calculate the pressure head in each of the landfill and unsaturated layers between the water table and the soil surface. Convert the calculated pressure heads to soil saturation. These calculations are both performed in the unsaturated zone module described in Section 3.

3. Calculate the soil moisture using the relationship that soil moisture is equal to soil saturation multiplied by effective porosity.

4. Calculate the depth weighted retention parameter from Equation 2.5. Calculate the surface runoff (RO) using Equation 2.3.

5. Calculate the actual evapotranspiration (ET) using Equations 2.6 to 2.8.

6. Calculate the surface water infiltration rate (I) using Equations 2.1 and 2.2.

7. Compare the infiltration rate (I) and the percolation rate (Q) assumed in Step 1.

   a. If $|I - Q|/Q$ < the convergence criteria, proceed to Step 9. The convergence criterion is 10^{-4} cm/day.

   b. If I > Q, increase Q. This corresponds to a case where infiltration from precipitation is sufficient to create perched water above the least conductive layer so that more percolation is forced through the layer. Portions of the profile will remain saturated under these conditions.

   c. If I < Q, decrease Q. This corresponds to case where infiltration from precipitation is so low that even the least conductive layer becomes unsaturated and less percolation moves through it.

8. With the new updated estimate of Q, apply Steps 2 through 8 iteratively until convergence is achieved or the maximum number of iterations is exceeded. If the maximum number of iterations is exceeded without meeting the convergence criteria in Step 7, check the relative convergence between Q and I. If *I-Q*/Q < the relative convergence criteria proceed to Step 9. The relative convergence criteria is 10^{-3}. Otherwise, print a convergence error message and stop.

9. Check the lateral drainage flag. If there is an active lateral drain in the profile, recalculate the percolation rate using the lateral drain option.

10. Repeat the entire procedure for each of the seasons. Output results for each season and convert the calculated seasonal infiltration rates to a steady-state average.

2.3 Assumptions and Limitations

The important simplifying assumption made in developing the landfill module include:

a) Lateral inflow, surface run-on, and transient climatic conditions are considered negligible. Degradation or aging of design components is not considered. However, the degree of failure of the liners may be specified.

b) The seasonal potential evapotranspiration rates are assumed to adequately characterize the dynamic variability of actual evapotranspiration demand.

c) The event-averaged infiltration rate is an adequate representation of the long-term average infiltration rate.

d) Groundwater is assumed to be below the bottom of the landfill.

e) No liquid is generated from the decomposition of waste or codisposal of wastes and sludges.

f) Lateral drains are fully efficient and remove all ponded water above the drainage layer.

2.4 Data Requirements

The landfill module has relatively modest data requirements. Table 2-1 lists the parameters required.

TABLE 2-1. PARAMETERS REQUIRED FOR THE LANDFILL MODULE

Parameters	Units

Climatic Data

For each season:

Typical storm precipitation amount	[cm]
Typical interval between storms	[d]
Potential evapotranspiration	[cm]

Design Specifications

SCS Curve Number II	[dimensionless]
Number of liners	[dimensionless]
Number of layers	[dimensionless]
Number of porous materials	[dimensionless]
Number of seasons	[dimensionless]
Location of the drainage layer	[dimensionless]
Thicknesses of the layers	[m]

For each liner:

Percent liner failure	[percent]
Thickness of liner	[m]
Hydraulic conductivity of liner	[m/yr]

For each porous material:

Saturated hydraulic conductivity	[cm/hr]
Porosity	[dimensionless]
Residual water content	[dimensionless]
Either:	
van Genuchten alpha coefficient	[1/cm]
van Genuchten beta coefficient	[dimensionless]
or	
Brooks and Corey exponent	[dimensionless]
van Genuchten alpha coefficient	[1/cm]
van Genuchten beta coefficient	[dimensionless]

)))

SECTION 3

The Unsaturated Zone Flow Module

3.1 Introduction

When the bottom of a waste disposal unit is located above the water table, leachate can migrate through the unsaturated zone and into a saturated aquifer. In such situations it is important to include the unsaturated zone in the analysis of contaminant fate and transport. A schematic diagram of the leachate migration is shown in Figure 3.1.

This chapter presents details of the semi-analytical unsaturated zone flow module included in MULTIMED. The flow module computes the water saturation values within the unsaturated zone which are used by the unsaturated zone transport module (described in Section 4) to compute one-dimensional vertical seepage velocities.

Two options, previously described in Section 2, are available for the simulation of leachate percolation through the unsaturated zone. Under Option 1, the user specifies the leachate rate, and the unsaturated zone module simulates the percolation of leachate to the water table. Under Option 2, the leachate rate is not specified, rather it is calculated by the landfill module (see Section 2). This calculation is dependent on the results of the unsaturated zone module. Therefore, an iterative scheme is used to calculate a leaching rate which satisfies both the surface water balance included in the landfill module and the unsaturated zone water saturation profile estimated by the unsaturated flow module.

This chapter is organized into four sections. Theoretical details of the flow module and the underlying assumptions are presented in Sections 3.2 and 3.3. Section 3.4 discusses the data requirements for this module. Note that the unsaturated flow and transport modules can not be run independent of each other. In addition, whenever the unsaturated flow and transport modules of MULTIMED are used, the saturated transport module must also be used.

3.2 GOVERNING EQUATIONS AND SOLUTION TECHNIQUES

The unsaturated zone flow module simulates steady downward flow to the water table. The governing equation is given by Darcy's law:

$$-K_v \, k_{rw} \, (\frac{\partial \psi}{\partial z} - 1) = Q \tag{3.1}$$

where

ψ = the pressure head [m]
z = the depth coordinate which is taken positive downward [m]
K_v = the saturated hydraulic conductivity [m/yr]
k_{rw} = the relative hydraulic conductivity [dimensionless]
Q = the percolation rate [m/yr]

The boundary condition at the water table is:

$$\psi(L) = 0 \tag{3.2}$$

where L is the thickness of the unsaturated zone [m].

To solve the above equations, it is necessary to specify the relationships of relative hydraulic conductivity (k_{rw}) versus water saturation (S_w), and of pressure head (ψ) versus water saturation. The relationship of pressure head to water saturation is described in the model by the following equation (van Genuchten, 1976; Mualum, 1976):

$$S_e = \begin{cases} [1 + (\alpha * \psi - \psi_a *)^{\beta}]^{-\gamma} & \psi < \psi_a \\ 1 & \psi \geq \psi_a \end{cases} \tag{3.3}$$

where

S_{wr} = the residual water saturation [dimensionless fraction]
β, γ = soil-specific empirical parameters [dimensionless]
α = soil-specific empirical parameter [1/m]
ψ_a = the air entry pressure head, subsequently assumed zero [m]
S_e = the effective saturation [dimensionless fraction]

and where S_e is related to the water saturation, S_w, as follows:

The parameters α, β, and γ are empirical coefficients defined by van Genuchten. The parameters β and γ are related through:

$$S_e = \frac{(S_w - S_{wr})}{(1 - S_{wr})} \tag{3.4}$$

$$\gamma = 1 - 1/\beta \tag{3.5}$$

Hence, the parameter γ need not be specified. Note that Equations 3.3 and 3.4 are not valid for $\beta \leq 1.0$ and $\gamma \leq 0.0$ because the effective saturation, S_e, can not be greater than one.

Two alternative functional expressions can be specified by the user to describe the relationship between relative hydraulic conductivity and water saturation. The van Genuchten relationship is:

$$k_{rw} = S_e^{1/2}[1 - (1 - S_e^{1/\gamma})^\gamma]^2 \tag{3.6}$$

Alternatively, the $k_{rw}(S_w)$ relationship presented by Brooks and Corey (1966) may be used. This relationship is given by:

$$k_{rw} = S_e^n \tag{3.7}$$

where n = soil specific parameter [dimensionless].

As a first step in the solution of Equations 3.1 and 3.2, the soil constitutive relations in Equations 3.3 and 3.6 are combined. Using van Genuchten's constitutive equations and assuming $\psi_a = 0$, leads to the following expression for $k_{rw}(\psi)$:

$$k_{rw} = \begin{cases} 1 & \psi \geq 0 \\[2ex] \dfrac{\{1 - (-\alpha\psi)^{\beta-1}[1 + (-\alpha\psi)^\beta]^{1/\beta-1}\}^2}{[1 + (-\alpha\psi)^\beta]^{(1/2-1/2\beta)}} & \psi < 0 \end{cases} \tag{3.8}$$

Next, Equation 3.8 is substituted into Equation 3.1 and the derivative $\partial\psi/\partial z$ is replaced by a backward finite difference approximation. This yields, after some rearranging:

$$\frac{K_v}{Q}\left(\frac{\psi_{z-\Delta z} - \psi_z}{\Delta z} + 1\right) - 1 = 0 \qquad \overline{\psi} \geq 0$$

$$\frac{K_v}{Q}\frac{\{1 - (-\alpha\overline{\psi}^{\,\beta-1}[1 + (-\alpha\overline{\psi})^\beta]^{1/\beta-1}\}^2}{[1 + (-\alpha\overline{\psi})^\beta]^{(1/2-1/2\beta)}}\left(\frac{\psi_{z-\Delta z} - \psi_z}{\Delta z} + 1\right) - 1 = 0 \qquad \overline{\psi} < 0 \tag{3.9}$$

where $\overline{\psi}$ is the representative pressure head for the soil layer between z and z−Δz.

If the Brooks and Corey (1966) relationship is used, the expression for relative hydraulic conductivity becomes:

$$k_{rw} = \begin{cases} 1 & \psi \geq 0 \\[1ex] (1 + (-\alpha\psi)^\beta)^{-n\gamma} & \psi < 0 \end{cases} \tag{3.10}$$

20

Substituting Equation 3.10 into Darcy's law (Equation 3.1), the resulting expression equivalent to Equation 3.9 is:

$$\frac{K_v}{Q} \left(\frac{\psi_{z-\Delta z} - \psi_z}{\Delta z} + 1 \right) - 1 = 0, \qquad\qquad \overline{\psi} \geq 0 \quad (3.11)$$

$$\frac{K_v}{Q} \left((1 + (-\alpha\overline{\psi})^\beta)^{-n\gamma} \left(\frac{\psi_{z-\Delta z} - \psi_z}{\Delta z} \right) + 1 \right) - 1 = 0, \qquad \overline{\psi} < 0$$

$\overline{\psi}$ can be written as a weighted average of ψ_z and $\psi_{z-\Delta z}$:

$$\overline{\psi} = \omega\psi_{z-\Delta z} + (1 - \omega)\psi_z \qquad\qquad\qquad (3.12)$$

where ω is a weighting coefficient ($0 \leq \omega \leq 1$). A value of ω equal to unity was found to give accurate results.

Using Equations 3.9 or 3.11 and 3.12 together with the lower boundary condition Equation 3.2 allows the solution for $\psi_1 = \psi_{L-\Delta z}$. This value for ψ_1 is then used in the place of ψ_z in Equation 3.9 or 3.11 and 3.12 and the equation is solved for the pressure head at the next desired distance upward from the water table. In this sequential manner, the pressure head at any depth in the unsaturated zone is computed. The Newton-Raphson method is used to solve the nonlinear root-finding problem (Equation 3.9 or 3.11). In the event that the Newton-Raphson method does not converge, the bisection method is used. The latter method is computationally slower but ensures convergence.

After the pressure head distribution in the unsaturated zone has been found, the corresponding saturation distribution, $S_w(z)$, is computed using Equations 3.4 and 3.5). In principle, the saturation distribution can be found without first solving for $\psi(z)$ by substituting Equation 3.3 or 3.7 rather than Equation 3.8 or 3.10 into Equation 3.1. The disadvantage of this approach is that it becomes more difficult to accommodate nonuniform material properties. Whereas the ψ-profile is continuous in the unsaturated zone, the S_w-profile is discontinuous at the interface of soil layers with contrasting hydraulic properties.

3.2.1 Spatial Discretization in the Unsaturated Flow Module

When the thickness of the unsaturated zone is specified as a constant (i.e., it is not a Monte Carlo parameter), up to 20 layers having unique flow properties may be simulated. Regardless of the number of layers, the finite-element grid used by the code is generated automatically. The code uses the following rules for generating the grid:

    (a)   If the depth is less than or equal to 50 m, the number of nodes is set equal to 50 and all layers are of equal thickness.

    (b)   If the generated value of depth lies between 50 m and 200 m, the number of nodes is obtained by rounding up the depth. Thus, if the generated value of the depth is 98.4 m, the number of nodes is 99. The nodes are all evenly spaced at 1 m intervals except for the distance between the first and second node, which equals a

distance necessary to obtain the proper depth. Thus, in the above
example, the distance between nodes 1 and 2 would be 0.4.

The minimum nodal spacing is 0.1 m. If the distance between nodes
1 and 2 is less than 0.1 m, then the total number of nodes is
decreased by one and the distance between nodes 1 and 2 is
increased by 1 m.

(c) If the depth is greater than 200 m, the number of nodes is set
equal to 200 and all layers are of equal thickness.

(d) If multiple layers are used, an additional node is inserted to
define the bottom of each layer.

*Note that if the depth of the unsaturated zone is generated randomly for each
run, the unsaturated zone is considered homogenous and composed of only one
material. Thus, only one layer and one material can be specified in both the
unsaturated flow and unsaturated transport modules.*

3.3 ASSUMPTIONS AND LIMITATIONS

The major assumptions on which the flow model is based are:

(a) Flow of the fluid phase is considered isothermal, one-dimensional,
and governed by Darcy's law.

(b) The flow field is considered to be steady.

(c) The simultaneous flow of the second phase (i.e., air) can be
disregarded.

(d) Hysteresis effects are neglected in the specification of the
characteristic curves.

3.4 DATA REQUIREMENTS

The data required by the unsaturated zone flow module are listed in Table 3-1.
Note that the van Genuchten parameters are required by the model to describe
the pressure head versus water saturation relationship. The user can specify
one of two options for describing the relationship between relative
permeability and water saturation: the van Genuchten or the Brooks and Corey
equation. If the Brooks and Corey option is used, a Brooks and Corey exponent
must be input in addition to the van Genuchten alpha and beta coefficients.

TABLE 3-1. Parameters required for the Unsaturated Zone Flow Module

Parameter	Units
Source-Specific Data	
Percolation rate from the facility	[m/yr]
Unsaturated Zone Data	
Number of layers	[dimensionless]
Number of porous materials	[dimensionless]
Thickness of each layer	[m]
Material associated with each layer	[dimensionless]
For each material:	
Air entry pressure head	[m]
Porosity	[dimensionless]
Saturated hydraulic conductivity	[cm/hr]
Residual saturation (water content)	[dimensionless]
Either:	
van Genuchten alpha coefficient	[1/cm]
van Genuchten beta coefficient	[dimensionless]
or	
Brooks and Corey exponent	[dimensionless]
van Genuchten alpha coefficient	[1/cm]
van Genuchten beta coefficient	[dimensionless]

Note: The model provides the option to use either van Genuchten's or Brooks and Corey's constitutive relationship for relative permeability versus water saturation. However, the relationship between pressure head and water saturation is expressed in terms of van Genuchten parameters.

Unsaturated Zone Transport Module

4.1 Introduction

This section presents the details of the unsaturated zone transport module
included in MULTIMED. As mentioned in Section 3, transport within the
unsaturated zone is important only when the bottom of the waste disposal unit
is located above the water table. Also, when the unsaturated zone modules are
used, the saturated zone module must also be used.

The theoretical basis of the unsaturated zone transport module and the
underlying assumptions are discussed in Sections 4.2 and 4.3. Section 4.4
addresses the data requirements for this module.

4.2 Governing Equations

4.2.1 Unsteady-State Transport

The transport of contaminants in the unsaturated zone is treated as a one-
dimensional problem. Important fate and transport mechanisms considered by
the model include dispersion in the vertical direction, linear adsorption, and
first-order decay of the contaminant. With these constraints, the transport
equation can be expressed as:

$$R_v \; \frac{\partial C}{\partial t} \; = \; D_v \; \frac{\partial^2 C}{\partial z^2} \; -V_v \; \frac{\partial C}{\partial z} \; - \; \lambda_v R_v C \qquad\qquad (4.1)$$

where

> C = the dissolved phase contaminant concentration in the
>   unsaturated zone [mg/ℓ],
> D_v = the dispersion coefficient in the unsaturated zone [m^2/yr]
> λ_v = the first-order degradation rate within the unsaturated zone
>   [1/yr]
> R_v = the unsaturated zone retardation factor [dimensionless]
> V_v = the steady-state unsaturated zone seepage velocity [m/yr]
> t =   time [yr]
> z = the vertical coordinate which is positive downwards [m]

The retardation factor in Equation 4.1 is computed using:

$$R_v = 1 + \frac{\rho_{bv} K_{dv}}{\theta S_w} \qquad\qquad (4.2)$$

where

ρ_{bv} = the bulk density of the unsaturated zone [g/cc]
K_{dv} = the contaminant distribution coefficient for the unsaturated zone [cc/g]
θ = the porosity of the unsaturated zone [dimensionless fraction]
S_w = the saturation within the unsaturated zone [dimensionless fraction]

The overall first-order degradation rate, λ_v, which is calculated using Equation 5.3 in Section 5, includes the effect of both biodegradation and chemical hydrolysis reactions. The latter is discussed in Section 5.5.2.

Further, the unsaturated zone seepage velocity in Equation 4.1 is computed using:

$$V_v = \frac{Q}{\theta S_w} \qquad\qquad (4.3)$$

where Q is the steady-state percolation rate within the unsaturated zone. Note that Q is assumed to be steady in MULTIMED. Also, the saturation, S_w, is computed by the unsaturated zone flow module, as discussed in Section 3.

Solution of the above differential equation requires two boundary conditions. The first boundary condition describes the source concentration and may be of the following form:

$$C(O,t) = C_o \qquad\qquad (4.4a)$$

or

$$C(O,t) = C_o \exp(-\Lambda t) \qquad\qquad (4.4b)$$

or

$$C(0,t) = C_o[1-s(t-T)] \qquad\qquad (4.4c)$$

where

Λ = the source concentration decay rate [1/yr]
s(t-T) = the unit step function with a value of unity for t>T and zero for t<T [t and T are in years]
C_o = the initial (or steady-state) concentration at the top of the unsaturated zone [mg/ℓ]

Note that Equation 4.4(a) represents a constant source concentration condition, Equation 4.4(b) an exponentially decaying source boundary concentration, and Equation 4.4(c) a finite (constant concentration) pulse source condition. The second boundary condition, applied at a large distance from the source, is:

$$C(\infty,t) = 0 \tag{4.5}$$

Background concentrations of the contaminant in the unsaturated zone are assumed to be negligible. Therefore, the initial condition is

$$C(z,0) = 0 \tag{4.6}$$

The analytical solution for the above system of equations has been presented by Marino (1974) and Van Genuchten and Alves (1982). Using the constant concentration boundary condition, Equation 4.4(a), the solution can be expressed as:

$$\frac{C}{C_o} = \frac{1}{2} \exp\left[\frac{(V_v - \Gamma)z}{2D_v}\right] erfc\left[\frac{R_v z - \Gamma t}{2\sqrt{D_v R_v t}}\right] + \frac{1}{2} \exp\left[\frac{(V_v + \Gamma)z}{2D_v}\right] erfc\left[\frac{R_v z \quad t}{2 \quad D_v R_v t}\right] \tag{4.7}$$

Using the exponentially decaying concentration boundary condition, the solution to Equation 4.1 becomes:

$$\frac{C}{C_o} = \frac{1}{2} \exp(-\Lambda t)\left\{\exp\left[\frac{z(V_v - \Gamma_1)}{2D_v}\right] erfc\left[\frac{R_v z - \Gamma_1 t}{2\sqrt{D_v R_v t}}\right]\right.$$
$$\left. + \exp\left[\frac{z(V_v + \Gamma_1)}{2D_v}\right] erfc\left[\frac{R_v z + \Gamma_1 t}{2\sqrt{D_v t R_v}}\right]\right\} \tag{4.8}$$

where Γ is given by:

$$\Gamma = (V_v^2 + 4D_v\lambda_v)^{1/2}$$
$$\Gamma_1 = [V_v^2 + 4D_v(\lambda_v - \Lambda R)]^{1/2} \tag{4.9}$$

The effect of variations in the degradation rate, dispersion coefficient, and seepage velocity is accounted for by dividing the unsaturated zone into a number of horizontal layers, each of which is assumed to be homogeneous. This is schematically shown in Figure 4.1. Equation 4.1 is sequentially solved for each layer. For the first layer, any one of the source boundary conditions (see Equations 4.4a, 4.4b, and 4.4c) can be specified. For the remaining layers, the following source boundary condition, which ensures continuity of concentration, is applied:

$$C_i(\ell_i, t) = C_{i+1}(0, t) \qquad (4.10)$$

where ℓ = the thickness of a layer and the subscripts i and i+1 refer to successive layers. Equation 4.10 implies that the source concentration at the top of any layer i+1 is set equal to the concentration computed at the bottom of the previous layer i. Note that the layers can be of different thickness.

The solution to the layered unsaturated zone is derived using Laplace transform techniques to transform the governing partial differential equation (Equation 4.1) and the boundary conditions to an ordinary differential equation in the Laplace domain. The ordinary differential equation is solved in the Laplace domain and then inverted using either the convolution theorem or the Stehfest algorithm (Stehfest, 1970; Moench and Ogata, 1981). The latter is a numerical inversion scheme. Both these solution schemes are included in the model. In general, the Stehfest algorithm is computationally faster. At very high Peclet numbers, however, there is a possibility that this numerical solution may not converge. For such cases, the convolution integration method may be used. Details of the solution scheme are presented by Shamir and Harleman (1967) and Hederman (1980).

4.2.2 Steady-State Transport

For the case of a steady-state continuous contaminant source, the governing Equation 4.1 can be simplified to yield:

$$D_v \frac{\partial^2 C}{\partial z^2} - V_v \frac{\partial C}{\partial z} - \lambda_v C R_v = 0 \qquad\qquad (4.11)$$

For this case the boundary conditions are:

$$C(z=0) = C_o \qquad\qquad (4.12a)$$

$$\frac{\partial C}{\partial z} (z=\infty) = 0 \qquad\qquad (4.12b)$$

The analytical solution to the above system of equations is:

$$C(z) = C_o \exp \{\frac{V_v z}{2D_v} - z(\lambda_v R_v/D_v + V_v^2/4D_v^2)^{1/2}\} \qquad\qquad (4.13a)$$

or

$$C(z) = C_o \exp \{\frac{z}{2\alpha_z} - \frac{z}{2\alpha_z} (1 + \frac{4\lambda_v \alpha_z R_v}{V_v})^{1/2}\} \qquad\qquad (4.13b)$$

$$\frac{C}{C_o} = \exp (\frac{-\lambda_v L R_v}{V_v}) \qquad\qquad (4.14)$$

In the event that dispersion within the unsaturated zone is neglected, the above equation reduces to:

where L = the depth of the unsaturated zone [m].

For a layered unsaturated zone, Equation 4.14 can be expressed as:

$$\frac{C}{C_o} = \exp\left(\sum_{i=1}^{n} \frac{-\lambda_{vi}\ell_i R_{vi}}{V_{vi}}\right) \tag{4.15}$$

where n = the number of homogenous layers within the unsaturated zone.

4.3 Assumptions and Limitations

The major assumptions on which the unsaturated zone transport model is based are:

(a) The flow field within the unsaturated zone is at steady state.

(b) The seepage velocity and other model parameters (e.g., the dispersion coefficient, partition coefficient) are uniform in each layer. In other words, each layer is homogeneous and isotropic.

(c) Transport is assumed to be strictly one dimensional. Lateral and transverse advection and dispersion are neglected.

(d) Adsorption and decay of the solute may be described by a linear equilibrium isotherm and a first-order decay constant respectively. The daughter products of chemical and biochemical decay are neglected.

(e) Each layer is approximated as being infinite in thickness. This assumption is valid and introduces negligible errors if the ratio of dispersivity to the layer thickness is small (<< 1.0).

4.4 Data Requirements

Table 4-1 lists the parameters required by the unsaturated zone transport module. These include:

(a) Three source-specific parameters. Note that the model is linear with respect to the source concentration. Thus, if the source concentration is set to unity, the model computes normalized downgradient well concentrations.

(b) Five chemical-specific parameters. Note that the overall decay coefficient and the distribution coefficient for the unsaturated zone can not be input directly. Rather they are computed from other parameters as discussed is Sections 4.4.1 and 4.4.2.

(c) Seven unsaturated zone transport parameters. Remember that the seepage velocity is computed using Equation 4.3, with the saturation values supplied by the unsaturated zone flow module. The computation of the dispersion coefficient by the code is discussed in Section 4.4.3.

(d) Two aquifer parameters. The pH and temperature of the unsaturated zone is assumed to be the same as for the saturated zone.

4.4.1 The Chemical Transformation Rate

The liquid-phase and sorbed-phase chemical decay coefficient are computed using the hydrolysis rate constants. The equations used are shown in Section 5.5.2.1. Note that the pH and temperature of the unsaturated zone can not be input; rather, the corresponding values for the saturated zone are used. The overall decay rate is then computed using Equation 5.3 in Section 5.

4.4.2 The Distribution Coefficient

The distribution coefficient is computed as the product of the normalized distribution coefficient and the fractional organic carbon content. However, the fractional organic carbon content is replaced by the percent organic matter divided by a conversion factor, using the following relationship (Enfield et al., 1982):

$$f_{oc} = \frac{f_{om}}{172.4} \qquad\qquad (4.16)$$

where

f_{oc} = fractional organic carbon content [dimensionless]
f_{om} = percent organic matter content [dimensionless]
172.4 = conversion factor from percent organic matter content to fractional organic carbon content

TABLE 4-1. Parameters Required for Unsaturated ZOne Transport Module

Parameters	Units

Source-Specific Parameters

Source decay constant	[1/yr]
Source concentration at top of unsaturated zone	[mg/ℓ]
Pulse duration (for unsteady state simulation)	[yr]

Unsaturated Zone-Specific Parameters

Number of layers used to simulate transport	[dimensionless]
Porosity of the unsaturated zone (specified in the unsaturated flow input)	[cc/cc]

For each layer:

Thickness	[m]
Longitudinal dispersivity	[m]
Bulk density of the soil	[g/cc]
Biodegradation rate,	[1/yr]
Percent organic matter	[dimensionless]

Saturated Zone-Specific Parameters

Temperature of the aquifer[a]	[°C]
pH of the aquifer[a]	[pH units]

Chemical-Specific Parameters

Normalized distribution coefficient (i.e., K_{oc})	[cc/g]
Reference Temperature	[°C]
Acid and base hydrolysis rates at reference temperature	[ℓ/mole-yr]
Neutral hydrolysis rate at reference temperature	[1/yr]

* *Note that the temperature and pH used in calculating the unsaturated zone overall decay rate are the temperature and pH specified for the aquifer.*

4.4.3 The Longitudinal Dispersion Coefficient

Longitudinal dispersion is computed using the relationship:

$$D_v = \alpha_v V_v \qquad (4.17)$$

where

D_v	=	the longitudinal dispersion coefficient [m²/yr]
V_v	=	the seepage velocity in the unsaturated zone [m/yr]
α_v	=	the longitudinal dispersivity [m]

The longitudinal dispersivity, α_v, can be either input directly by the user or derived by the code. The equation used in the model to derive dispersivity values is based on an analysis of data presented by Gelhar et al. (1985) and shown in Table 4-2. Using regression analysis, the following relation was developed:

$$\alpha_v = .02 + .022L, \quad R^2 = 66\% \tag{4.18}$$

where L is the thickness of the unsaturated zone. To avoid excessively high values of dispersivity for deep unsaturated zones, a maximum dispersivity of 1.0 m is used. Thus, for all depths greater than 44.5 m, α_v is set equal to 1.0 m. Additional details of the above regression are presented in Salhotra (1988).

TABLE 4-2. Compilation of Field Dispersivity Values (Gelhar et al., 1985)

Author	Type of Experiment	Vertical Scale of Experiment (m)	Longitudinal Dispersivity α_v (m)
Yule and Gardner (1978)	Laboratory	0.23	0.0022
Hildebrand and Himmelblau (1977)	Laboratory	0.79	0.0018
Kirda et al. (1973)	Laboratory	0.60	0.004
Gaudet et al. (1977)	Laboratory	0.94	0.01
Brissaud et al. (1983)	Field	1.00	0.0011, 0.002
Warrick et al. (1971)	Field	1.20	0.027
Van de Pol et al. (1977)	Field	1.50	0.0941
Biggar and Nielsen (1976)	Field	1.83	0.05
Kies (1981)	Field	2.00	0.168
Jury et al. (1982)	Field	2.00	0.0945
Andersen et al. (1968)	Field	20.00	0.70
Oakes (1977)	Field	20.00	0.20

The Saturated Zone Transport Module

5.1   Introduction

This chapter presents details of the module used to simulate contaminant fate
and transport within the saturated porous zone. Recall that the contaminant
can enter the saturated formation by direct leaching from a source (in the
absence of an unsaturated zone) or by percolation through the unsaturated
zone. MULTIMED allows either option to be specified. In both cases the
governing equations and the semi-analytical solution for transport in the
saturated zone are the same. Flow in the saturated zone is assumed to be
steady.

The following sections describe the governing equations, boundary and initial
conditions, model limitations, and parameters associated with the saturated
zone transport module.

5.2 Governing Equations

The three-dimensional solute transport equation on which the model is based
can be written as:

$$D_x \frac{\partial^2 C}{\partial x^2} + D_y \frac{\partial^2 C}{\partial y^2} + D_z \frac{\partial^2 C}{\partial z^2} - V_s \frac{\partial C}{\partial x} = R_s \frac{\partial C}{\partial t} + R_s \lambda_s C + R_s \frac{qC}{B} \qquad (5.1)$$

where
   x, y, z = spatial coordinates in the longitudinal, lateral and vertical
              directions, respectively [m]
   C   = dissolved concentration of chemical [mg/ℓ, g/m^3]
   D_x, D_y, D_z = dispersion coefficients in the x, y and z directions,
              respectively [m^2/yr]
   V_s = one dimensional, uniform seepage velocity in the x direction
              [m/yr]
   R_s = retardation factor in the saturated zone [dimensionless]
   t   = elapsed time [yr]
   λ_s = effective first-order decay coefficient in the saturated zone
              [1/yr]
   q   = net recharge outside the facility percolating directly into and
              diluting the contaminant plume [m/yr]
   B   = the thickness of the saturated zone [m]
   θ = effective porosity for the saturated zone [dimensionless]

In Equation 5.1, the retardation factor and the effective decay coefficient
are defined as:

$$R_s = 1 + \frac{\rho_b K_d}{\theta} \qquad (5.2)$$

and

$$\lambda_s = \frac{\lambda_1 \theta + \lambda_2 \rho_b K_d}{\theta + \rho_b K_d} + \lambda_b \qquad\qquad (5.3)$$

where

ρ_b = bulk density of the porous media [g/cc]
K_d = distribution coefficient [cc/g]
λ_1 = first-order decay constant for dissolved phase [1/yr]
λ_2 = first-order decay constant for the sorbed phase [1/yr]
λ_b = first-order lumped biodegradation rate in the saturated zone [1/yr]

The flow domain is regarded as semi-infinite in the x direction ($0 \le x \le \infty$), infinite in the y-direction ($-\infty \le y \le \infty$) and finite in the z-direction ($0 \le z \le B$).

Solution of Equation 5.1 requires two boundary conditions in each of the x, y, and z directions and an initial condition. At the source (downgradient edge of the waste disposal unit) the model allows a choice between two boundary conditions with respect to the distribution of contaminant along the vertical source plane. The first boundary condition specifies the contaminant concentration as a gaussian distribution in the lateral direction and uniform over the vertical mixing or source penetration depth, H. A schematic description of the flow domain and this source boundary condition is shown in Figure 5.1(a). Mathematically, the boundary condition can be expressed as:

$$C(0,y,z,t) = \begin{cases} C_o \exp[-y^2/(2\sigma^2)] & 0 \le z \le H \\ 0 & H < z \le B \end{cases} \qquad (5.4)$$

In Equation 5.4, C_o [mg/ℓ] is the maximum dissolved concentration of the solute at the source and occurs at the center of the gaussian distribution. The standard deviation, σ, is a measure of the width of the source.

Changes in the maximum dissolved concentration, C_o, over time are modeled using one of three options. The value of C_o can be constant for all time (steady-state):

$$C_o = C_\ell \qquad t > 0 \tag{5.5}$$

or a finite pulse, T_s years in duration, of constant concentration:

$$C_o = C_\ell \qquad 0 \leq t \leq T_s \tag{5.6}$$

or finally, an exponentially decaying pulse given by:

$$C_o = C_\ell \exp(\Lambda t) \qquad t > 0 \tag{5.7}$$

where

C_ℓ = user-specified leachate concentration [mg/ℓ]
Λ = source decay rate constant [1/yr]

The second, alternative source boundary condition allowed by the model is a rectangular patch source of thickness H and width $2y_o$. A schematic diagram of this boundary condition is shown in Figure 5.1(b). It can be mathematically expressed as:

$$C(0,y,z,t) = \begin{cases} C_o & -y_o \leq y \leq y_o \text{ and } 0 \leq z \leq H \\ 0 & (y_o < y \text{ or } y < -y_o) \text{ and } H < z \leq B \end{cases} \tag{5.8}$$

In Equation 5.8, C_o [mg/ℓ] is the dissolved concentration of the solute at the source. It is assumed to be uniform over the effective width of the facility and the depth of the source and varies in time as shown in Equations 5.5 through 5.7.

$$C(x,y,z,0) = 0 \tag{5.9a}$$

$$C(x,\pm\infty,z,t) = 0 \tag{5.9c}$$

$$C(\infty,y,z,t) = 0 \tag{5.9b}$$

$$\frac{\partial C}{\partial z}(x,y,B,t) = 0 \tag{5.9e}$$

$$\frac{\partial C}{\partial z}(x,y,0,t) = 0 \tag{5.9d}$$

In addition to the source boundary condition, the initial and additional boundary conditions used by the model can be expressed as:

$$C(x,y,z,t) = \frac{H}{B} C_f(x,y,t) + \Delta C_p(x,y,z,t)$$ (5.10)

Equation 5.9a implies that background concentrations of the contaminant in the aquifer are zero. Equations 5.9d and 5.9e imply that there is zero flux of contaminant at z = 0 and z = B.

5.2.1 Solution to the Gaussian Source Boundary Condition

Huyakorn et al. (1987) and USEPA (1985) have presented analytical solutions for the system of Equations 5.1 to 5.4 and Equation 5.9. The general solution can be expressed as:

where C_f and ΔC_p are functions given by:

$$C_f(x,y,t) = \xi \int_0^t F(x,y,\tau) \exp(-\eta\tau)\, d\tau$$ (5.11)

$$\Delta C_p(x,y,z,t) = \frac{2\xi}{\Pi} \sum_{n=1}^{\infty} \frac{1}{n} \cos\left(\frac{n\Pi z}{B}\right) \sin\left(\frac{n\Pi H}{B}\right) \cdot$$
$$\int_0^t F(x,y,\tau)\, \exp(-\beta_n \tau)\, d\tau$$ (5.12)

in which

$$\xi = \frac{C_o \sigma x}{(2\Pi D_x^*)^{1/2}} \exp\left(\frac{V_s^* x}{2 D_x^*}\right)$$ (5.14)

$$F(x,y,\tau) = \frac{1}{\tau^{3/2}(2\sigma^2 + 4 D_y^* \tau)^{1/2}} \cdot \exp\left(-\frac{x^2}{4 D_x^* \tau} - \frac{y^2}{4 D_y^* \tau + 2\sigma^2}\right)$$ (5.13)

$$\eta = \frac{V_s^{*2}}{4D_x^*} + \lambda \tag{5.15}$$

where

D_x^*, D_y^*, and D_z^* = the retarded dispersion coefficients (D_x/R_s, D_y/R_s, D_z/R_s) in the x, y and z direction

V_s^* = the retarded solute (seepage) velocity [$V_s^* = V_s/R_s$]

τ = the variable of integration

Note that in the event that H = B (i.e., the source fully penetrates the saturated formation), $\Delta C_p = 0$ in Equation 5.10. At any distance, x, from the source, the maximum contaminant concentration occurs at the centerline of the plume and can be represented as:

$$C(x,0,0,t) = \frac{H}{B} C_f(x,0,t) + \Delta C_p(x,0,0,t) \tag{5.17}$$

where $C_f(x,0,t)$ and $\Delta C_p(x,0,0,t)$ are given by Equations 5.11 and 5.12 with arguments y and z set equal to zero, and the function $F(x,0,\tau)$ defined as:

$$F(x,0,\tau) = \frac{\exp(-x^2/4D_x^*\tau)}{\tau^{3/2}(2\sigma^2 + 4D_y^*\tau)^{1/2}} \tag{5.18}$$

As t approaches infinity, a steady-state condition is reached. The steady-state concentration along the plume centerline can be expressed as:

$$C^*(x,0,0) = \frac{H}{B} C_f^*(x,0) + \Delta C_p^*(x,0,0) \tag{5.19}$$

where

$$C_f^*(x,0) = \xi^* \int_0^\infty \exp\left[-\frac{\sigma^2 u^2}{2} - x\left(\frac{u^2 D_y^*}{D_x^*} + \frac{\eta}{D_x^*}\right)^{1/2}\right]du \tag{5.20}$$

$$\Delta C_p^*(x,0,0) = \frac{2\xi^*}{\Pi} \sum_{n=1}^\infty \frac{1}{n} \sin\left(\frac{n\Pi H}{B}\right)$$
$$\cdot \int_0^\infty \exp\left[-\frac{\sigma^2 u^2}{2} - x\left(\frac{u^2 D_y^*}{D_x^*} + \frac{\beta n}{D_x^*}\right)^{1/2}\right]du \tag{5.21}$$

and

$$\xi^* = \frac{2C_o\sigma}{(2\Pi)^{1/2}} \exp\left(\frac{V_s^* x}{2D_x^*}\right) \tag{5.22}$$

The solution for the transient state (i.e., Equations 5.10 to 5.16) in MULTIMED is achieved by incorporating a pre-existing code, EPATMOD (Huyakorn et al., 1986). Similarly, the steady-state solution (i.e., Equations 5.19 through 5.22) in MULTIMED makes use of a pre-existing code named EPASMOD (Huyakorn et al., 1986).

Note that for large pulse durations, the transient solution is identical to the steady-state solution. However, the steady-state solution is significantly faster than the transient solution and should be used for steady-state computations. Finally, note that the model uses the principle of superposition to compute the plume concentration for a pulse source, i.e., a contaminant source of finite duration, T_s.

5.2.2 Solution to the Patch Source Boundary Condition

Sudicky et al. (1988) have presented the analytical solution to the system of Equations 5.1 through 5.3, 5.8, and 5.9. The general solution can be expressed as:

$$
\begin{aligned}
C\,(x,y,z,t) &= C_o\ \frac{x(z_2-z_1)}{4B(\Pi D_x^*)^{1/2}}\ \int_0^t \exp\left\{-\frac{(x-V_s^*\tau)^2}{4D_x^*\tau}-\Lambda\,(t\quad)\right. \\[2mm]
&\cdot\ \frac{1}{\tau^{3/2}}\ \left[erfc\left\{\frac{Y-Y_o}{2(D_y^*\tau)^{1/2}}\right\}-erfc\left\{\frac{Y+Y_o}{2(D_y^*\tau)^{1/2}}\right\}\right]d\tau \\[2mm]
&+\ C_o\ \frac{x}{2D_x^{*1/2}\Pi^{3/2}}\ \int_0^t\ \exp\left\{-\frac{(x-V_s^*\tau)^2}{4D_x^*\tau}-\Lambda(t-\tau)-\lambda\tau\right\}\frac{1}{\tau^{3/2}} \\[2mm]
&\cdot\ \left[erfc\left\{\frac{Y-Y_o}{2(D_y^*\tau)^{1/2}}\right\}-erfc\left\{\frac{Y+Y_o}{2(D_y^*\tau)^{1/2}}\right\}\right]\cdot\sum_{n=1}^{\infty}\ \frac{1}{n} \\[2mm]
&\cdot\ \left[\sin\left\{\frac{n\Pi z_2}{B}\right\}-\sin\left\{\frac{n\Pi z_1}{B}\right\}\right]\cos\left(\frac{n\Pi z}{B}\right)\exp\left\{-\frac{n^2\Pi^2 D_z^*\tau}{B^2}\right\}d\tau
\end{aligned}
\tag{5.23a}
$$

where

$$z_1 = 0 \tag{5.23b}$$

and

$$z_2 = H \tag{5.23c}$$

If the solution is desired along the plane y = 0, Equation 5.23a can be simplified by noting that the term

$$erfc\ \{\frac{y-y_o}{2(D_y^* \tau)^{1/2}}\}\ -\ erfc\ \{\frac{y+y_o}{2(D_y^* \tau)^{1/2}}\} \tag{5.24a}$$

reduces to:

$$2\ -\ 2\ erfc\ \{\frac{y_o}{2(D_y^* \tau)^{1/2}}\} \tag{5.24b}$$

When z = 0, the term $\cos(n\pi z/B)$ becomes 1. A more substantial simplification results in the case of a fully penetrating source (i.e., $z_1 = 0$ and $z_2 = B$). In this case, the entire second integral term in Equation 5.23 vanishes.

Similarly, for the steady-state case the solution is:

$$C\ (x,y,z)\ =\ C_o\ \frac{(z_2-z_1)x}{\pi B(D_x^* D_y^*)^{1/2}}\ (\lambda\ +\ V_s^{*^2}/4D_x^*)^{1/2}\ \exp\ (\frac{V_s^* x}{2D_x^*})$$

$$\cdot \int_{-y_0}^{y_0} \frac{1}{\sqrt{\dfrac{x^2}{D_x^2} + \dfrac{(y-y^*)^2}{D_y^*}}}\ K_1\ [\{(\lambda\ +\ V_s^{*^2}/4D_x^*)\ (\frac{x^2}{D_x^*}\ +\ \frac{(y-y^*)^2}{D_y^*})\}^{1/2}]\ dy$$

$$+\ \frac{2C_o x}{\pi^2\ (D_x^* D_y^*)^{1/2}}\ \exp\ (\frac{V_s^* x}{2D_x^*}) \sum_{n=1}^{\infty}\ \frac{1}{n}\ [\sin\ (\frac{n\pi z_2}{B})\ -\ \sin\ (\frac{n\pi z_1}{B})]\ \cos\ (\frac{n\ z}{B}) \tag{5.25}$$

$$\cdot\ (\lambda\ +\ V_s^2/4D_x^*\ +\ n^2\pi^2 D_z^*/B^2)^{1/2}\ \int_{-y_0}^{y_0} \frac{1}{\sqrt{\dfrac{x^2}{D_x^*} + \dfrac{(y-y^*)^2}{D_y^*}}}$$

$$\cdot\ K_1\ [\sqrt{(\lambda\ +\ V_s^{*^2}/4D_x^*\ +\ n^2\pi^2 D_z^*/B^2)\ (\frac{x^2}{D_x^*}\ +\ \frac{(y-y^*)^2}{D_y^*})}]\ dy^*$$

39

where K_1 is the modified Bessel function of the first kind and first order. Note that the second integral term in Equation 5.25 vanishes again in the case of a fully penetrating source.

An alternative formulation of the steady-state solution for the case where $y = 0$ is:

$$C(x,0,z) = \frac{C_o(z_2-z_1)x}{2(\Pi D_x^*)^{1/2}B} (\lambda + V^{*2}/4D_x^*)^{1/2} \exp\left(\frac{V_s^*x}{2D_x^*}\right) \int_0^\infty \frac{1}{\tau^{3/2}}$$

$$\exp\left\{-\tau - \frac{m_o^2a^2}{4\tau}\right\} erf\left(\frac{m_oY_o}{2\tau^{1/2}}\right) d\tau$$

$$+ \frac{C_ox}{\Pi(\Pi D_x^*)^{1/2}} \exp\left(\frac{V_s^*x}{2D_x^*}\right) \sum_{n=1}^{\infty} \frac{1}{n} \left[\sin\left(\frac{n\Pi z_2}{B}\right) - \sin\left(\frac{n\Pi z_1}{B}\right)\right] \cos\left(\frac{n\,z}{B}\right)$$

$$\cdot (\lambda + V_s^{*2}4D_x^* + n^2\Pi^2 D_z^*/B^2)^{1/2} \int_0^\infty \frac{1}{\tau^{3/2}} \exp\left\{-\tau - \frac{m_n^2a^2}{4\tau}\right\} erf\left(\frac{m_nY_o}{2^{1/2}}\right) dt \quad (5.26)$$

with

$$a^2 = \frac{x^2 D_x'}{D_y'} \quad (5.27)$$

$$m_o = \left\{\frac{\lambda + V'^2/4D_x'}{D_y'}\right\}^{1/2} \quad (5.28)$$

$$m_n = \left\{\frac{\lambda + V'^2/4D_x + n^2\Pi^2 D_z'/B^2}{D_y'}\right\} \quad (5.29)$$

As before, for the case of a fully penetrating source and/or when $z = 0$, this solution can be further simplified. The above solutions, Equations 5.23 to 5.26, were earlier programmed in a code named PATCH3D. This code has been incorporated into MULTIMED.

5.2.3 Receptor Well or Stream Location

A schematic of the receptor location relative to the waste facility is presented in Figure 5.2. The location of a well is determined by specifying in the input the radial distance to the well, the angle between the plume centerline and the radial location of the well measured counterclockwise, and the depth of penetration of the well. The code computes the cartesian coordinates of the well location as:

$$x_r = R \cos \psi \quad (5.30)$$

$$y_r = R \, Sin \, \psi \tag{5.31}$$

where

      R = the radial distance to the well [m]
      ψ = the angle measured counterclockwise from the plume centerline [degrees]
      x_r, y_r = the cartesian coordinates of the well location [m]

The z coordinate of the well is specified in the input as a fraction of the total depth of the aquifer, measured from the water table downward. Based on the input, the code calculates the z-distance in meters from the water table to the well. The well is assumed to have a single slot at that depth.

When the surface water module is used, a stream is the receptor instead of a well. The stream location is determined from the radial distance to the receptor alone (i.e., the angle off-center and z-distance are not used).

5.2.4 Time Values for Saturated Zone Concentrations

When operated in transient mode, MULTIMED requires that time values for calculating the groundwater concentration at the well be entered by the user. (The steady-state model does not require time values.) The source term for the transient model can be either a square wave pulse, formed by a constant leachate concentration of finite duration, or an exponentially decaying pulse, formed by specifying a source decay rate. In either case, the concentration at the well builds gradually, reaches some peak value, and declines as the dispersed pulse passes the well. The user must enter the time values that capture the various components of the pulse as it passes the well, such as the break-through time or the time of maximum concentration. An analytical technique to exactly predict when the pulse will reach the well or when the maximum concentration will occur has not been developed. However, the following equations may provide a reasonable estimate of the time, T_{mc}, when maximum concentration will be reached:

$$T_{mc} = xR_s/V_s + 0.5T_s \tag{5.32}$$

where

      x = x-distance to the well
      R_s = retardation factor in the saturated zone
      V_s = groundwater seepage velocity
      T_s = duration of the leakage pulse

Using this as a starting time, the user can begin a search that should lead quickly to the time values of interest. A good time step, T_{step}, to use in the search is given by:

$$T_{step} = 0.4T_{mc} \tag{5.33}$$

If the unsaturated zone is included in the simulation, T_s should be set to the time when the unsaturated zone concentration has passed its maximum and is about half way back to zero. This can be found by making an initial model run and examining the resulting unsaturated zone time series found in the output file VTRNSPT.OUT.

41

5.3 Assumptions and Limitations

Following are the list of assumptions inherent in the saturated zone transport module:

(a)   A single aquifer with uniform thickness is modeled. The saturated, porous medium properties are isotropic and homogeneous. The module cannot be used to simulate transport in fractured media unless the fractured medium is represented as an equivalent porous formation.

(b)   The ground water flow velocity is steady and uniform. This implies that the recharge through the facility and into the groundwater plume is small compared to the natural (regional) flow.

(c)   Contaminant degradation/transformation follows the first-order rate law and is restricted to biodegradation and hydrolysis. The latter is a second order process from which the first order rate is obtained using the existing environmental pH. This assumption is conservative since it neglects degradation due to other mechanisms such as oxidation, reduction, etc. Further, the model does not include by-products of degradation.

(d)   Contaminant sorption follows a linear adsorption isotherm. Adsorption takes place instantaneously and the adsorbed phase is in local equilibrium.

(e)   The initial contaminant concentration in the aquifer is zero. Assumptions regarding the source boundary conditions and the extent of the formation have been discussed in Section 5.2.

5.4 Coupling of the Unsaturated and Unsaturated Zone Modules

When modeling the transport of contaminants through the unsaturated and the saturated zones, an important requirement is that the principle of conservation of mass be satisfied (i.e., the mass flux of contaminant that leaches from the bottom of the unsaturated zone (or out of the facility in the absence of an unsaturated zone) must be equal to the mass flux that enters the saturated zone). This mass flux consists of the sum of advective and dispersive mass fluxes.

5.4.1 Steady-State Coupling

The mass that reaches the water table from the facility can be expressed as:

$$M_L = A_w \, Q_f \, C_\ell \tag{5.34}$$

where

$\begin{aligned}
M_L \quad &= \text{ the mass that leaches out of the facility [g/yr]} \\
A_w \quad &= \text{ the area of the facility [m}^2\text{]} \\
Q_f \quad &= \text{ percolation rate [m/yr]} \\
C_\ell \quad &= \text{ concentration in the leachate from the facility [g/m}^3\text{] if} \\
& \text{ attenuation within the unsaturated zone is neglected or the} \\
& \text{ unsaturated zone is absent. Alternatively, } C_\ell \text{ is the} \\
& \text{ concentration at the bottom of the unsaturated zone.}
\end{aligned}$

42

The mass flux that is *advected* into the saturated zone is calculated by integrating the source concentration in the y direction from $-\infty$ to $+\infty$ and over the depth z = 0 to z = H. Thus the mass flux advected into the aquifer is:

$$M_a = \int_{z=0}^{H} \int_{y=-\infty}^{+\infty} C(x = 0,y,z) \, V_s \theta \; dydz \qquad (5.35)$$

where

M_a = mass flux advected into the aquifer [g/yr]
$C(x=0,y,z)$ = concentration as a function of y and z at the source [g/m^3, mg/ℓ] as expressed by Equation 5.4 or 5.8
V_s = the seepage velocity in the saturated zone [m/yr]
θ = effective porosity of the saturated zone (cc/cc)

Similarly, the mass flux that enters the saturated zone due to dispersion can be expressed as:

where
M_d = mass flux dispersed into the aquifer [g/m^3]
D_x = dispersion coefficient in the x direction [m^2/yr]

5.4.1.1 The Gaussian Source Boundary Condition--

Substituting Equation 5.4 into Equation 5.35 and integrating, with C_o assumed uniform over the source depth H, yields:

$$M_d = \int_{z=0}^{H} \int_{y=-\infty}^{+\infty} \theta \; D_x \; \frac{\delta C}{\delta x} \Big|_{x=0} dydz \qquad (5.36)$$

Ungs (1987) has evaluated the integral in Equation 5.36 to yield:

$$M_a = (2\pi)^{1/2} \sigma V_s \theta H C_o \qquad (5.37)$$

$$M_d = (2\pi)^{1/2} \sigma V_s \theta H C_o \left[-1/2 + 1/2 \left(1 + \frac{4\lambda_s R_s D_x}{V_s^{\,2}}\right)^{1/2} \right] \qquad (5.38)$$

where

λ_s = the first-order decay coefficient [1/yr]
R_s = the linear retardation factor [dimensionless]
D_x = the longitudinal dispersion coefficient [m^2/yr]

Note that in the event, that $D_x = 0$, the dispersive flux, M_d, is zero.

The total flux into the saturated zone is given by the sum of advective (Equation 5.37) and dispersive (Equation 5.38) fluxes:

$$M_T = (2\pi)^{1/2} \sigma V_s \theta H C_o \zeta_D \qquad (5.39)$$

where

λ_s = the first-order decay coefficient [1/yr]
R_s = the linear retardation factor [dimensionless]
D_x = the longitudinal dispersion coefficient [m^2/yr]

Note that if ζ_D is set equal to unity, it implies that the dispersive flux is neglected.

$$\zeta_D = [\frac{1}{2} + \frac{1}{2} (1 + \frac{4\lambda_s R_s D_x}{V_s^2})^{1/2}] \qquad (5.40)$$

Equating Equations 5.34 and 5.40 yields the following expression of the mass balance:

$$A_w Q_f C_\ell = (2\pi)^{1/2} \sigma V_s \theta H C_o \zeta_D \qquad (5.41)$$

The above equation is used to couple the unsaturated and the saturated zone models under steady-state conditions.

Equation 5.41 can be rearranged to yield:

$$C_o = \frac{A_w Q_f}{(2\pi)^{1/2} V_s \theta H \sigma \zeta_D} C_\ell \qquad (5.42)$$

or

$$C_o = (NMF) C_\ell \qquad (5.43)$$

The factor NMF can be thought of as representing a near-field dilution effect or the effect of mixing below the facility. Based on purely physical considerations, this factor should be less than or at most equal to unity.

5.4.1.2 *The Patch Source Boundary Condition*

Substituting Equation 5.8 into Equation 5.35 and substituting Equation 5.23a into Equation 5.36 and integrating, the total mass entering the saturated zone can be expressed as:

$$M_T = 2y_o V_s \theta H C_o + 2y_o V_s \theta H C_o \{-1/2 + 1/2 (1 + \frac{4\lambda_s R_s D_x}{V_s^2})^{1/2}\} \qquad (5.44)$$

or letting

$$\zeta_D = [\frac{1}{2} + \frac{1}{2} (1 + \frac{4\lambda_s R_s D_x}{V_s^2})^{1/2}] \qquad (5.45)$$

45

then,

$$M_T = 2y_o V_s \theta H C_o \zeta_D \qquad (5.46)$$

In Equation 5.44 the first term represents the advective mass flux and the second term represents the dispersive mass flux entering the saturated zone. Equating Equation 5.46 to Equation 5.34 yields the mass balance expression used to couple the unsaturated and saturated zone (patch source) model under steady-state conditions:

$$C_o = \frac{A_w Q_f}{2y_o V_s \theta H \zeta_D} C_\ell \qquad (5.47)$$

5.4.2 Unsteady-State Coupling

For the case of unsteady-state transport in the unsaturated zone, the mass flux at the water table varies in time and the above approach for coupling the unsaturated and the saturated zone is no longer valid. In the unsteady state, concentrations in the saturated zone are determined using the convolution integral approach that superimposes the effects of source changes over time as follows:

$$C(x,y,z,t) = \int_0^t \frac{\partial C^*}{\partial \tau} \Big|_\tau f(x,y,z,t-\tau) \, d\tau \qquad (5.48)$$

where
$C^*(t)$ = the concentration at the water table at time t [mg/ℓ]
$f(x,y,z,t)$ = the normalized (with respect to source concentration) solution of the saturated zone analytical solution [mg/ℓ]

In Equation 5.48, the value of $f(x,y,z,t)$ is obtained using Equations 5.10 to 5.16 (with $C_o = 1$) for the case of a gaussian source boundary condition or Equation 5.23a (with $C_o = 1$) for a patch source boundary condition. In the computer code, the integral is numerically evaluated using the trapezoidal rule.

5.5 Data Requirements

Table 5-1 lists the primary input parameters required to compute the contaminant concentrations in the saturated zone. These parameters are classified into the following groups:

    (1)   Source-specific parameters
    (2)   Chemical-specific parameters
    (3)   Aquifer-specific parameters

A number of the parameters listed in Table 5-1 can be derived using other variables (presented in Table 5-2) and a set of empirical, semi-empirical or exact relationships. The derivation of parameters by the code is discussed below.

5.5.1 Source-Specific Parameters

46

The source-specific parameters which can be derived are the spread of the source, the source width, the source length, and the source thickness (which is actually classified as an aquifer parameter in the input). These are discussed below in terms of the Gaussian and the Patch boundary conditions.

5.5.1.1 *The Gaussian Source Boundary Condition*

As described in Section 5.2, the gaussian source boundary condition is uniquely specified when σ (the standard deviation of the gaussian source), H (the thickness of the source) and C_o (the maximum gaussian concentration) are specified. Note that in the event of a finite duration source, an additional parameter, T_s (the duration of the source), is necessary.

Source Thickness (Mixing Zone Depth) -- Percolation of water through the facility (and unsaturated zone, if it exists) results in the development of a mixing zone below the facility. This is shown in Figure 5.2. In the saturated zone module, this mixing zone is the "source" of the contaminants, hence the term source thickness is used interchangeably with the term mixing zone depth. The thickness, H, of the mixing zone depends on the vertical dispersivity of the media. If a value for H is not known, it can be derived using the following relationship:

$$H = (2\alpha_V L)^{1/2} + B(1 - \exp(-\frac{LQ_f}{V_s \theta B})) \tag{5.49}$$

where

α_V = the vertical dispersivity [m]
L = the length scale of the facility--i.e., the dimension of the facility parallel to the flow direction [m]
B = the thickness of the saturated zone [m]

In Equation 5.49, the first term represents the thickness of the mixing zone due to vertical dispersion and the second term represents the thickness of the mixing zone due to the vertical velocity below the facility resulting from percolation. The derivation of the second term is presented in Appendix A. While implementing this alternative, the code checks that the computed value of the thickness of the source, H, is not greater than the thickness of the aquifer, B.

The Spread of the Gaussian Source -- The standard deviation of the gaussian source is a measure of the spread of the source. It can be derived by the code using:

$\sigma = W/6$

where

W = the width scale of the facility--i.e., the dimension of the facility orthogonal to the groundwater flow direction [m]Dividing by 6 implies that 99.86 percent of the area under the gaussian source is flanked by the width of the facility.

The Length Scale and the Width Scale--If the length, L, or the width, W, of the source is not known, they can be derived by assuming that the waste disposal facility has a square shape and taking the square root of the area:

$$L = (A_w)^{1/2} \tag{5.51}$$

5.5.1.2 The Patch Source Boundary Condition

The patch source boundary condition is uniquely specified when the width of the source, $2y_o$, the source thickness, H, and the uniform concentration, C_o, are specified. The first two of these parameters can be derived.

TABLE 5-1. Primary Parameters Used in the Saturated Zone Transport Module

Parameters	Units
Source-Specific Parameters	
Area of the land disposal facility	[m^2]
Leachate concentration at the waste facility	[mg/l, g/m^3]
Either:	
Standard deviation of the source (Gaussian)	[m]
or	
Width of source (Patch)	[m]
Infiltration rate	[m/yr]
Recharge rate into the plume	[m/yr]
Duration of the pulse	[yr]
Source decay constant	[1/yr]
Aquifer-Specific Parameters	
Porosity	[cc/cc]
Thickness of the aquifer	[m]
Thickness of source	[m]
Seepage velocity	[m/yr]
Dispersivities (longitudinal, transverse, vertical)	[m]
Retardation coefficient	[dimensionless]
Radial distance from the site to the receptor	[m]
Angle between the plume center and the receptor	[degrees]
Well vertical distance	[fraction]
Time value at which concentration is required	[yr]
Chemical-Specific Parameters	
Effective first-order decay coefficient	[1/yr]
Distribution coefficient	[cc/g]
Overall Chemical Decay Coefficient	
Solid phase decay coefficient	[1/yr]
Dissolved phase decay coefficient	[1/yr]
Bulk density	[g/cc]
Distribution coefficient	[cc/g]
Porosity	[cc/cc]

TABLE 5-2. Parameters Used to Derive Other Saturated Zone Transport Module
Parameters

Parameters	Units
Solid and Dissolved Phase Decay Coefficients	
Reference temperature	[°C]
Aquifer temperature	[°C]
Second-order acid-catalysis hydrolysis rate constant at reference temperature	[ℓ/mole-yr]
Second-order base-catalysis hydrolysis rate constant at reference temperature	[ℓ/mole-yr]
Neutral hydrolysis rate constant at reference temperature	[l/yr]
pH of the aquifer	[pH units]
Retardation Coefficient	
Bulk density	[g/cc]
Distribution (i.e., adsorption) coefficient	[cc/g]
Porosity	[cc/cc]
Bulk Density	
Porosity	[cc/cc]
Porosity	
Mean particle diameter of the porous medium	[cm]
Particle Diameter	
Porosity	[cc/cc]
Distribution Coefficient	
Normalized distribution coefficient for organic carbon, K_{oc}	[cc/g]
Fractional organic carbon content	[dimensionless]
Seepage Velocity	
Hydraulic gradient	[m/m]
Hydraulic conductivity	[m/yr]
Porosity	[cc/cc]

TABLE 5-2. Parameters Used to Derive Other Saturated Zone Transport Module Parameters *(concluded)*

Parameters	Units
Hydraulic Conductivity	
Porosity	[cc/cc]
Mean particle diameter of the porous medium	[cm]
Thickness of the Source (Mixing Zone Depth)	
Length of the land disposal facility	[m]
Thickness of the aquifer	[m]
Seepage velocity	[m/yr]
Porosity	[cc/cc]
Infiltration rate through the facility	[m/yr]
Vertical dispersivity	[m]
Standard Deviation of the Source	
Width of the land disposal facility	[m]
Length and Width of the Facility	
Area of the land disposal facility	[m^2]
Dispersivities	
Radial distance from the site to the receptor	[m]

Source Thickness (Mixing Zone Depth)--If the source thickness is not specified directly, it is derived in the same way as for the Gaussian source.

Width of the Patch Source--The width of the patch source should be input as a user-specified value. However, the width of the source can be derived as the square root of the area using Equation 5.51.

5.5.2 Chemical-Specific Parameters

Two chemical-specific parameters shown in Table 5-1 can be derived from other parameters: the overall chemical decay coefficient and the distribution coefficient. Two additional chemical-specific parameters (shown in Table 5-2) can be derived as well. They are the solid phase and the liquid phase decay coefficients.

5.5.2.1 The Overall Chemical Decay Coefficient

The overall chemical decay coefficient for the saturated zone can be input directly. When it is not known, it can be derived by the code using the first term in Equation 5.3. If the solid-phase and the liquid-phase decay coefficients are unknown, they too can be derived from temperature-corrected values for hydrolysis rates, as described below. Note that chemical degradation within the saturated zone is limited to hydrolysis and the by-products of hydrolysis are assumed to be non-hazardous.

The acid-catalyzed, neutral and base-catalyzed hydrolysis rates are all influenced by groundwater temperature. This effect is quantified in the code using the Arrhenius equation, that yields:

$$K_{a,n,b}^{T} = K_{a,n,b}^{T_r} \exp[E_a/R_g \ (\frac{1}{T_r + 273} - \frac{1}{T + 273})] \tag{5.52}$$

where

$K_{a,b}^{Tr}$ and $K_{a,b}^{T}$ =   the second-order acid- and base-catalysis hydrolysis rate
                  at temperature T_r and T respectively [ℓ/mole-yr]
K_{n}^{Tr} and K_{n}^{T} =   the neutral hydrolysis rate at temperatures T_r and T
                  respectively [1/yr]
T   = temperature of the groundwater [°C]
T_r = reference temperature [°C]
R_g = universal gas constant [1.987E-3 kcal/deg-mole]
E_a = Arrhenius activation energy [kcal/mole]

Note that, using the generic activation energy of 20 kcal/mole recommended by
Wolfe (1985), the factor E_a/R_g has a value of about 10,000.

The acid catalyzed, base catalyzed and neutral hydrolysis rate constants are
combined (Mill et al., 1981) to yield the composite, first order, dissolved
phase hydrolysis rate:

$$\lambda_1 = K_a^T[H^+] + K_n^T + K_b^T[OH^-] \tag{5.53}$$

where

[H^+] = the hydrogen ion concentration [mole/ℓ]
[OH^-] = the hydroxyl ion concentration [mole/ℓ]

Note that [H^+] and [OH^-] are both computed from the pH of the aquifer, i.e.,

$$[H^+] = 10^{-pH} \tag{5.54}$$

$$[OH^-] = 10^{-(14-pH)} \tag{5.55}$$

For the case of sorbed phase hydrolysis, evidence suggests that base
neutralized hydrolysis can be neglected and that the acid neutralized
hydrolysis rate is enhanced by a factor of α. Thus, the effective sorbed
phase decay rate is expressed as:

$$\lambda_2 = \alpha K_a^T[H^+] + K_n^T \tag{5.56}$$

where α is the acid-catalysis hydrolysis rate enhancement factor for the
sorbed phase with a typical value of 10.0.

5.5.2.2 The Distribution Coefficient

The relationship most suited for relating the chemical distribution
coefficient, K_d, to soil or porous medium properties is discussed in detail by
Karickhoff (1984). In the absence of user-specified values, hydrophobic
binding is assumed to dominate the sorption process. For this case, the
distribution coefficient can be related directly to soil organic carbon
content using:

$$K_d = K_{oc} f_{oc} \tag{5.57}$$

where

   K_{oc} = normalized distribution coefficient for the chemical on organic carbon [ml/g]

   f_{oc} = organic carbon content in the saturated zone [dimensionless fraction]

5.5.3 Aquifer-Specific Parameters

Of the 12 aquifer-specific input parameters shown in Table 5-1, six can be either input directly or derived. In addition, some of the parameters used to derive these primary parameters (see Table 5-2) can also be derived.

5.5.3.1 Retardation Coefficient

The retardation coefficient can be derived in the code using Equation 5.2.

5.5.3.2 Porosity and Mean Particle Diameter

In the absence of a user-supplied value for porosity, θ, it can be calculated from the particle diameter using the following empirical relationship (Federal Register, Vol. 51, No. 9, pp. 1649, 1986):

$$\theta = 0.261 - 0.0385 \ln(d) \tag{5.58}$$

where

      d = the mean particle diameter [cm].

Using the same relationship, the mean particle diameter can be derived from a user-supplied value for porosity. Thus, only one or the other may be derived in a given simulation.

5.5.3.3 Bulk Density

The soil bulk density directly influences the retardation of solutes and is related to the soil structure. An exact relationship between the soil porosity, particle density, and the bulk density can be derived (Freeze and Cherry, 1979). This relationship is used in the code to derive bulk density. Assuming the particle density to be 2.65 g/cc, the relationship is expressed as:

$$\rho_b = 2.65(1 - \theta) \tag{5.59}$$

where

      ρ_b = the bulk density of the soil [g/cc].

5.5.3.4 Seepage Velocity

The seepage velocity is related to aquifer properties through Darcy's Law. Assuming a uniform, saturated porous medium, the seepage velocity can be derived in the code using the following relationship:

$$V_s = \frac{KS}{\theta} \tag{5.60}$$

where

        K   = the hydraulic conductivity of the formation [m/yr]
        S   = the hydraulic gradient [m/m]
        θ = porosity [dimensionless]

Note that in general, the hydraulic gradient is a function of the local topography, groundwater recharge volume and location, and the volume and location of groundwater withdrawals. Further, it may also be related to the porous media properties.

5.5.3.5 Hydraulic Conductivity

In the absence of site-specific measurements, a hydraulic conductivity value can be derived using approximate functional relationships. One such relationship, the Kozeny-Carman equation (Bear, 1979), is included in the model:

$$K = \frac{\rho g}{\mu} \; \frac{\theta^3}{(1-\theta)^2} \; \frac{d^2}{1.8}$$

(5.61)

where

        K   = the hydraulic conductivity [cm/s]
        ρ = the density of water [kg/m^3]
        g   = acceleration due to gravity [m/s^2]
        μ = the dynamic viscosity of water [N-s/m^2]
        d   = mean particle diameter [cm]

In Equation 5.61 the constant 1.8 includes a unit conversion factor. Both the density of water, ρ, and the dynamic viscosity of water, μ, are functions of temperature and are computed using regression equations presented in CRC (1981). Note that at 15°C, the value of [$\rho g/1.8\mu$] is about 478. After using Equation 5.61 to derive a value for hydraulic conductivity, the code converts the value to units of meters per year.

The only use of the hydraulic conductivity parameter in MULTIMED is to compute the seepage velocity. Therefore, if the user chooses to input the seepage velocity directly, instead of specifying it as a derived parameter, the hydraulic conductivity value is not needed.

5.5.3.6 Dispersion Coefficients

The model computes the longitudinal, lateral and vertical dispersion coefficients as the product of the seepage velocity and longitudinal (α_L), transverse (α_T), and vertical (α_V) dispersivities. In the absence of user specified values for dispersivities, the model allows two alternatives.

Alternative one is based on the values presented in Gelhar and Axness (1981). Dispersivities are calculated as a fraction of the distance to the downgradient receptor well, as follows:

$$\alpha_L = 0.1 \, x_r$$

(5.62)

$$\alpha_T = \frac{\alpha_L}{3.0} \tag{5.63}$$

$$\alpha_V = 0.056\alpha_L \tag{5.64}$$

where x_r = the distance to the receptor well [m]. Option one is summarized in Table 5-3(a).

Alternative two allows a probabilistic formulation for the longitudinal dispersivity as shown in Tables 5-3(a) and 5-3(b) [Gelhar (personal communication), 1986]. The longitudinal dispersivity is assumed to be uniform within each of the three intervals shown in Table 5-3(b). Note that the values of longitudinal dispersivity shown are based on a receptor well distance of 152.4 m. For other distances, the following equation is used:

$$\alpha_L(x_r) = \alpha_L(x_r = 152.4)(x_r/152.4)^{0.5} \tag{5.65}$$

TABLE 5-3(a). Alternatives for Including Dispersivities in the Saturated Zone Flow Module

Dispersivity	Alternative 1 Existing Values	Alternative 2 Gelhar's Recommendation
α_L [m]	0.1 x_r	Probabilistic Formulation (See Table 5-3(b))
α_T [m]	0.333 α_L	$\alpha_L/8$
α_V [m]	0.056 α_L	$\alpha_L/160$
α_L/α_T	3	8
α_L/α_V	approx. 18	160

TABLE 5-3(b). Probabilistic Representation of Longitudinal Dispersivity for a Distance of 152.4 m

Class	1	2	3
α_L (m)	0.1-1	1-10	10-100
Probability	0.1	0.6	0.3
Cumulative Probability	0.1	0.7	1.0

The transverse and vertical dispersivity are assumed to have the following values:

$$\alpha_T = \alpha_L/8 \tag{5.66}$$

$$\alpha_V = \alpha_L/160 \tag{5.67}$$

5.5.3.7 Source Thickness (Mixing Zone Depth)

The derivation of this aquifer-specific parameter is discussed in Section 5.5.1.1.

SECTION 6

The Surface Water Module

6.1 Introduction

This chapter presents details about the fate and transport of a toxic chemical pollutant in a surface stream as included in MULTIMED. As illustrated in Figure 6.1(a and b), the module is based on the assumption that contamination of the stream occurs due to the complete interception of a steady-state groundwater plume. Interception of a finite pulse source can not be simulated. Also, the case of partial penetration of the plume is not considered. Further, the case of stream contamination due to direct overland runoff from a 'failed' waste containment facility is not discussed. This route of exposure has been analyzed and discussed in detail by Ambrose et al. (1985).

The technical approach presented in the following sections is based on the surface water exposure assessment model developed by Ambrose et al. (1985), and an enhanced version of that surface water model, termed SARAH2 (Vandergrift and Ambrose, 1988).

6.2 Mathematical Description of the Surface Water Module

The surface water model assumes complete interception of a contaminant plume by a stream perpendicular to the stream as shown in Figures 6-1(a) and 6-1(b). Further it is assumed that at x=0 (the downstream edge of the near-field mixing region), the river is laterally as well as vertically mixed. With these assumptions, the following mass balance equation can be written:

$$M_g = C_s \ (Q_g + Q_s) \tag{6.1}$$

where

M_g = contaminant mass flux entering the stream, [g/yr]
C_s = the near-field fully mixed contaminant concentration in the stream [g/m^3 or mg/ℓ]
Q_g = groundwater discharge [m^3/yr]
Q_s = stream discharge [m^3/yr]

The stream discharge is supplied by the user. The groundwater discharge, Q_g, is calculated as:

$$Q_g = V_s^* \theta \ (H + 2\sqrt{\alpha_V x_s}) \ (3.92\sigma + 2\sqrt{\alpha_T x_s}) \tag{6.2}$$

where

V_s^* = the steady-state retarded seepage velocity [m/yr]
θ = the porosity [cc/cc]
H = the depth of penetration of the source [m]
α_V, α_T = the vertical and transverse dispersivity [m]
x_s = the distance of stream from the downgradient edge of the waste disposal unit [m]
σ = the standard deviation of the source [m]

Equation 6.2 calculates the volumetric flux from the groundwater, Q_g, using a steady-state retarded seepage velocity and an estimate of the cross-sectional area of the plume that intercepts the stream. The cross-sectional area is estimated based on the vertical and lateral spread of the plume under uniform flow conditions. Note that in Equation 6.2, the factor 3.92 accounts for 95% of the area of the initial gaussian source. In the event that the patch source boundary for the saturated zone model is used, the term 3.92σ in Equation 6.2 is replaced by W, the width of the patch source.

For a continuous, steady source of contaminant at the waste disposal facility, the mass loading to the stream, M_g, for steady-state conditions is:

where

$$M_g = M_L \exp\left(-\frac{\lambda_v d_v}{V_v^*}\right) \exp\left(-\frac{\lambda_s x_s}{V_s^*}\right) \tag{6.3}$$

M_L = mass flux of contaminant leaching from the land disposal facility [kg/yr] (also see Equation 5.34)
λ_v = the overall decay coefficient in the unsaturated zone [1/yr]
d_v = the distance traveled by the contaminant within the unsaturated zone [m]
V_v^* = the retarded seepage velocity in the unsaturated zone [m/yr]
λ_s, x_s, V_s^* = the corresponding quantities for the saturated zone

In the event that the unsaturated zone is simulated as a layered system consisting of n layers, Equation 6.3 can be modified as:

$$M_g = M_L \exp\left[-\sum_{i=1}^{n}\left(\frac{\lambda_v d_v}{V_v^*}\right)_i\right] \exp\left[-\frac{\lambda_s x_s}{V_s^*}\right] \tag{6.4}$$

Combining equations 6.1 and 6.3 or 6.4 gives the concentration of the contaminant in the fully mixed portion of the stream at the downstream edge of the near field mixing zone. At a downstream location within the stream, the contaminant concentration [mg/ℓ] is reduced due to degradation. Assuming a first order degradation rate, the downstream concentration is:

$$C_R(x_R) = C_s \exp\left(\frac{-\lambda_R x_R}{V_R}\right) \tag{6.5}$$

where

        $C_R(x_R)$ = contaminant concentration in the stream [mg/ℓ]
        λ_R = the in-stream decay rate [1/yr]
        x_R = the distance from the downstream edge of the mixing zone to the point of interest [m]
        V_R = the mean in-stream velocity of flow [m/yr]

The model estimates the in-stream decay rate, λ_R, and the mean in-stream velocity of flow, V_R, by methods described below.

6.2.1 Computation of the In-Stream Decay Coefficient

The in-stream fate processes of volatilization and hydrolysis are included in the model and assumed to be first order reactions. The overall decay coefficient is represented as:

where

$$\lambda_R = (K_{VR} + K_{HR}^{T}) \; X \; 3.15E7$$

        K_{HR}^{T} = the hydrolysis rate constant at the in-stream temperature, T [1/yr]
        K_{VR} = the volatilization rate constant [1/yr]

The factor 3.15E7 changes the units of λ_R from [1/s] to [1/yr]. The nominal hydrolysis rate constant is calculated from the acid-catalyzed, neutral and base-catalyzed hydrolysis rate constants (Burns et al., 1982; Mill et al., 1981):

$$K_{HR}^{T_r} = K_a^{T_r} \, [H+] \; (\alpha f_s + f_D) + K_n^{T_r} + K_b^{T_r} \, [OH^-] \, f_D$$

where

        K_a^{Tr} and K_b^{Tr} = the second-order acid-catalysis and base-catalysis hydrolysis rate constant at the reference temperature, T_r [ℓ/mole-yr]
        K_n^{Tr} = the neutral hydrolysis rate at temperature, T_r [1/yr]
        $[H^+]$ = hydrogen ion concentration
        α = sorption catalysis hydrolysis rate enhancement factor for the sorbed compound [dimensionless]
        K_n = neutral hydrolysis rate constant at the reference temperature [1/yr]
        f_s = fraction of the chemical that is sorbed [dimensionless]
        f_D = fraction of the chemical that is dissolved [dimensionless]
        $[OH^-]$ = the hydroxyl ion concentration [mole/ℓ]

Note that $[H^+]$ and $[OH^-]$ can be computed from the pH of the stream.

The hydrolysis rate constants can be expressed as a function of temperature by using the Arrhenius equation:

$$K_{HR}^{T} = A \exp \left[-E_a/R_g T \right] \tag{6.8}$$

60

where

E_a = the Arrhenius activation energy [kcal/mol]
R_g = the gas constant [1.987E-3 kcal/deg-mol]
T = the temperature [K]

The pre-exponential factor, A, has the same units as the hydrolysis rate constant. Using the above equation, the hydrolysis rate constant is corrected to ambient stream temperature by using the following expression:

$$K_{HR}^{T} = K_{HR}^{T_R} \exp \left[\frac{E_a}{R_g} \left(\frac{1}{T_R + 273} - \frac{1}{T + 273} \right) \right] \tag{6.9}$$

where T_R and T are the reference temperature and in-stream water temperature in °C. Note for the case when the activation energy is 20 kcal/mole, the value of E_a/R_g is 10,000. This value is used in the model.

The second transformation pathway considered is volatilization. The volatilization rate constant is calculated from the Whitman, or two-resistance model (Whitman, 1923; Burns et al., 1982):

$$K_{VR} = \frac{1}{D_s} \frac{1}{R_L + R_G} f_D \tag{6.10}$$

where

K_{VR} = the volatilization rate constant [1/s]
D_s = mean stream depth [m]
R_L = liquid phase resistance [s/m]
R_G = gas phase resistance [s/m]

The second term in Equation 6.10 represents the conductivity of the compound through a liquid and a gas boundary layer at the water surface. The liquid phase resistance to the compound is assumed to be proportional to the transfer rate of oxygen, which is limited by the liquid phase only:

$$R_L = \frac{1}{K_{02} D_s \sqrt{32/MW}} \tag{6.11}$$

where

K_{02} = reaeration rate constant [1/s]
MW = molecular weight of the compound [g/mole]
32 = molecular weight of oxygen [g/mole]

The gas phase resistance to the compound is assumed to be proportional to the transfer rate of water vapor, which is limited by the gas phase only:

$$R_G = \frac{1}{(H^{/}/RT) WAT (18/MW)} \tag{6.12}$$

where

        WAT   = vapor exchange constant [m/sec]
        H'   = Henry's law constant [atm-m^3/mole]
        R   = ideal gas constant [8.206 x 10^{-5} m^3-atm/mol°K]
        T   = stream water temperature [°K]
        18   = the molecular weight of water [g/mole]

The reaeration and water vapor exchange constants will vary with stream reach and time of year. They can be calculated using one of several empirical formulations. In this model the reaeration rate constant is calculated by the Covar method using stream velocity, V_R, and depth, D_s, corrected for temperature (Covar, 1976). The water vapor exchange constant is calculated using wind speed and a regression relation proposed by Liss (1973):

$$WAT = 5.16 \ x \ 10^{-5} + 3.156 \ x \ 10^{-3} \ W \tag{6.13}$$

where W = mean wind speed at 10 cm above surface [m/sec].

Wind speed measured above 10 cm is adjusted to the 10 cm height assuming a logarithmic velocity profile and a roughness height of 1 mm (Israelsen and Hansen, 1962):

$$W = W_z \ \log \ (0.1/0.001)/\log(z/0.001) \tag{6.14}$$

where

        W_z = wind speed at height z [m/sec]
        z   = wind measurement height [m]

6.2.2 Calculation of the Mean In-Stream Velocity

The mean in-stream velocity, V_R, is estimated in MULTIMED as:

$$V_R = (D_s)^{2/3}(SLOPE/n)^{1/2} \tag{6.15}$$

where

        D_s = mean stream depth [m]
        SLOPE   = channel slope [dimensionless]
        n   = Mannings roughness coefficient [dimensionless]

6.3 Exposure Due to Surface Water Contamination

6.3.1 Routes of Exposure

Three routes of exposure to toxic substances in surface streams are considered in the model. These are human exposure due to drinking contaminated water, human exposure due to the consumption of fish exposed to the contaminated water, and exposure to aquatic organisms. Figures 6.2(a), 6.2(b) and 6.2(c) show flow charts of the various stages between failure of the waste containment facility and these exposure routes. MULTIMED uses the concentrations, C_R and C_s, to predict the concentration of a contaminant in

drinking water, fish, and/or aquatic organisms. Based on these results and using procedures discussed in Section 9.6, the user can manually back-calculate the maximum allowable concentration of the contaminant in the waste disposal facility that is protective of human health and toxic aquatic effects.

6.3.2 Human Exposure to Toxics through Drinking Water

Human exposure to dissolved chemicals in drinking water is assumed to occur through water obtained from a treatment plant located downstream from the initial mixing zone. The water is assumed to be treated by a primary settling process allowing suspended solids and adsorbed chemicals to settle. The influent concentration, C_R is reduced to a concentration of C_{DW} in the effluent drinking water from the water treatment plant. This concentration is represented by:

$$C_{DW} = f_D \, C_R \tag{6.16}$$

where f_D is equal to the fraction of the contaminant that is dissolved. It can be expressed as:

$$f_D = \frac{C_R}{C_R + C_{ad}} \tag{6.17}$$

where C_{ad} = sorbed concentration [mg/ℓ]. The dissolved aqueous concentration, C_R, and the sorbed concentration, C_{ad}, can be related by:

$$K_p = \frac{C_{ad}}{C_R S} \tag{6.18}$$

where

$$\begin{aligned} S \quad &= \text{sediment concentration [mg/ℓ]} \\ K_p \quad &= \text{the equilibrium distribution coefficient [ℓ/mg]} \end{aligned}$$

Further, it can be shown that for the sorption of hydrophobic organic compounds:

$$K_p = K_{oc} \, f_{oc} \tag{6.19}$$

where

$$\begin{aligned} K_{oc} \quad &= \text{the organic carbon partition coefficient [ℓ/kg]} \\ f_{oc} \quad &= \text{organic carbon content of suspended solids [fraction]} \end{aligned}$$

Substituting Equations 6.18 and 6.19 into Equation 6.18, f_D is expressed as:

$$f_D = \frac{1}{K_{oc} f_{oc} S + 1} \tag{6.20}$$

and the fraction of sorbed contaminant is $(1 - f_D)$.

6.3.3 Human Exposure to Toxics Due to Fish Consumption

Dissolved neutral organic compounds in the water can be taken up by fish through exchange across the gill and gut membranes, and through the skin. Contaminated food can be ingested, resulting in further exchange of compounds across the gut membrane. Concentration levels in the fish rise until the activity of a compound in the blood equals the activity of that compound in the water. This condition represents chemical equilibrium. Further uptake of the compound, which results in higher blood concentrations, will lead to net exchange out of the fish through the gill, gut, kidney and skin. The whole-fish concentration of the pollutant can be expressed as:

$$C_F = K_F \, f_D \, C_s \tag{6.21}$$

where K_F equals the entire fish partition coefficient or the bioconcentration factor. Note that the use of the near-field, in-stream concentration, C_s, in Equation 6.21 rather than the downstream, attenuated concentration, C_R, assumes that the fish reside continuously within the most polluted reach of the stream and, hence, is a conservative assumption.

If the fish is exposed to a steady aqueous concentration over a long period of time, the distribution of the compound within the lipid and non-lipid tissues of the fish will equilibrate so that:

$$C_\ell = K_\ell \, C_B \tag{6.22}$$

and

$$C_{n\ell} = K_{n\ell} \, C_B \tag{6.23}$$

where

$$
\begin{array}{lll}
C_\ell & = & \text{the lipid phase biomass concentration [mg/kg]} \\
C_B & = & \text{the concentration in the blood[mg/\(\ell\)]} \\
K_\ell & = & \text{the lipid phase partition coefficient [\(\ell\)/kg]} \\
C_{n\ell} & = & \text{the non-lipid (blood, muscle) phase biomass concentration} \\
& & \text{[mg/kg]} \\
K_{n\ell} & = & \text{the non-lipid phase partition coefficient [\(\ell\)/kg]}
\end{array}
$$

Neglecting bioaccumulation, the equilibrium concentration in the blood will not exceed the dissolved concentration in the river, i.e.,

$$C_B = f_D C_s \tag{6.24}$$

The average whole fish concentration, C_F [mg/kg], can be expressed as the weighted sum of the tissue concentrations:

$$C_F = f_\ell \, C_\ell + (1 - f_\ell) \, C_{n\ell} \tag{6.25}$$

64

where f_ℓ = lipid fraction of the fish biomass [dimensionless].

Combining Equations 6.22 to 6.25 with Equation 6.21, C_F can be expressed as:

$$C_F = [f_\ell K_\ell + (1-f_\ell) K_{n\ell}]\, f_D\, C_s \qquad (6.26)$$

Comparing Equation 6.21 and Equation 6.26, the entire fish partition coefficient can be expressed as:

$$K_F = [f_\ell K_\ell + (1-f_\ell) K_{n\ell}] \qquad (6.27)$$

For less hydrophobic compounds, $K_{n\ell}$ may contribute significantly to K_F. Non-lipid tissue is composed primarily of water along with protein and carbohydrates. By replacing $K_{n\ell}$ with the octanol-water partition coefficient and assuming that partitioning to non-lipids is less than or equal to 1% of the partitioning to lipids, the model calculates a conservative estimate of K_F as:

$$K_F = K_{ow}\, (f_\ell + 0.01) \qquad (6.28)$$

The octanol water partition coefficient, K_{ow}, is approximated using the correlation with K_{oc} developed by Karickhoff et al. (1979):

$$K_{oc} = 0.41\, K_{ow} \qquad (6.29)$$

6.3.4 Exposure of Aquatic Organisms to Toxics

Aquatic organisms are exposed to contaminants present in the stream. Only dissolved species of a compound cross the membranes of aquatic organisms and cause internal exposure. There is some evidence, however, that the presence of suspended contaminant solids can enhance the rate of uptake and the internal exposure to a compound. Also, the Criterion Continuous Concentration (CCC), which is set to protect against toxic effects to aquatic organisms, is usually referenced to the total concentration of the contaminant in the stream. Therefore, exposure to aquatic organisms is estimated by using the total concentration of the compound in the stream.

6.4 Assumptions and Limitations

Following is a list of important assumptions on which the surface water module is based:

> **(a)** The surface stream model considers the case of complete plume interception only.

> **(b)** The module considers only the case of a steady-state continuous source at the landfill.

> **(c)** The stream is laterally and vertically well mixed. This implies that the stream is relatively small.

(d) The only in-stream transport process considered is lumped first order decay due to volatilization and hydrolysis.

(e) The municipal water treatment plant assumes removal of contaminants by adsorption onto particles that are removed by sedimentation or filtration processes.

(f) The concentration of the contaminant in fish is assumed to be at equilibrium with the near-field, in-stream concentration.

6.5 Data Requirements

Table 6-1 lists the surface water and chemical input parameters required to compute the in-stream concentration, as well as concentrations in drinking water, fish, or aquatic organisms. The surface water module must be run in conjunction with the saturated transport module (and the unsaturated zone modules, if needed). The saturated zone parameters are listed in Tables 5-1 and 5-2. Note that the location of the stream is specified using saturated zone parameters (see Section 5.2.3).

TABLE 6-1. Parameters Required for the Surface Water Module

Parameters	Units
Surface Stream Specific Data	
Stream discharge	[m^3/sec]
Distance to drinking water plant intake	[m]
Mean stream depth	[m]
Mannings roughness coefficient	[dimensionless]
Channel slope	[dimensionless]
Sediment concentration	[mg/ℓ]
Organic carbon fraction of suspended solids	[dimensionless]
pH of the stream	[pH units]
In-stream temperature	[°C]
Fraction of fish that is lipid	[dimensionless]
Wind speed	[m/s]
Height at which wind speed is measured	[m]
Chemical Specific Data	
Reference temperature	[°C]
Second-order acid catalysis hydrolysis rate constant at reference temperature	[ℓ/mole-yr]
Second-order base catalysis hydrolysis rate constant at reference temperature	[ℓ/mole/yr]
Neutral hydrolysis rate constant at reference temperature	[1/yr]
Henry's law constant	[atm-m^3/mole]
Molecular weight of the contaminant	[g/mole]
Normalized partition coefficient (i.e., K_{oc})	[mℓ/g]

For Monte Carlo simulations, the parameters shown in Table 6-1 may be input as constant values or as distributions. The values of some of these parameters can be computed indirectly using the parameter estimation methods discussed in the MULTIMED user's manual.

The Air Emissions Module

7.1 Introduction

This chapter describes the algorithm used to estimate the air emission of toxic substances from land-based waste disposal facilities. The current version of the air emissions module includes an algorithm to simulate the emissions from Subtitle C facilities. Algorithms to estimate emissions from impoundments and Subtitle D facilities are currently not included in MULTIMED's air emissions module.

The model accounts for diffusive transport through porous media based on Fick's law. The effect of atmospheric pressure fluctuations and other transport processes is accounted for by empirical factors. Approximate values of these parameters, based on available numerical and analytical studies, are included.

The current version of the air emissions module assumes that the wastes contained in the facility are suitably segregated into cells so that there is no chemical or biochemical activity within the facility. The case of co-disposal with municipal or liquid wastes is not considered here. This suggests that the possibility of gas generation within the landfill is highly unlikely. Further, the waste is considered to be covered with soil. Thus, the complex process of emissions from uncovered wastes is not included in the model.

The model's air emissions estimates are independent of predictions of unsaturated/saturated transport. Therefore, in the current version of the code, the air emission and dispersion simulations are run separately from subsurface transport simulations.

This chapter is restricted to the air-emissions module only and does not include any discussion of near field or far-field dispersion or transport processes. The latter is discussed in Section 8.

7.2 Governing Equations

7.2.1 The Air Emissions Diffusion Model

The model described below was first developed by Farmer et. al. (1978) for computing the vapor flux of hexachlorobenzene through a dry soil cover from a landfill. This method treats the waste volatilization or vapor loss of the chemical from a landfill as a diffusion controlled process using Fick's Law for steady-state diffusion. The diffusion into the atmosphere is assumed to emanate from a plane surface with a constant concentration. The emission rate is expressed as:

$$E_i = \frac{A_w}{L} D_{ei} (C_{si} - C_{ai}) TSEC \qquad (7.1)$$

where

> E_i = the emission rate of chemical i [g/yr]
> L = mean depth of the soil cover [cm]
> D_{ei} = effective diffusion coefficient for chemical i in soil [cm^2/s]
> C_{si} = pore space concentration of chemical i [g/cc]
> C_{ai} = concentration of the chemical i in air [g/cc]
> A_w = area of the land disposal facility [cm^2]
> TSEC = the number of seconds in a year [s]

7.2.2 The Effect of Atmospheric Pressure Fluctuations

The model, as presented above, accounts for only the diffusive transport of vapors through the porous media. The effect of atmospheric pressure fluctuations that 'pump' chemical vapors from the waste disposal facility is not considered. Typical ranges of atmospheric pressure fluctuations are presented in Table 7-1.

The occurrence of large barometric changes is associated with the passage of weather fronts, typically 4 to 8 days in duration. Clements and Wilkening (1974) investigated the effect of large scale atmospheric changes in ^{222}Rn flux across a soil-air interface. Field data show that pressure changes of 1 to 2 percent associated with the passage of frontal systems produce changes in the ^{222}Rn flux from 20 to 60 percent, depending on the rate of change of pressure and its duration. This finding was confirmed in a laboratory experiment using a vertical column of ^{226}Ra-bearing sand. Lu and Matuszek (1978) observed similar atmospheric pressure-induced gas flow of tritiated compounds from waste in a commercial radioactive-waste land burial site.

TABLE 7-1. General Characteristics of Atmospheric Pressure Fluctuations[*]

Parameter	Frontal Passage	Diurnal Variation	Local Gustiness
Pressure Amplitude (mm Hg)	10-20	1-3	0.1-0.2
Duration	4-8(d)	24(h)	10-30(s)

[*]*Springer et al. (1986)*

The pumping effect of diurnal barometric variations in extracting gases and vapors from subsurface porous formations apparently has not been investigated in detail. Fukuda (1955) investigated air and vapor movement in soil due to wind gustiness. The soil depth to which air can penetrate as a result of wind gustiness is very small. It was found that in sandy soil with mean particle diameters of 0.25 to 0.5 mm, air penetrates only about 5 mm below the surface.

Models that simulate the effect of pressure fluctuations (Thibodeaux, 1982) have not been sufficiently calibrated and verified. However, this effect has been incorporated into MULTIMED by using an empirical factor, e_{BP}. Thibodeaux (1982) computed a value of 1.13 for this factor using a numerical simulation model and two weeks of atmospheric pressure data.

7.2.3. Other Transport Processes

Thibodeaux et al. (1986) compared the flux estimated using Equation 7.1 with experimental data (without atmospheric pressure fluctuations). Their results indicate that Equation 7.1 underestimates fluxes by a factor of approximately three . This anomaly between the measured and computed values has been ascribed to the process of surface diffusion (Cussler, 1983) that occurs on

68

the walls of soil grains. This is a relatively fast process and could
account, in part, for the enhanced fluxes.

In the absence of detailed physical understanding of this process, it is best
to incorporate its effect as an empirical enhancement factor, e_f.
Incorporating the two empirical factors, e_f and e_{BP}, into Equation 7.1, the
model equation can be expressed as:

$$E_i = \frac{A_w}{L} D_{ei} (C_{si} - C_{ai}) e_{BP} e_f TSEC \qquad (7.2)$$

The concentration of the chemical in air, C_{ai}, is assumed to be zero in the
code. This is valid for the case of high wind velocities at the surface that
rapidly transport vapor emissions away from the land disposal unit.

7.2.4 Computation of the Diffusion Coefficient

The effective diffusion coefficient for a chemical in soil, D_{ei}, is computed in
the code using a general, empirical relationship proposed by Currie (1961).
The relationship, which is based on a hydrogen diffusion experiment, accounts
for the effect of moisture content:

$$D_{ei} = \gamma D_{oi} \theta_t^{\mu - \sigma} (\theta_a)^{\sigma} \qquad (7.3)$$

where

> D_{oi} = diffusion coefficient for chemical i in air [cm^2/s]
> θ_a = air-filled porosity of soil [cc/cc]
> θ_t = total porosity of soil [cc/cc]
> σ = exponent which is 4.0 for granular material subject to moisture
>   testing
> γ = factor which varies with soil type (0.8 to 1.0)
> μ = exponent which varies with soil type (1.4 for spherical grains
>   (sand), 2.6 for kaolin (clay) and 11.0 for plate minerals)

The effect of temperature on the diffusion coefficient is considered in the
code using:

$$D_{oT} = D_{oR} (\frac{T}{T_R})^{1.5} \qquad (7.4)$$

where D_{oR} and D_{oT} = the diffusion coefficients at the reference temperature, T_R,
and temperature of the waste disposal unit, T, respectively.

7.2.4.1 Effect of Engineering Controls

The current version of MULTIMED can not account for the effect of engineering
controls. If the effect of composite engineering controls, such as vegetative
soil, a synthetic membrane, or a drain layer, is important to results,
Equation 7.2 can be solved by manual calculation using the resistances-in-
series concept. The total effective diffusion for the cover can be computed
as:

$$D_{total,i} = \frac{L_{total}}{\sum_N (\frac{L_n}{D_{eni}})}$$ (7.5)

where

L_n = the thickness of each layer [cm]
D_{eni} = the effective diffusion coefficient for chemical i in layer n [cm^2/sec]
N = total number of layers
L_{total} = sum of thickness of the N layers [cm]

7.2.5 Computation of Vapor Concentration, C_{si}

The accuracy of the emission estimates obtained using the above model significantly depends on the accuracy with which the vapor concentration in the pore spaces of the waste disposal unit is computed. This concentration depends on the properties of the chemical species, the chemical quantity in the cell, and the state of the chemical with respect to the other materials in the cell. Table 7-2 (Thibodeaux, 1982) shows a categorization of the various states of chemical substances in landfills and the equilibrium laws that can be used to determine the pore space chemical concentration. Further details about these methods is available in Groves et al. (1984).

Application of these eight different theories to compute the pore space concentration requires detailed information that is typically not available for a waste facility. MULTIMED air emission module assumes that the information is not available and therefore adopts a conservative approach. Maximum vapor phase chemical concentrations of solid wastes in pure form or as mixtures of solid flakes and granules are considered. For such conditions, it is safe to assume that a chemical will exert pure component vapor pressure. Thus, the saturation vapor concentration for a chemical in the waste can be determined using the ideal gas law:

$$C_{si} = \frac{X_i P_{oi} M_i}{RT}$$ (7.6)

where

M_i = mole weight of chemical i [gm/mole]
R = molar gas constant (mm Hg-cm^3/$^{\circ}$K-mole)
T = temperature of the landfill [$^{\circ}$K]
X_i = mole fraction of chemical i in the mixture [dimensionless]
P_{oi} = vapor pressure of chemical i [mm of mercury]

7.3 Assumptions and Limitations

Following is the list of assumptions on which the air emissions algorithm is based:

(a) The air emissions algorithm is not applicable to the case where landfill gas is generated within the facility.

70

(b) Far field atmospheric dispersion of the contaminants is treated separately as discussed in Section 8.

(c) Enhancement in the rate of emissions due to barometric pumping and other, as yet undefined processes, is included using empirical factors.

(d) The vapor phase contaminant concentration within the land disposal unit is computed assuming that the unit contains chemicals in pure solid state. This is a conservative approach in that it tends to overpredict the emission of contaminants.

7.4 Data Requirements

The data required for the air emissions model are shown in Table 7-3.

TABLE 7-3. Parameters Required for the Air Emissions Module

Parameters	Units
Air Emission-Specific Parameters	
Effective depth of the soil cover	[cm]
Water content of the soil	[cc/cc]
Total porosity of the soil	[cc/cc]
Empirical coefficients to compute diffusion coefficient in soil from a known diffusion coefficient in air	γ, μ, σ [dimensionless]
Flux enhancement factor due to barometric pressure fluctuations	[dimensionless]
Enhancement factor due to other transport processes	[dimensionless]
Temperature of the landfill	[$^{\circ}$C]
Chemical-Specific Parameters	
Mole weight of the chemical	[g/mole]
Mole fraction of chemical in landfill	[dimensionless]
Vapor pressure of chemical	[mm of mercury]
Diffusion coefficient for chemical in air at a reference temperature	[cm^2/s]
Reference temperature for air diffusion	[$^{\circ}$C]
Source-Specific Parameters	
Area of the land disposal facility (converted to cm^2 in program)	[m^2]

SECTION 8

Air Dispersion Module

8.1 Introduction

This section describes the air dispersion module used to calculate the atmospheric transport of vapor emissions from a Subtitle C landfill. It must be run in conjunction with the air emission model described in Section 7.

Pollutants emitted from landfills will be transported by advection due to the mean wind field and by dispersion due to vertical and horizontal turbulent wind fluctuations. During development of MULTIMED, over 60 air dispersion models that simulate these transport processes were reviewed and classified into the following five categories:

> **(i)**   Grid models
> **(ii)**   Trajectory models
> **(iii)** Gaussian models
> **(iv)**   Screening level models
> **(v)**   Miscellaneous models

As will be discussed in subsequent sections, the model selected for inclusion is a long-term gaussian plume model similar to the VALLEY model (U.S. EPA, 1977). This type of model has been verified through extensive use, accounts for long-term variations in meteorological conditions, and involves a level of computational effort appropriate for MULTIMED. In the current version of the model, the air dispersion module has received only limited testing.

8.2 Governing Equations

8.2.1 The Gaussian Dispersion Equation

The general gaussian equation for the ground-level concentration of a pollutant at a receptor located at a distance, x, from a point source (Wark and Warner, 1981) is:

$$C = \frac{QRD}{2\pi U \sigma_y \sigma_z} \exp\left[-\frac{1}{2}\left(\frac{Y}{\sigma_y}\right)^2\right] \qquad\qquad (8.1)$$

where

> C   = ground level pollutant concentration at distance, x, from the source [mg/ℓ]
> Q   = source emission rate [g/s]
> R   = term that accounts for vertical plume dispersion and reflection, computed using Equation 8.2
> D   = term that accounts for chemical decay, computed using Equation 8.3
> U   = wind speed [m/s]
> σ_y = horizontal (transverse) dispersion coefficient [m]
> σ_z = vertical dispersion coefficient [m]

y   = transverse distance from the plume centerline [m]

This equation is derived by solving the one-dimensional, advection-dispersion equation and assuming a gaussian distribution of pollutant in the transverse and vertical directions. Note that the horizontal and vertical dispersion coefficients are functions of atmospheric stability and the distance between the source and the receptor.

The term, R, that accounts for vertical dispersion and the reflection of the plume at the ground surface and at the top of the atmospheric mixing layer, is computed using:

$$R = \sum_{n=-\infty}^{\infty} \{ \exp [-\frac{1}{2}(\frac{2nL - H_a}{\sigma_z})^2] + \exp [-\frac{1}{2}(\frac{2nL + H_a}{\sigma_z})^2]\} \qquad (8.2)$$

where

  H_a = height of the plume centerline above ground [m]
  L   = thickness of the atmospheric mixing layer [m]

Further, in Equation 8.1, D is an exponential decay term used to account for the transformation and chemical degradation of pollutants:

$$D = \exp (-k \frac{x}{U}) \qquad (8.3)$$

where

  k   = a first-order decay rate constant (1/s)

Equation 8.1 assumes constant meteorological (wind speed, direction, stability) and source emission conditions in level terrain, and is valid only for calculating steady-state ground-level concentrations. To estimate the long-term (i.e., seasonal, annual) average concentrations for periods during which meteorological conditions change, a frequency-weighting approach, which calculates concentrations for all possible combinations of wind direction, wind speed, and stability class, is used.

The distribution of meteorological conditions over time is described by a joint frequency distribution of wind direction, wind speed, and stability. The range of possible wind directions in an area is represented by dividing the areal x-y plane into 16 equal wind direction sectors each subtending an angle of 2π/16 radians at the location of the point source (see Figure 8.1). Wind speeds are similarly described by dividing the range of possible wind speeds into six equal intervals, with each interval represented by a single average wind speed. The six average wind speeds commonly used for reporting meteorological data are supplied as defaults in the MULTIMED preprocessor. They can be modified by the user, if desired.

Atmospheric stability is a measure of the turbulence in the atmosphere. The two types of turbulence present in the environment are convective and mechanical. Convective turbulence describes the turbulence caused by differences between temperature at different heights (i.e., heat flux). Mechanical turbulence describes the mixing caused by wind shear. Atmospheric stability is represented by the Pasquill-Gifford (PG) classification scheme, composed of the six discrete categories A through F defined in Table 8-1. Stability Class A, the most unstable class, is dominated by convective

activities typical of a sunny day with light winds. Stability Class D, or
neutral stability, describes a well-mixed atmosphere and is dominated by
mechanical turbulence. Stability Class F, the most stable class, describes a
stratified atmosphere where temperature increases with height and winds are
light. This is typical of a clear calm winter evening. Pollutant releases
disperse the most under unstable conditions and the least under stable
conditions.

To account for the variability of wind direction, pollutant concentrations are
averaged in the y-direction across each wind direction sector:

$$C_i = \frac{16}{2\Pi x_c} \frac{QRD}{U\sigma_z \sqrt{2\Pi}}$$
(8.4)

where

$\quad$ C_i $\quad$ = average ground level pollutant concentration in sector
$\quad\quad\quad\quad$ i [mg/ℓ]

$\quad$ x_c $\quad$ = distance from the source to the receptor along the plume
$\quad\quad\quad\quad$ centerline [m]

Note that the transverse dispersion terms in Equation 8.1 have been replaced
by the inverse of the sector width ($2\Pi x_c$ /16).

The long-term average concentration is then computed by weighting
concentrations for each combination of wind speed, wind direction, and
stability class by the corresponding joint frequency of occurrence. Thus the
long-term average concentration from a point source is expressed as (U.S. EPA,
1977):

$$C_L = \frac{16}{2\Pi} \sum_{i=1}^{16} \sum_{j=1}^{6} \sum_{k=1}^{6} f_{ijk} \left[\frac{QRS_i D}{U_j \sigma_z x_C \sqrt{2\Pi}} \right]$$
(8.5)

where

$\quad$ C_L $\quad$ = long-term average ground-level pollutant concentration [mg/ℓ]

$\quad$ f_{ijk} $\quad$ = the joint frequency of occurrence of the ith wind direction,
$\quad\quad\quad\quad$ j[th] wind speed, and k[th] stability class [dimensionless]

$\quad$ S_i $\quad$ = a smoothing function computed using Equation 8.6
$\quad\quad\quad\quad$ [dimensionless]

TABLE 8-1. Atmospheric Stability Categories

Category	Description
A	Extremely unstable
B	Moderately unstable
C	Slightly unstable
D	Neutral
E	Slightly stable
F	Moderately stable

In Equation 8.5, S_i is a smoothing function used to eliminate discontinuities in concentrations calculated near the boundaries of the wind direction sectors. Frequencies for a wind direction sector may be very different from those in the two adjacent sectors, resulting in unrealistic discontinuities at the sector boundaries. To avoid this effect, the receptor concentrations are calculated as weighted averages of concentrations in the wind direction sector in which the receptor is located and the two adjacent sectors. The weighting (or smoothing) factor is the normalized distance of the receptor from sector centerlines as shown in Figure 8.1. Thus:

$$S_i = \frac{w - Y_i}{w} \qquad\qquad\qquad (8.6)$$

where

w = the distance between sector centerlines at the receptor [m]
Y_i = the distance of the receptor from the centerline of sector i [m]

Equation 8.5 is the key equation used by the air dispersion module to calculate ground-level concentrations at various distances from the waste disposal facility. The following sections describe the application of the gaussian equation to area sources, the estimation of plume rise, methods for calculating vertical dispersion coefficients, and terrain corrections.

8.2.2 Area Source Approximations

Area sources are used to represent emissions from landfills and from areas where point sources are too numerous to simulate individually. Emissions from these sources are expressed as mass fluxes per unit area. Concentrations resulting from area sources are calculated from the gaussian point source dispersion equation using the virtual point source approximation. The location of the virtual point source is determined such that the horizontal plume dispersion at the centroid of the area source is equal to the width of the area source. For long-term sector averaging models, the virtual point source is located such that the distance between the wind direction sectors at the centroid of the area source is equal to the width of the area source (Figure 8.2).

Thus, the distance, x_c, used in Equation 8.5 is the distance from the virtual point source to the receptor along the sector centerline. However, the distance used in calculating the decay term (Equation 8.3) is the distance from the centroid of the area source to the receptor (i.e., the actual distance traveled by the pollutant).

The air dispersion module has an additional correction to the virtual source approximation to account for receptors very close to the source. Receptors near the source will not be affected by the entire area source, since contributions from portions of the area will be carried past the receptor. In these cases the effective source area is reduced as shown in Figure 8.3. The emission rate used in Equation 8.5 is then the product of the effective source area and the landfill emission rate per unit area.

8.2.3 Plume Rise

Gaussian plume models calculate dispersion after the plume has stabilized to its initial height of rise. During emission the plume may rise vertically due to initial buoyancy and momentum. However, emissions from landfills and other area sources will often have negligible buoyancy or momentum. These emissions occur by diffusion through the landfill cap material and will in general have a temperature close to the ambient temperature. Area sources are therefore usually modeled by assuming that the plume centerline does not rise above the elevation of the source during emission. An option is available, however, to estimate initial plume rise by assuming that the height of rise from area sources is linearly proportional to wind speed (Irwin et al., 1985):

$$h = (\frac{U}{5}) \, \Delta h_5 \tag{8.7}$$

where

   h   = height of plume rise [m]
   Δh_5 = height of rise at U = 5 m/s [m]

In the above relationship, Δh_5 is a model input parameter which must be determined by the user from field studies or other estimation methods.

8.2.4 Estimation of Vertical Dispersion Coefficient

The vertical dispersion coefficient determines the vertical distribution of pollutant in the plume and is a critical parameter in estimating ground level receptor concentrations. The vertical dispersion coefficient increases with turbulence and with distance from the source. The model allows the user to select between two options for estimating this parameter. The first is the Pasquill-Gifford family of curves derived using the expression:

$$\sigma_z = a \, x^b + c \tag{8.8}$$

where a, b, and c are experimentally derived constants associated with the six meteorological stability classes. The values of a, b, and c for the six stability classes, which are listed in Table 8-2, are included in the code as data statements.

TABLE 8-2. Constants for PASQUILL-GIFFORD Curves for each Stability Class

x ≥ 1000 m						
Stability =	A	B	C	D	E	F
a	.001	.0476	.1192	.615	2.63	3.6
b	1.89	1.1	1.91	5.4	5.1	5.14
c	9.6	2.00	-25	.5-	126.	-75.

100 m ≤ x 1000 m						
Stability =	A	B	C	D	E	F
a	.001	.0476	.119	.187	.1345	.362
b	1.89	1.11	.915	.755	.745	.55
c	9.6	2.00	-1.4	-1.1	-2.7	

x < 100 m						
Stability =	A	B	C	D	E	F
a	.1742	.1426	.1233	.0804	.06	.0434
b	.936	.922	.905	.881	.854	.814
c	0	0	0	0	0	0

Source: U.S. EPA (1977).

The Pasquill-Gifford curves were derived from a series of experiments on dispersion in flat terrain, and may not be applicable to all locations. If data on wind turbulence are available for the site, the vertical dispersion coefficient can be calculated by the model from the standard deviation of the wind elevation angle. This is the second option:

$$\sigma_z = \frac{2\sigma_e r_o}{\ln[\frac{\sigma_e(x + r_o) + h}{\sigma_e(x - r_o) + h}]} \tag{8.9}$$

where

σ_e = the standard deviation of the wind elevation angle [radians]
r_o = radius of source [m]

Note that the standard deviation of the wind elevation angle, σ_e, is also referred to as the vertical turbulence intensity and is defined as the standard deviation of vertical wind velocity fluctuations divided by the mean wind speed. The radius of the source is calculated as the square root of the area of the facility divided by two.

8.2.5 Terrain Effects

No gaussian model explicitly simulates the effects of terrain on meteorology or on the trajectory of the plume (i.e., trapping in valleys, obstruction by hills, etc.). However, MULTIMED does account for the effect of elevation on the height of the plume centerline above the ground surface. The plume centerline is assumed to remain at a constant elevation; the effective height of the plume is then modified for receptors higher or lower than the source:

$$H_a = \begin{cases} h - (Z_r - Z_s) & (Z_r - Z_s) \leq h \\ 0 & (Z_r - Z_s) > h \end{cases} \qquad (8.10)$$

where

> H_a = effective height of plume centerline above receptor [m]
> h   = the height above ground of the plume centerline at the source [m]
> Z_r = elevation of the receptor [m]
> Z_s = elevation of the ground at the source, assumed zero in the model [m]

When $(Z_r - Z_s) > h$, the model assumes that the plume centerline is at the ground surface.

The model also has two options for using a terrain correction, which is a function of the atmospheric stability. Under stable conditions, the terrain correction is calculated as described above. For unstable and neutral conditions the model assumes that the plume always remains at the initial height above the ground surface. Under these conditions the plume centerline essentially parallels the ground surface.

8.3 Assumptions and Limitations

The following assumptions and limitations apply to the air dispersion module of MULTIMED:

> **(a)** The concentration profile of the pollutant is assumed to be gaussian in the transverse and vertical directions.

> **(b)** Calculated concentrations are long-term averages and will not indicate the maximum concentrations which might result from extreme meteorological conditions.

> **(c)** The model does not account for the effects of terrain on the shape of the plume or the trajectory of the plume.

> **(d)** The pollutant is assumed to be a non-buoyant vapor which neither rises nor settles out of the plume due to gravitational forces.

> **(e)** Sources are assumed to be square areas with constant emission rates.

> **(f)** Chemical transformation of the pollutant is modeled by lumped first-order decay; no mechanistic descriptions of processes such as photolysis are included in the model.

8.4 Data Requirements

Input data for the air dispersion module include parameters describing the receptor, the source, and the local meteorology. The data requirements are listed in Table 8-3. Note that in MULTIMED the source emission rates are estimated by the air emissions module, described previously in Section 7.

The code allows the user either to assign a constant wind and stability condition or to use a wind-stability frequency-weighting approach. For the first condition, Equation 8.5 is solved using a constant wind speed and constant stability condition, supplied in the input. The direction of the wind is assumed to be the same as the direction of the receptor.

For the second approach, a separate input file of joint frequency distributions is required to solve Equation 8.5. This joint frequency distribution of stability, wind speed, and wind direction is used to compute seasonal average concentrations. For the usual configuration of 16 wind direction sectors, 6 wind speeds, and 6 stability classes, 576 (16 x 6 x 6) joint frequency entries are required. Typically this joint frequency distribution is available as STAR (Stability Array data) summaries for airports but may be difficult to find for other locations.

TABLE 8-3. Parameters Required for the Air Dispersion Module

Parameters	Units
Source-Specific Parameters	
Area of the land disposal facility (converted to cm^2 in the code)	[m^2]
Air Dispersion-Specific Parameters	
Height of plume rise at a wind speed of 5 m/s	[m]
Mixing layer thickness	[m]
Standard deviation of wind elevation angle	[radians]
Receptor elevation	[m]
Receptor distance from the source	[m]
Receptor angle from the source	[radians]
Decay coefficient for pollutant in air	[s^{-1}]
Either:	
Constant wind speed	[m/s]
Constant stability condition	[dimensionless]
or	
Wind speeds for 6 classes	[m/s]
Joint frequency distribution for each wind speed, direction, and stability class	[dimensionless]

SECTION 9

Uncertainty Analysis

9.1 Introduction

As described in the previous sections, MULTIMED simulates the movement of contaminants emanating from a waste disposal facility. The model includes algorithms that simulate the movement of the contaminant within the unsaturated zone, the saturated zone, a surface stream, and the atmosphere based on a number of user-specified parameters. These include chemical-specific, media-specific, source-specific and receptor location-specific parameters.

Typically the values of these parameters are not known exactly due to measurement errors and/or inherent spatial and temporal variability. Therefore, it is often more appropriate to express their value in terms of a probability distribution rather than a single deterministic value and to use an uncertainty propagation model to assess the effect of the variability on the model output.

This section presents the uncertainty propagation method implemented in the MULTIMED code. The method allows a quantitative estimate of the uncertainty in the concentration at a downgradient receptor location due to uncertainty in the model input parameters.

9.2 Statement of the Problem and Technical Approach

The objective of the uncertainty analysis/propagation approach is to estimate the uncertainty in the receptor concentration given the uncertainty in the input parameters. In other words, the objective is to estimate the cumulative probability distribution of the downgradient well concentration given the probability distribution of the input parameters. As an example, C_w represents the downgradient well concentration:

$$C_w = g(\underline{X}) \tag{9.1}$$

where $\underline{X}$ represents the vector of model inputs and g represents the computational algorithms for transport in the unsaturated and the saturated zones. Some or all of the components of $\underline{X}$ may vary in an uncertain way (i.e.,

$$F_{C_w}(C'_w) = Probability(C_w \leq C'_w) \tag{9.2}$$

they are random variables defined by cumulative probability distribution functions). The goal is to calculate the cumulative distribution function, $F_{C_w}(C'_w)$, given a probabilistic characterization of $\underline{X}$. Note that $F_{C_w}(C'_w)$ is defined as:
where C'_w is a given downgradient well concentration.

Five methods of evaluating $F_{C_w}(C_w^{'})$ were examined in order to select the most appropriate method for MULTIMED (WCC, 1986). The methods are:

    1. First-Order and First-Order-Second-Moment Analysis (FO, FOSM);

    2. Monte Carlo Simulation (MC);

    3. Discretization of Probability Distributions (DPD);

    4. Response Surface Analysis (RS); and

    5. Rackwitz-Fiessler Method and its variants (RF).

The selection criteria included:

    1. *Computational efficiency,* measured by the number of response calculations required to achieve a given level of precision in estimation of an output statistic (in this case, the 90th percentile of the output distribution).

    2. *Accuracy* in evaluation of the output statistic (e.g., a specified percentile value).

    3. *Generality* of application, so that a number of modules and input conditions, and all sources of uncertainty, can be accommodated by the same uncertainty-propagation method.

    4. *Simplicity* of usage, measured by the number of parameters that must be specified by the user for each application.

    5. *Completeness of the information produced,* which may include only the mean and variance of the output distribution or may be the whole distribution, and which may or may not contain information useful for uncertainty decomposition.

    6. *Flexibility with respect to input distributions*, so that the method would be able to accommodate a number of different input distributions.

Using the above criteria, a qualitative comparison of the various uncertainty-propagation methods is included in Table 9-1. Based on the evaluation of the methods and a knowledge of MULTIMED, the Monte Carlo simulation method was selected. This approach is simple, unbiased and completely general. Further the method is especially attractive when there are many input variables that are randomly distributed, because the efficiency does not depend on the dimensionality of the input vector. Further, because the model is analytical, it is not very expensive to run a large number of independent executions of the model to achieve satisfactory confidence limits on the downgradient well concentration. Details of the Monte Carlo method are discussed below.

TABLE 9-1. Qualitative Comparison of Uncertainty-Propogation Methods

Criterion	FO, FOSM	MC	DPD	RS	RF
Computational Efficiency	***	**	--	**	*
Accuracy	*	*	*	**	**
Generality	**	***	*	*	*
Simplicity	***	***	***	**	*
Information Produced	**	*	**	**	***
Variation of F_X	**	**	**	***	*

```
--  - criteria not satisfied
*   - criteria partially satisfied
**  - criteria satisfied in general
*** - criteria satisfied
```

9.3 The Monte Carlo Analysis Technique

Figure 9.1 illustrates the Monte Carlo method used in MULTIMED. Given a set of deterministic values for each of the input parameters, X_1, X_2 . . . X_n, the composite model computes the downgradient receptor concentration, C_w, i.e.:

$$C_w = g\ (X_1, X_2, X_3\ .\ .\ .\ X_n) \tag{9.3}$$

Application of the Monte Carlo simulation procedure requires that at least one of the input variables, X_1 . . . X_n, be uncertain, with the uncertainty represented by a cumulative probability distribution. The method involves the repeated generation of pseudo-random values of the uncertain input variable(s). The pseudo-random values are drawn from the specified distribution and are within the range of any imposed bounds. Then the model is applied, using these values, to generate a series of model responses (i.e., values of C_w). These responses are statistically analyzed to yield the cumulative probability distribution of the model response. Thus, the various steps for the application of the Monte Carlo simulation technique involve:

(a) Selection of representative cumulative probability distribution functions for the relevant input variables.

(b) Generation of a pseudo-random number from the distributions selected in (a). These values represent a possible set of values for the input variables.

(c) Application of the model to compute the derived inputs and output(s).

(d) Repeated application of steps (b) and (c).

(e) Presentation of the series of output (random) values generated in step (c) as a cumulative probability distribution function (CDF).

(f) Further analysis and application of the cumulative probability
distribution as a tool for decision making.

9.4 Uncertainty in the Input Variables

The variables required by MULTIMED can be broadly classified into two different sets that exhibit different uncertainty characteristics. These are:

(a) Variables that describe the chemical, biochemical, and toxicological properties of the hazardous constituent. Examples of these variables include the Henry's law constant, the acid, neutral, and base catalyzed hydrolysis rates, and the soil adsorption coefficient.

(b) Variables that describe the environmental properties of the various media and impact the fate and transport of the pollutant within each medium. Examples of these variables include the hydraulic conductivity, porosity, organic carbon content, and dispersivity values.

Uncertainty in the first set of variables primarily arises due to laboratory measurement errors or theoretical analysis used to estimate the numerical values. In addition to experimental precision and accuracy, errors may arise due to extrapolations from controlled (laboratory) measurement conditions to uncontrolled environmental (field) conditions. Further, for some variables, semi-empirical methods are used to estimate the values. In this case, errors in using the empirical relationships also contribute to variability in the model outputs.

Uncertainty in the second set of variables may include both measurement and extrapolation errors. However, the dominant source of uncertainty in these is their inherent natural (spatial and temporal) variability. This variability can be interpreted as site-specific or within-site variation in the event that the model is used to analyze exposure due to a specific land-disposal unit. Alternatively it can represent a larger scale (regional/national) uncertainty if the model is used to conduct exposure analysis for a specific chemical or specific disposal technology on a generic, nation-wide or regional basis. Note that the distributional properties of the variables may change significantly depending upon the nature of the application.

Whatever the source of uncertainty, the uncertainty preprocessor developed for the model requires that the uncertainty be quantified by the user. This implies that for each input parameter deemed to be uncertain, the user selects a distribution and specifies the parameters that describe the distribution.

Currently, the user can select one of the following distributions:

(a) Normal
(b) Lognormal
(c) Uniform
(d) Log uniform
(e) Exponential
(f) Empirical
(g) Johnson SB distribution.

The first two distributions require the user to specify the mean and the variance. The third and the fourth require minimum and maximum values. The fifth distribution requires only one parameter--the mean of the distribution. For the empirical distribution, the user is required to input the coordinates of the cumulative probability distribution function (minimum 2 pairs, maximum 20 pairs) which is subsequently treated as a piece-wise linear curve.

Finally, the Johnson SB distribution requires four parameters--mean, variance, the lower and upper bounds.

In all cases, MULTIMED requires the upper and lower bounds for all the distribution types. If a value which is randomly generated during any Monte Carlo run is outside the user-specified bounds, it is rejected by the code and a new number is generated.

Of the seven distributions, the characteristics of the first six are readily available in literature (Benjamin and Cornell, 1970). Details of the Johnson system of distributions are presented in McGrath and Irving (1973) and Johnson and Kotz (1970). The distribution types are briefly summarized in Section 9.5 below. Note that Section 9.5 is copied, with slight modifications, from Volume 1 of the RUSTIC documentation (Dean et al., 1989).

9.5 Description of the Parameter Distributions

This description of the distributions which can be specified in the MULTIMED Monte Carlo option includes: 1) the parameters of the distributions, 2) the equations for the probability and cumulative density functions, and 3) a brief discussion of the properties of each distribution.

9.5.1 Normal Distribution

The term "normal distribution" refers to the well known bell-shaped probability distribution. Normal distributions are symmetrical about a mean value and are unbounded, although values further from the mean occur less frequently. The spread of the distribution is generally described by the standard deviation. The normal distribution has only two parameters: the mean and the standard deviation. Although the distribution is unbounded, the user must enter minimum and maximum values for individual parameter distributions. Generated values outside these bounds are not used by the model.

The probability density function of x is given by:

$$f_n(x) = \frac{1}{S_x \sqrt{2\pi}} \exp\left[-0.5\left(\frac{x - m_x}{S_x}\right)^2\right] \tag{9.4}$$

where S_x is the standard deviation, and m_x is the mean of x. The cumulative distribution is the integral of the probability density function:

$$F_n(x) = \int_{-\infty}^{x} f_n(x)dx \tag{9.5}$$

The above integration must be performed numerically, but tables of numerically-integrated values of $F_n(x)$ are widely available in the statistical literature.

9.5.2 Log-Normal Distribution

The log-normal distribution is a skewed distribution in which the natural log of variable x is normally distributed. Thus, if y is the natural log of x, then the probability distribution of y is normal with mean, m_y, and standard

deviation, S_y, and a probability density function similar to Equation 9.4. The mean and standard deviation of x (m_x and S_x) are related to the log-normal parameters m_y and S_y as follows:

$$m_x = \exp[m_y + 0.5(S_y)^2] \tag{9.6}$$

$$S_x^2 = m_x^2 [\exp(S_y^2) - 1] \tag{9.7}$$

To preserve the observed mean and standard deviation of x, the parameters of the log-normal distribution (m_y and S_y) are therefore selected such that the above relationships are satisfied. Note that m_y and S_y do not equal the natural logs of m_x and S_x respectively. Log-normal distributions have an absolute lower bound of 0.0 and no absolute upper bound, and are often used to describe positive data with skewed observed probability distributions. As stated above, within the absolute bounds, the user must input minimum and maximum bounds for individual parameters.

Note that when a lognormal distribution is selected in MULTIMED, the user should input the mean and standard deviation of the data (arithmetic space). The transformation to the mean and standard deviation in lognormal space is performed by the code.

9.5.3 Uniform Distribution

A uniform distribution is a symmetrical probability distribution in which all values within a given range have an equal chance of occurrence. A uniform distribution is completely described by two parameters: 1) the minimum value (lower bound), A, and 2) the maximum value (upper bound), B. The equation for the uniform probability density distribution of variable x is given by:

$$f_u(x) = 1/(B - A) \tag{9.8}$$

where $f_u(x)$ is the value of the probability density function for x. The cumulative distribution F(x) is obtained by integrating Equation 9.8. This yields the probability distribution:

$$F_u(x) = (x - A)/(B - A) \tag{9.9}$$

where F(x) is the probability that a value less than or equal to x will occur.

9.5.4 Log-uniform Distribution

The log-uniform distribution type requires only a lower and an upper bound; the mean and standard deviation are not used. This distribution results in values between the lower and upper bounds having equal probability of occurrence (as in a standard uniform distribution) but with relative magnitudes that follow a logarithmic scale.

9.5.5 Exponential Distribution

The probability density function for an exponential distribution is described by an exponential equation:

$$f_e(x) = \frac{\exp(-x/m_x)}{m_x} \tag{9.10}$$

where m_x is the mean of x. The cumulative distribution is given by:

$$F_e(x) = 1 - \exp(-x/m_x) \qquad\qquad\qquad (9.11)$$

The exponential distribution is bounded by zero; the probability density function peaks at zero and decreases exponentially as x increases in magnitude.

9.5.6 Empirical Distribution

At times it may be difficult to fit a standard statistical distribution to observed data. In these cases it is more appropriate to use an empirical piecewise-linear description of the observed cumulative distribution for the variable of interest.

Cumulative probabilities can be estimated from observed data by ranking the data from lowest (rank = 1) to highest (rank = number of samples) value. The cumulative probability associated with a value of x is then calculated as a function of the rank of x and the total number of samples. The cumulative probabilities of values between observed data can be estimated by linear interpolation.

9.5.7 The Johnson System of Distributions

The Johnson system involves three main distribution types, one of which, the SB (Log-ratio or bounded), is included in MULTIMED. The Johnson SB distribution basically represents a log-ratio or bounded transformation applied to the random variable such that the transformed variable is normally distributed.

$$SB: Y = \ell n \left(\frac{(X-A)}{(B-X)} \right) \qquad\qquad\qquad (9.12)$$

where

ln	= natural logarithm transformation
X	= untransformed variable with limits of variation from A to B
Y	= the transformed variable with a normal distribution

To determine if the Johnson SB distribution is appropriate for a sample data set, the skewness and kurtosis of the sample data should be plotted as shown in Figure 9.2. If the sample point is located in the region for the SB distribution, it can be used for the sample data. For additional details about the Johnson system of distributions, the reader is referred to McGrath et al. (1973) and Johnson and Kotz (1970).

9.6 The Random Number Generator

Having selected a distribution for each of the input parameters to be Monte Carloed, the model generates random values of these parameters. This requires the use of pseudo-random number generating algorithms. Numerous non-proprietary subroutines exist that can be used to generate random numbers. A number of these are comparable in terms of their computational efficiency, accuracy and precision. The specific routines included in this code are those described by McGrath et al. (1973).

The performance of these algorithms has been checked to ensure that they accurately reproduce the parameters of the distributions that are being

sampled. In order to test the algorithms two sets of runs were made. For Run
1, 500 random numbers were generated; for Run 2, 1000 random numbers were
generated. For the five distributions tested, the input parameters and the
results are shown in Tables 9-2(a) and (b). In each case, the output
statistics for the randomly generated variables closely match the input
values.

For Run 2, the randomly generated variables were arranged in ascending order
and the cumulative probability distributions were plotted. The results are
shown in Figures 9.3 to 9.7. Visual inspection of these figures further
testifies to the accuracy of these algorithms.

Note that more rigorous statistical tests could be used to further test the
accuracy of the algorithms. However, the above simplified analysis and the
additional testing performed by Marin (1988) has provided sufficient proof of
the accuracy of the results and indicated that these algorithms satisfactorily
reproduce the input statistics and distributions of the variables.

9.7 Analysis of the Model Output

Using the randomly generated parameter values, the model is used to estimate
values of concentrations at a point located downgradient from the waste
facility. If C_w represents the normalized, steady-state concentration at the
receptor location calculated by the model when the leachate concentration at
the waste disposal facility is unity, and C_T is the (health based maximum
allowable) threshold concentration for the chemical at the receptor, the
maximum allowable leachate concentration at the waste facility can be back-
calculated by hand using:

$$C_\ell = \frac{C_T}{C_w} \qquad\qquad (9.13)$$

The maximum allowable leachate concentration defined by Equation 9.13 is the
leachate concentration for which the downgradient receptor concentration does
not exceed the threshold concentration.

Alternatively,

$$\frac{1}{C_w} = \frac{C_\ell}{C_T} \qquad\qquad (9.14)$$

Equation 9.14 states that the reciprocal of the computed normalized
concentration represents the maximum allowable ratio of leachate concentration
to the threshold concentration. Thus, for a simulated normalized
concentration of $C_w = 0.05$ mg/ℓ, Equation 9.14 implies that the maximum
allowable leachate concentration from the landfill could be 20 times the
threshold value for the chemical. Note that both C_w and C_T are chemical
specific.

Combining the above back calculation procedure with the Monte Carlo analysis
allows the maximum leachate concentration to be couched in a probabilistic
framework. For each chemical, application of the Monte Carlo method results
in an array of values for normalized concentration, each representing a
feasible result for the waste disposal facility-environmental scenario. These
values are statistically analyzed to derive the cumulative probability

90

distribution function as shown in Figure 9.8. The cumulative probability distribution, $F_{C_w}(C_w')$ together with the allowable threshold value, C_T, and the back calculation procedure (Equations 9.13 and 9.14) provide the information necessary to calculate the maximum allowable leachate concentration. In particular, the value of leachate concentration, C_ℓ, that leads to p% of the realizations in compliance--i.e., the receptor well concentration is less than or equal to the threshold concentration, is:

$$C_\ell = \frac{C_T}{C_p} \qquad\qquad\qquad (9.15)$$

where C_p is the p-percentile concentration obtained from the cumulative distribution function of the downgradient well concentration.

9.8 Confidence Bounds for the Estimated Percentile

As described above, the Monte Carlo simulation provides an estimate of C_p, the p-percentile concentration obtained from a sample of n model simulations. Since the sample size is finite, estimates of C_p will be uncertain, with the degree of uncertainty decreasing with increasing sample size.

A quantitative estimate of the uncertainty in the estimate of C_p can be obtained by computing a confidence interval around the estimate C_p. The upper and the lower bounds of this confidence interval are defined such that:

$$Probability\,(C_L < C_p < C_U) = 1 - \alpha \qquad\qquad (9.16)$$

where

C_L	= the lower bound of the confidence interval [mg/ℓ]
C_U	= the upper bound of the confidence interval [mg/ℓ]
α	= significance level [dimensionless]

The interval C_L to C_U is usually referred to as the $100(1 - \alpha)$ confidence interval and implies that the true value of the estimate of the quantile C_p lies within the interval C_L to C_U with a probability of $100(1 - \alpha)$. The confidence interval is estimated using the binomial distribution as described below.

Define an indicator (Bernoulli) random variable, I, such that:

$$I = \begin{cases} 1 & \text{if } C_w < C_p \\ 0 & \text{if } C_w > C_p \end{cases} \qquad\qquad (9.17)$$

Also, define a random variable, K, equal to the number of trials for which I = 1 from the Monte Carlo simulations. The random variable K is then binomially distributed with a mean of np and a variance of np(1 - p), i.e.,

$$Probability\left\{\sum_{i=1}^{n} I_i = k\right\} = \frac{n!}{k!(n-k)!}\, p^k (1-p)^{n-k} \qquad (9.18)$$

where n is the number of independent realizations of C_w (by Monte Carlo simulations) corresponding to n independent realizations of I.

The probability that K is less than a given positive integer is also the probability that $C_{(K)} < C_p$ where $C_{(K)}$ is the Kth smallest simulated value of the concentration. Thus a confidence interval on K, based on the binomial distribution, can be used to establish the confidence interval, C_p.

Conover (1980) describes a procedure for obtaining a confidence interval for C_p that essentially involves looking up values in a table of cumulative probabilities of the binomial distribution (i.e., Prob $\{K \leq k\}$) to find the k values corresponding to probabilities of $\alpha/2$ and $1 - \alpha/2$. For sample sizes greater than 20, he provides an alternate procedure based on the normal approximation to binomial probabilities for large n. This simple approximation requires the calculation of two values, r and s:

$$r = np + z_{\alpha/2}[np(1 - p)]^{1/2} \tag{9.19}$$

$$s = np + z_{1-\alpha/2}[np(1 - p)]^{1/2} \tag{9.20}$$

where $z_{\alpha/2}$ and $z_{1-\alpha/2}$ are quantiles of the standard normal (mean = 0, variance = 1) distribution (note that $z_{\alpha/2} = -z_{1-\alpha/2}$). Conover recommends rounding up these values of r and s to the next higher integers and estimate the corresponding values of $C_{(r)}$ and $C_{(s)}$, as the rth and s^{th} smallest values of C_w. The confidence interval is then of the form:

$$Prob \{C_{(r)} \leq C_p \leq C_{(s)}\} = (1 - \alpha)100\% \tag{9.21}$$

This approach was used by Carsel et al. (1985) and WCC (1986, Appendix C) and is incorporated in the current version of MULTIMED.

9.9 The Number of Monte Carlo Simulation Runs

Unfortunately, there is no way to a priori calculate the number of Monte Carlo simulations required to establish a confidence interval on C_p with a given width without first having a very good estimate of the shape of $F_{C_w}(C_w')$ in the region of C_p. It is easy, however, to calculate the number of realizations required to bring the ranks r and s as close together as desired. For realistically large n (typically in the hundreds or more for simulation applications), the normal approximation applies and n can be found by fixing (s - r) to the width desired and solving for n using Equations 9.19 and 9.20. Thus,

$$n = \frac{(s - r)^2}{4p(1 - p)(z_{1-\alpha/2})^2} \tag{9.22}$$

Notice that the smaller the specified range (s - r), the smaller the number of realizations required. This should not be counterintuitive, because a fixed confidence interval on the C_w scale should naturally contain more simulated values (and thus a large value for s - r) if more simulations are performed.

An alternative criterion for specifying n might be the fraction of the range of simulated ranks to be covered by the confidence interval. Thus,

$$\frac{s - r}{n} = f = \frac{2z_{1-\alpha/2}[np(1-p)]^{1/2}}{n} \tag{9.23}$$

or, solving for n:

$$n = \frac{4p(1 - p)(z_{1-\alpha/2})^2}{f^2} \tag{9.24}$$

SECTION 10

References

Ambrose, R.B., L.A. Mulkey, and P.S. Huyakorn (1985), "A Methodology for Assessing Surface Water Contamination due to Land Disposal of Hazardous Waste." *USEPA,* Athens, GA.

Anatra, M., S. Bosch, P. Durkin, D.A. Gray, and D. Hohreiter (1986), "Investigation of the Uncertainty in the Acceptable Daily Intake (ADI)." *Syracuse Research Corporation report submitted to Woodward-Clyde Consultants,* USEPA Project No. 68-03-6304, Cincinnati, Ohio.

Anderson, M.P. (1979), "Using Models to Simulate the Movement of Contaminants through Groundwater Flow System." *CRC Critical Reviews in Environmental Control,* Vol. 9, Issue 2, pp. 97-156.

Arthur D. Little, Inc. (1984), "Evaluation of Emission Controls for Hazardous Waste Treatment, Storage and Disposal Facilities." *EPA-650/3-84-017. Office of Air Quality Planning and Standards,* Research Triangle Park, North Carolina.

Bear, J. (1979), *Hydraulics of Groundwater,* McGraw Hill, New York.

Benjamin, J.R., and C.A. Cornell (1970), *Probability, Statistics, and Decision for Civil Engineers*. McGraw Hill Book Company.

Bicknell, Brian R. (1984), "Modeling Chemical Emissions from Lagoons and Landfills." *Anderson-Nichols and Co., Inc.,* Palo Alto, CA 94303.

Brooks, R.H., and A.T. Corey (1966), "Properties of Porous Media Affecting Fluid Flow." *ASCE J. Irrig. Drain. Div.* 92(2):61-68.

Burns, L.A., D.M. Cline, and R.R. Lassiter (1982), "Exposure Analysis Modeling System (EXAMS): User Manual and System Documentation." *USEPA, -600/3-82-023,* Athens, GA.

Carnahan, B., H.A. Luther, and J.O. Wilkes (1969), *"Applied Numerical Methods",* John Wiley.

Carsel, R.F., and R.S. Parrish (1988), "A Method for Developing Joint Probability Distribution of Soil-Water Retention Characteristics." *Water Resources Research* 24(5):755-769.

Carsel, R.F., R.S. Parrish, R.L. Jones, J.L. Hansen, R.L. Lamb (1985), "Characterizing the Uncertainty of Pesticide Leaching in Agricultural Soils." *Draft submitted to J. Env. Qual.*

Carsel, R.F, et al. (1985), "Characterizing the Uncertainty of Pesticide Leaching in Agricultural Soils." *Draft Report* U.S. EPA Environmental Research Laboratory, Athens, Georgia 30613.

Carsel, R.F., C.N. Smith, L.A. Mulkey, J.D. Dean, and P. Jowise. (1984) User's Manual for the Pesticide Root Zone Model (PRZM) Release 1. *EPA-600/3-84-109,* 16-17.

Carsel, R.F., and R.S. Parrish. (1988) A Method for Developing Joint Probability Distribution of Soil-Water Retention Characteristics. *Water Resource Research* 24(5), 755-769.

Clements, W.F., and M.H. Wilkening (1974), "Atmospheric Pressure Effects on ^{222}Rn Transport across the Earth-Air Interface." *J. Geophysical Research*, Vol. 79, No. 33.

Code of Federal Regulations. 40 CFR. Part 264.

Cohen, Y. (1986), "Organic Pollutant Transport. Improved Multimedia Modeling Techniques Are the Key to Predicting the Environmental Fate of Organic Pollutants." *Environ. Sci. Technol.*, Vol. 20, No. 6.

Conover, W.J. (1980), *Practical Nonparametric Statistics.* 2nd ed., John Wiley and Sons, New York, 493 pp.

Covar, A.P. (1976), "Selecting Proper Recreation Coefficient for Use in Water Quality Models." Presented at the USEPA *Conference on Environmental Simulation and Modeling,* April 19-22, 1976.

CRC (1981), *Handbook of Chemistry and Physics,* 62nd edition, CRC Press.

Currie, J.A. (1961), "Gaseous Diffusion in Porous Media. Part 3 - Wet Granular Materials." *British Journal of Applied Physics,* June 1961.

Currie, J.A. (1960), "Gaseous Diffusion in Porous Media. Part 2 - Dry Granular Materials." *British Journal of Applied Physics,* Vol. 11, August 1960.

Cussler, E.L. (1983), *"Diffusion: Mass Transfer in Fluid System,"* pp. 188-189, 1st Ed., Cambridge University Press.

Dass, P., G.R. Tamke, and C.M. Stoffel. (1977) Leachate Production at Sanitary Landfills. *ASCE, Jour. Env. Eng. Div.,* 103 (EE6).

E.C. Jordan Co. (1987), Technical Memorandums dated June 2, 1987, and September 1987, submitted to *USEPA,* OSW, Washington, D.C.

E.C. Jordan Co. (1985), "Analysis of Engineered Controls of Subtitle C Facilities for Land Disposal Restrictions Determinations. Revised Distribution of Leaching Rates." Draft Report *ECJ Project No. 4756-01* prepared for Research Triangle Institute, North Carolina, and USEPA, OSW, Washington, D.C.

Electric Power Research Institute (1985), "A Review of Field Scale Physical Solute Transport Processes in Saturated and Unsaturated Porous Media." *EPRI EA-4190, Project 2485-5,* Palo Alto, California.

Enfield, C.G., et al. (1982), "Approximating Pollutant Transport to Ground Water." *Ground Water,* Vol. 20, No. 6, pp. 711-722.

Farmer, W.J., et al. (1978), "Land Disposal of Hexachlorobenzene Wastes: Controlling Vapor Movement in Soils." *Proceedings of the 4th Annual Research Symposium* held at San Antonio, Texas, March 6-8.

Federal Register (1986), "Hazardous Waste Management System: Land Disposal Restrictions." *USEPA*, Vol. 15, No. 9.

Freeze and Cherry (1979), *"Groundwater."* Prentice Hall, Englewoods Cliffs, New Jersey.

Freeze, R.A., and J.A. Cherry. (1979) *Groundwater.* Prentice-Hall Inc., Englewood Cliffs, N.J., 30-36.

Fukuda, H. (1955), "Air and Vapor Movement in Soil Due to Wind Gustiness." *Soil Science* 79:249-258.

Gelhar, L.W. and Axness, C.J. (1981), "Stochastic Analysis of Macro-Dispersion in Three-Dimensionally Heterogeneous Aquifers." *Report No. H-8, Hydraulic Research Program.* New Mexico Institute of Mining and Technology, Soccorro, New Mexico. 140 p.

Groves, F.R., D.D. Reible, and L.J. Thibodeaux (1984), "Estimation of Physical and Chemical Properties of Waste Organic Mixtures Associated with Land Pollution." Section 3 in Exposure Assessment Involving Mixtures of Environmental Pollutants, Ed. J.D. Dean et al., *Office of Health and Environmental Assessment,* DRD, USEPA, Washington, D.C.

Haderman, J. (1980), "Radionuclide Transport through Heterogenous Media." *Nuclear Technology* 47:312-323, February 1980.

Hermann, D.J., and S.B. Tuttle. (1981) Performance Studies of Various Landfill and Impoundment Liners. *Fourth Annual Madison Conference of Applied Research and Practice on Municipal and Industrial Waste.* University of Wisconsin, Madison, WI, 250-265.

Huyakorn, P.S., M.J. Ungs, L.A. Mulkey, and E.A. Sudicky (1987), "A Three-Dimensional Analytical Method for Predicting Leachate Migration." *Groundwater,* Vol. 25, No. 5. September-October 1982.

Huyakorn, P.S., M.J. Ungs, E.D. Sudicky, L.A. Mulkey, and T.D. Wadsworth. 1986. "RCRA Hazardous Waste Identification and Land Disposal Restriction Groundwater Screening Procedure." *USEPA,* Washington, D.C.

Irwin, J.S., T. Chico, and J. Catalano. 1985. *CDM 2.0 -- Climatological Dispersion Model -- User's Guide.* U.S. Environmental Protection Agency, Research Triangle Park, North Carolina.

Israelsen, D.W., and V.E. Hansen (1962), *"Irrigation Principles and Practices."* John Wiley and Sons, Inc., New York. 447 pages.

Johnson, N.L., and S. Kotz (1970), *Distributions in Statistics: Continuous Univariate Distributions*, Houghton Mifflin Company, Boston.

Karickhoff, S.W. (1984), "Organic Pollutant Sorption in Aquatic Systems."
    ASCE J. Hyd. Div. 110(6):707-735.

Karickhoff, S.W., D.S. Brown, and T.A. Brown (1979), "Sorption of Hydrophobic
    Pollutants on Natural Sediments." *Water Res.* 13:241-248.

Knisel, W.J., Jr., Ed. (1980) CREAMS, A Field Scale Model for Chemical Runoff and Erosion from Agricultural Management Systems. Vols. I, II, and III, *Draft Copy, USDA-SEA, AR, Cons. Res. Report 24.*

Kulkarni R.B., G. Luster, G. Rao and A.M. Salhotra (1988) Enhanced Methods for Characterizing Uncertainties in Numerical Models. Volume I: Methodology Development and Validation and Volume II: User's Manual and Programmers Guide. Report prepared for U.S. Environmental Protection Agency, Office of Research and Development, Athens, GA Contract No. 68-03-6309

Lester, B.H., P.S. Huyakorn, H.O. White, Jr., T.D. Washworth, and J.E. Buckley (1986), "EPACML Composite Analytical-Numerical Model for Simulating Leachate Migration in Unconfined Aquifers." *Prepared by GeoTrans, Inc.*

Liss, P.S. (1973), "Process of Gas Exchange across an Air-Water Interface." *Deep-Sea Research* 20:221-238.

Lu, A.H., and J.M. Matuszek (1978), "Transport through a Trench Cover of Gaseous Tritiated Compounds from Buried Radioactive Waste," presented at *Symposium on the Behavior of Tritium in the Environment,* held at San Francisco.

Lu, J.C.S., B. Eichenberger, and R.J. Stearns. (1985) *Leachate from Municipal Landfills Production and Management*. Noyes Publications, Park Ridge, N.J., 7-94.

Lyman et al. (1982), *"Handbook of Chemical Property Estimation Methods. Environmental Behavior of Organic Compounds."* McGraw-Hill Book Company.

Marin, C. (1988), Personal Communication.

Marino, M.A. (1974), "Distribution of Contaminants in Porous Media Flow." *Water Resources Research* 10(5):1013-1018.

McGrath, E.J., and D.C. Irving (1973), Techniques for Efficient Monte Carlo Simulation, Volume II. Random Number Generation for Selected Probability Distributions. *Report prepared for Office of Naval Research.* Project No. NR 364-074/1-5-72, Code 462.

McKoy and Associates (1986), "Predicting Volatile Organic Emissions through Soil Covers." *The Hazardous Waste Consultant,* September 1986.

Meeks, Y, P. Mangarella, G. Palhegyi, and A. M. Salhotra (1988), "Landfill Source Model." *Report Prepared for U.S. Environmental Protection Agency* under EPA Contract No. 68-03-6304. Environmental Research Laboratory, Athens, Georgia.

Mill, T., et al. (1981), "Laboratory Protocols for Evaluating the Fate of Organic Chemicals in Air and Water." *Final Draft, Prepared for U.S. EPA Technology Development and Applications Branch* under EPA Contract No. 68-03-2227. Environmental Research Laboratory, Athens, Georgia.

Millington, R.J., and J.P. Quirk (1961), "Permeability of Porous Solids." *Trans. Faraday Soc.* 57:1200-1207.

Moench, A.F., and A. Ogata (1981), "Numerical Inversion of the Laplace Transform Solution to Radial Dispersion in a Porous Medium." *Water Resources Research* 17(1):250-252.

Mood, A.M., F.A. Graybill, and D.C. Boes (1974), *Introduction to the Theory of Statistics,* third edition. McGraw-Hill Book Co., New York. 564 pages.

Mualem, Y. (1976), "A New Model for Predicting the Hydraulic Conductivity of Unsaturated Porous Media." *Water Resources Research* 12(3):513-522.

Mulkey, L.A., and T. Allison (1988), "Transient versus Steady-State Land Disposal Model Comparisons." *Report prepared for EPA OSW Environmental Research Laboratory.*

Olkin, I., L.J. Gleser, and C. Derman (1978), *Probability Models and Applications.* Macmillan, New York, 576 pp.

Perrier, E.R., and A.C. Gibson (1980), "Hydrologic Simulation on Solid Waste Disposal Sites." *SW-868, U.S. E.P.A*, Cincinnati, OH.

Renyi, A. (1953), "On the Theory of Order Statistics." *Acta Mathematica Academiae Scientiarum Hungarical* 4(3-4):191-231.

Schanz, R., and A.M. Salhotra (1988), "A Water Treatment Plant Model for Pollutant Exposure Assessment." *Final Report submitted to Environmental Research Laboratory,* Office of Research and Development, Athens, GA.

Schroeder, P.R., J.M. Morgan, T.M. Waloki, and A.C. Gibson (1984), "The Hydrologic Evaluation and Landfill Performance (HELP) Model." *Interagency Agreement Number AD-96-F-2-A140,* U.S. Army Engineer Waterways Experiment Station, Vicksburg, MS 39180.

Shamir, V.Y., and D.R.F. Harleman (1967), "Dispersion in Layered Porous Media." *Journal of Hydraulics Division,* ASCC-HYS, pp. 237-260.

Shen, Thomas T. (1981), "Estimating Hazardous Air Emissions from Disposal Sites." *Pollution Engineering.*

Shen, T.T. (1979), "Emission Estimation of Toxic Pollutants from Hazardous Waste Disposal Sites." *Unpublished report, Division of Air Resources,* NYS Department of Environmental Conservation.

Shen, Thomas T., and T.J. Tofflemire (1980), "Air Pollution Aspects of Land Disposal of Toxic Wastes." *ASCE,* Vol. 106 EE1.

Salhotra, A. (1988), "Dispersivity Values for the Unsaturated Zone," Technical Memo submitted to *EPA/OSW* dated February 10, 1988.

Schroeder, P.R., J.M. Morgan, T.M. Walski, and A.C. Gibson (1984a), "Hydrologic Evaluation of Landfill Performance (HELP) Model: Volume I. User's Guide for Version 1." Municipal Environmental Research Laboratory, U.S. Environmental Protection Agency, Cincinnati, OH. *EPA/530-SW-84-009.*

Schroeder, P.R., A.C. Gibson, and M.D. Smolen (1984b), "Hydrologic Evaluation of Landfill Performance (HELP) Model: Volume II. Documentation for Version 1." Municipal Environmental Research Laboratory, U.S. Environmental Protection Agency, Cincinnati, OH. *EPA/1530-SW-84-009.*

Sharp-Hansen, S., C. Travers, P. Hummel, and T. Allison (1990), "A Subtitle D Landfill Application Manual for the Multimedia Exposure Assessment Model (MULTIMED)." Prepared for the Environmental Research Laboratory, U.S. Environmental Protection Agency, Athens, GA.

Spear, R.C. (1970a), "The Application of Kolmogorov-Renyi Statistics to Problems of Parameter Uncertainty in Systems Design." *International Journal of Control* 11(5):771-778.

Spear, R.C. (1970b), "Monte Carlo Method for Component Sizing." *Journal of Spacecraft and Rockets* 7(9):1127-1129.

Springer, C., P.D. Lunrey, K.T. Valsaraj, L.J. Thibodeaux, and S.C. James (1986), "Emissions of Hazardous Chemicals from Surface and Near Surface Impoundments to Air," Part B Landfills, *Project No. CR 808161-02, Office of Research and Development*, USEPA, Cincinnati, Ohio.

Stehfest, H. (1970), "Numerical Inversion of Laplace Transforms." *Commun. ACM* 13(1):47-49.

Sudicky, E.A., M.J. Ungs, and P.S. Huyakorn (1986), "Three Dimensional Analytical Solution for Transport from Gaussian Source in Uniform Ground Water Flow." Submitted to *Water Resources Research.*

Sudicky, E.A., T.D. Wadsworth, J.B. Kool, and P.S. Huyakorn (1988), "PATCH3D - - Three Dimensional Analytical Solution for Transport in a Finite Thickness Aquifer with First-Type Rectangular Patch Source." *Report prepared for Woodward-Clyde Consultants.* January 1988.

Swann, R.L., Eschenroeder, A., eds. (1983), "Fate of Chemicals in the Environment." *ACS Symposium Series 225,* American Chemical Society, Washington, D.C.

Todd, D.K. (1970) *The Water Encyclopedia: A Compendium of Useful Information on Water Resources.* Water Information Center, Port Washington, N.Y.

Thibodeaux, L.J., C. Springer, and G. Hildebrand (1986), "Transport of Chemical Vapours through Soil--a Landfill Cover Simulation Experiment," *presented at 1986 Summer National American Institute of Chemical Engineers*, August 24-27, 1986, Boston, Massachusetts.

Thibodeaux, L.J., et. al. (1982), "Models of Mechanisms for the Vapor Phase Emission of Hazardous Chemicals from Landfills." *Jour. of Hazardous Materials* 7(1982):63-74.

Ungs, M. J. (1986), "Mathematical Analysis and Validation of the Monte Carlo Uncertainty Analysis for the Surface Water Component of the Land Disposal Restriction Determinations." *Draft Report Prepared for U.S. EPA Office of Solid Waste* under EPA Contract No. 68-01-7266, Work Assignment No. 13.

Ungs, M.J. (1987), Unpublished manuscript submitted to Woodward-Clyde Consultants and U.S. EPA ERL Athens.

USDA, Soil Conservation Service. (1972) *National Engineering Handbook, Section 4, Hydrology*. U.S. Government Printing Office, Washington, D.C.

USEPA (1985), "Development of Land Disposal Banning Decisions Under Uncertainty." *USEPA Environmental Research Laboratory*, Athens, Georgia.

USEPA (1984), "Evaluation and Selection of Models for Estimating Air Emissions from Hazardous Waste Treatment, Storage and Disposal Facilities." *(EPA-450/3-84-020) Office of Air Quality Planning and Standards*, Research Triangle Park, North Carolina.

USEPA (1977), *User's Guide to the VALLEY Model*, Office of Air Quality Planning and Standards, Research Triangle Park, North Carolina.

Vandergrift, S.B., and R.B. Ambrose, Jr. (1988), "SARAH2, A Near Field Exposure Assessment Model for Surface Water." U.S. EPA, Athens, GA. *EPA/600/3-88/020.*

Van Genuchten, M. (1976), "A Closed Form Equation for Predicting the Hydraulic Conductivity of Unsaturated Soils." *Soil Sci. Soc. J.* 44(5):892-898.

Van Genuchten, M., and W.J. Alves (1982), "Analytical Solutions of the One-dimensional Convective-Dispersive Solute Transport Equation." *Technical Bulletin No. 1611*, United States Department of Agriculture.

Van Genuchten, M. Th., G.F. Pinder, and W.P. Saukin (1977), "Modeling of Leachate and Soil Interactions in an Aquifer, Management of Gas and Leachate in Landfills." *Rep. EPA -600/9-77-026*, pp. 95-102, USEPA, Cincinnati, Ohio.

Veneziano, D., R. Kulkarni, G. Luster, G. Rao, and A. Salhotra (1987, in press), "Improving the Efficiency of Monte Carlo Simulation for Ground-Water Transport Models." *Proceeding of DOE/AECL 87 Conference on Geostatistical, Sensitivity, and Uncertainty Methods for Ground-Water Flow and Radionuclide Transport Modeling, San Francisco, 1987.*

Wark, K., and C.F. Warner (1981), *Air Pollution -- Its Origin and Control*. Harper and Row. New York.

Whitman, R.G. (1923), "A Preliminary Experimental Confirmation of the Two Film Theory of Gas Absorption." *Chem. Metallurgy Eng.* 29:146-148.

Wolfe, N.L. (1985), "Screening of Hydrolytic Reactivity of OSW Chemicals." *USEPA Athens Environmental Research Laboratory*, Athens, Georgia.

Wolfe, N.L. (1987), Personal Communication.

Woodward-Clyde Consultants (1986), "Development of an Approach for Conducting Uncertainty Analyses in Multimedia Modeling." *Draft Report Prepared for USEPA Technology Development and Applications Branch, Athens*. Project No. 68-03-6304. Work Assignment B-2.

Woodward-Clyde Consultants. (1988) SYNOP, Rainfall Analysis Algorithm. Report under preparation.

APPENDIX A

Simplified Estimation for the Mixing Zone Depth

The mixing zone depth of a solute plume under a waste facility can be estimated by adding the contributions due to advection and dispersion, i.e.:

$$H = h_{adv} + h_{disp} \qquad\qquad\qquad\qquad (A.1)$$

where

       H = the total depth of penetration [m]
       h_{adv} = the vertically adveced component of the penetration depth [m]
       h_{disp} = the vertically dispersed component of the penetration depth [m]

The advected depth, h_{adv}, is the depth to which a particle would be transported under the influence of vertical advection and is given by:

$$h_{adv} = \int_{t=0}^{\tau} V_z dt \qquad\qquad\qquad\qquad (A.2)$$

where

       V_z = the vertical seepage velocity [m/yr]
       τ = time of travel [yr]

If the vertical seepage velocity is constant with depth, then:

$$h_{adv} = V_z t \qquad\qquad\qquad\qquad (A.3)$$

However, a better assumption is that the vertical seepage velocity varies linearly with depth, with a maximum value at the water table and zero at the bottom of the aquifer. This variation can be mathematically expressed as:

$$V_z = V_{zo}(1-z/B) \qquad\qquad\qquad\qquad (A.4)$$

where

       B = the saturated aquifer thickness [m]
       z = the depth from the top of the water table [m]
       V_{zo} = the maximum vertical seepage velocity [m/yr]

V_{zo} can be estimated from the net vertical recharge rate.

Equation 2 cannot be integrated since V_z is not an explicit function of time. Consider the following differential equation for the vertical seepage velocity:

$$\frac{dz}{dt} = V_z(z) \tag{A.5}$$

Rearrange terms in Equation 5 and integrate to depth h_{adv}:

$$\int_{z=0}^{h_{adv}} \frac{dz}{V_z(z)} = \int_{t=0}^{\tau} dt \qquad (A.6)$$

Substitute Equation 4 into Equation 6 and integrate to get:

$$\frac{-B}{V_{zo}} \ln(1-h_{adv}/B) = \tau \qquad (A.7)$$

Solve for h_{adv} from Equation 7:

$$h_{adv} = B(1 - e^{\frac{-V_{zo}\tau}{B}}) \qquad (A.8)$$

The time of travel, τ, can be estimated as the time it takes for a particle to be advected horizontally under the facility of length, L, i.e.,

$$\tau = \frac{L}{V_x} \qquad (A.9)$$

where V_x is the horizontal seepage velocity and is assumed to be a constant.

Prickett, Naymik, and Lonnquist (1981) estimate the magnitude of the effect of dispersion on particle transport as:

$$\Delta_{long} = \sqrt{2\alpha_L V \tau} \qquad (A.10)$$

$$\Delta_{vert} = \sqrt{2\alpha_V V \tau} \qquad (A.11)$$

where

α_L, α_V = the longitudinal and vertical dispersivities [m]
V   = the magnitude of the seepage velocity [m/yr]
Δ_{long}, Δ_{vert} = the longitudinal and vertical dispersed distances that
                  correspond to one standard deviation of random transport
                  [m]

If the effect of the horizontal seepage velocity is assumed to be much larger than that of the vertical, then the dispersed depth is estimated from Equation 11 as:

$$h_{disp} = \sqrt{2\alpha_V v_x t} \tag{A.12}$$

Hence, the total depth of penetration is the sum of the vertically advected and dispersed components. Substitute Equations A.8 and A.12 into Equation A.1 to obtain the total estimated depth of penetration.

$$H = B(1-e^{\frac{-V_{zo}t}{B}}) + \sqrt{2\alpha_V v_x t} \tag{A.13}$$

The solution to Equation A.13 needs to be checked when evaluating any particular case so that a value of H greater than the aquifer thickness, B, is not used. If the computed H is greater than B, set H equal to B.

Reference

Prickett, T., T. Naymik, and C. Lonnquist (1981), A Random-Walk Solute Transport Model for Selected Groundwater Quality Evaluations. *Bulletin 65,* Illinois State Water Survey, Department of Energy and Natural Resources, Champaign, Illinois. 103 pages.

PRECIPITATION

EVAPOTRANSPIRATION

INFLITRATION

RUNOFF

Vegetation

UPPER SUBPROFILE

VEGETATIVE LAYER.

LATERAL DRAINAGE LAYER

BARRIER SOIL LAYER

CAP OR COVER

LOWER SUBPROFILE

REFUSE LAYER

LATERAL DRAINAGE LAYER

LATERAL DRAINAGE
(FROM BASE OF LANDFILL)

drain

BARRIER SOIL LAYER

LINER

PERCOLATION
(FROM BASE OF LANDFILL)
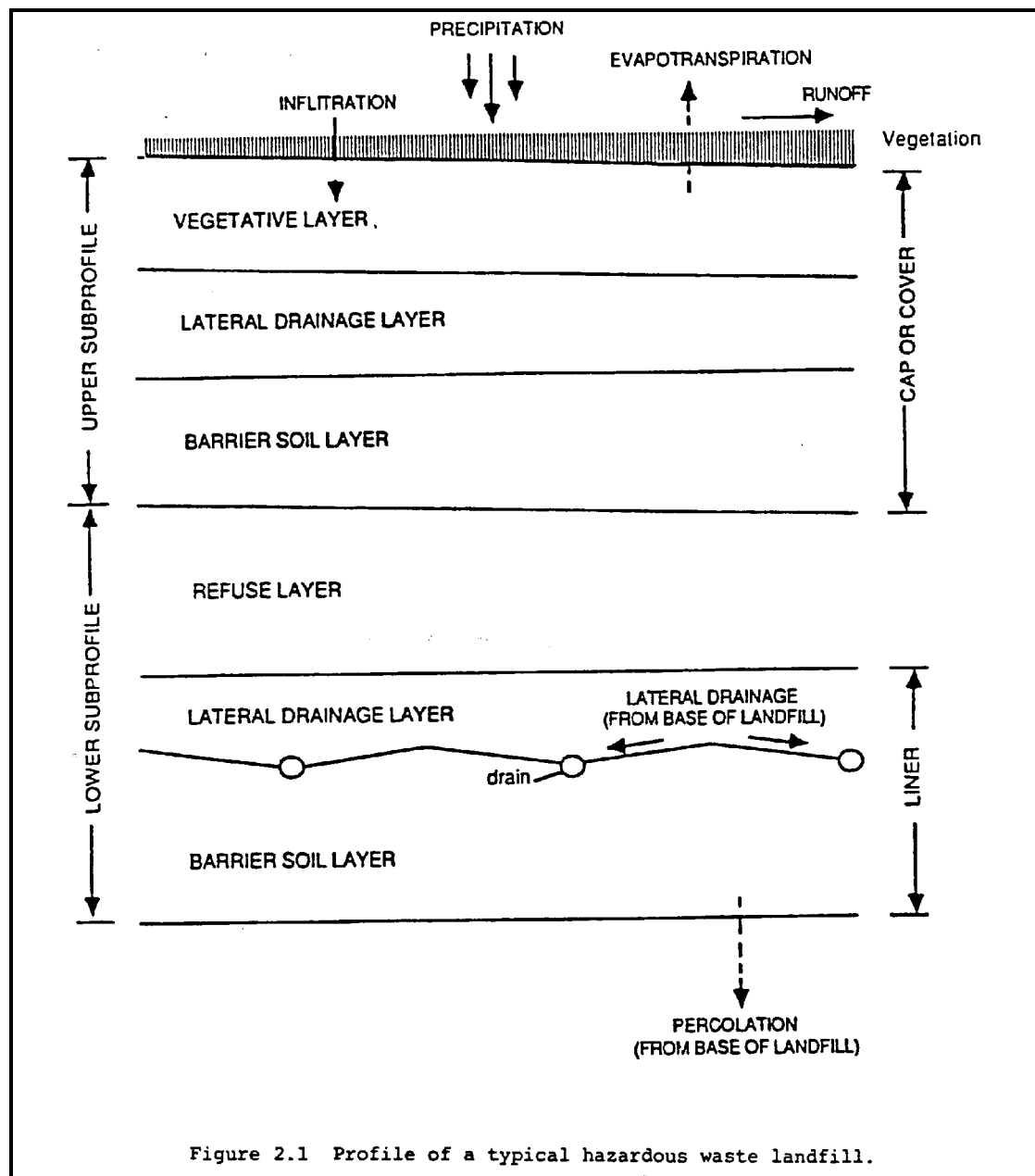
Figure 2.1 Profile of a typical hazardous waste landfill.
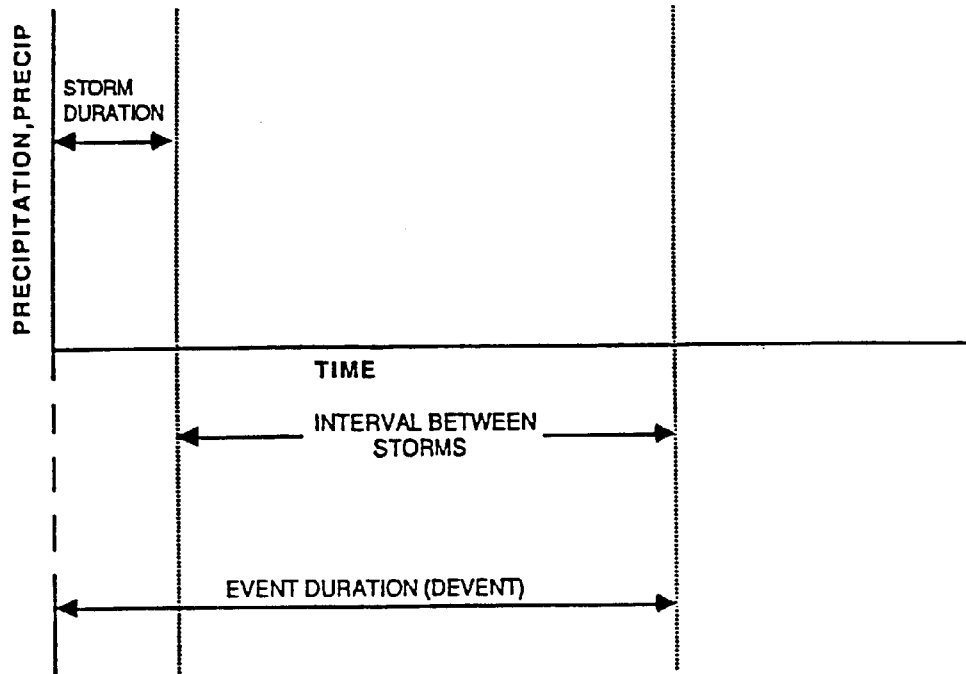
INFIL = PRECIP - RO - ET

$$I = \frac{INFIL}{DEVENT}$$

where

INFIL   = Water available for infiltration during the event (cm)
PRECIP = Storm precipitation (cm)
RO   = Runoff during the event (cm)
DEVENT = Event duration (d)
I   = Infiltration rate (cm/d)
ET   = Evapotranspiration during the event (cm)

Figure 2.2   Depiction of a typical event duration.

SOIL MOISTURE CONTENT

Wilting Point · Saturation · Vegetation

Available Soil Moisture
Moisture Distribution

Uppermost Landfill Layer

Second Landfill Layer

PLAN VIEW

Monitoring Well

Waste Facility

W

L

x

y

Contaminant Plume

SECTION VIEW

Monitoring Well
Ground Surface

Waste Facility

Unsaturated Zone

Water Table

H

Aquifer

B

V

V
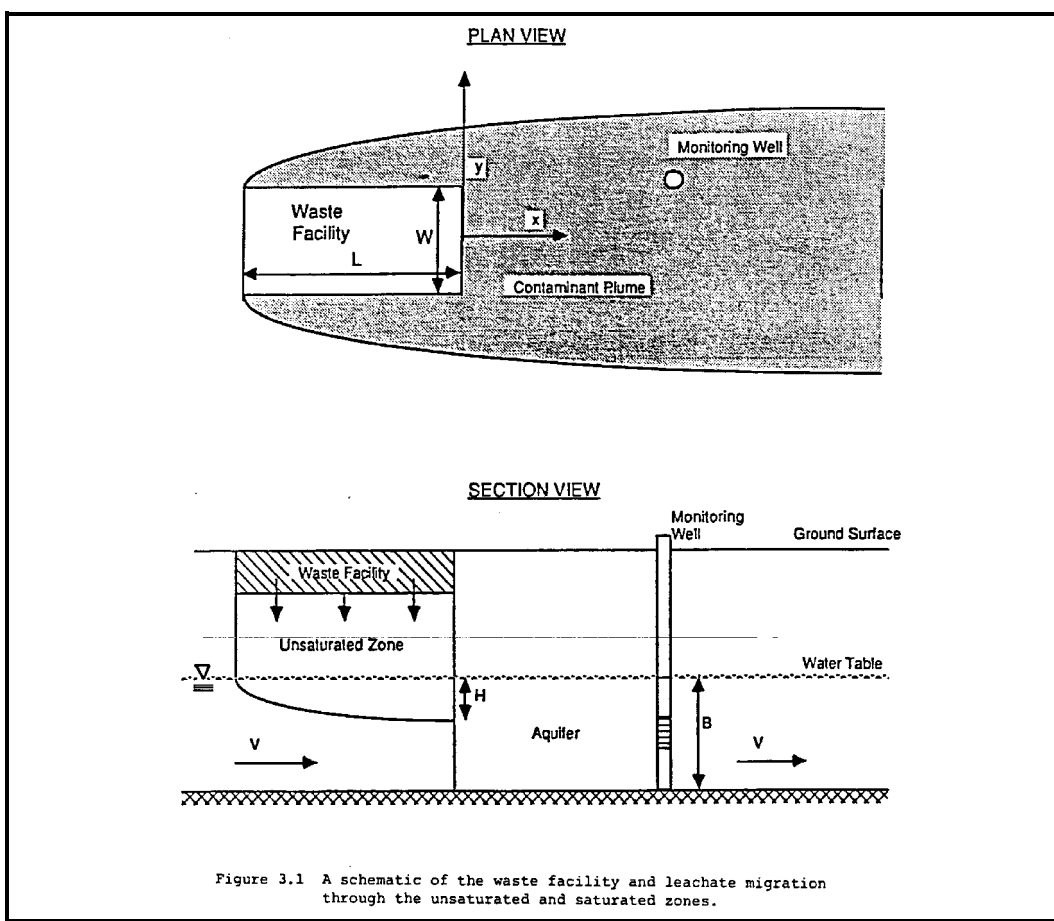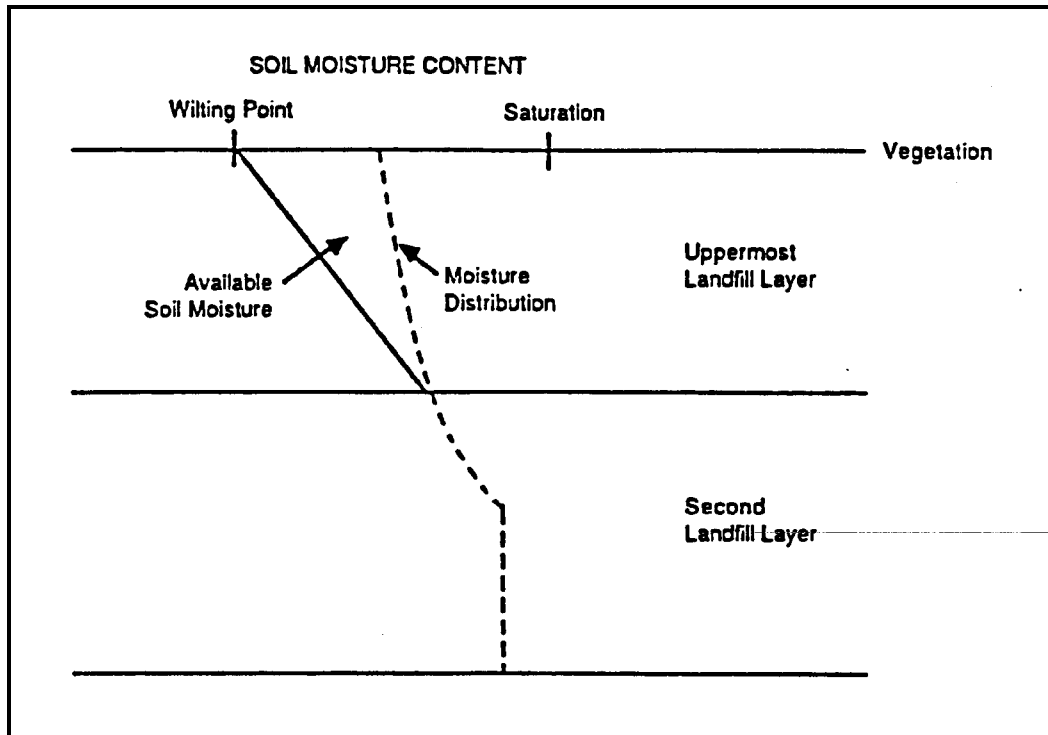
Figure 3.1   A schematic of the waste facility and leachate migration
through the unsaturated and saturated zones.

Flow

C/C$_0$

1   z=0

t

z_1

Layer 1 l_1

C/C$_0$

1   z= l_1

t

z_2

Layer 2 l_2

C/C$_0$

1   z= l_1+ l_2

t

z_3

Layer 3 l_3

C/C$_0$

1

z= l_1 + l_2 + l_3

t

Figure 4.1 A schematic of transport through the layered unsaturated
zone.
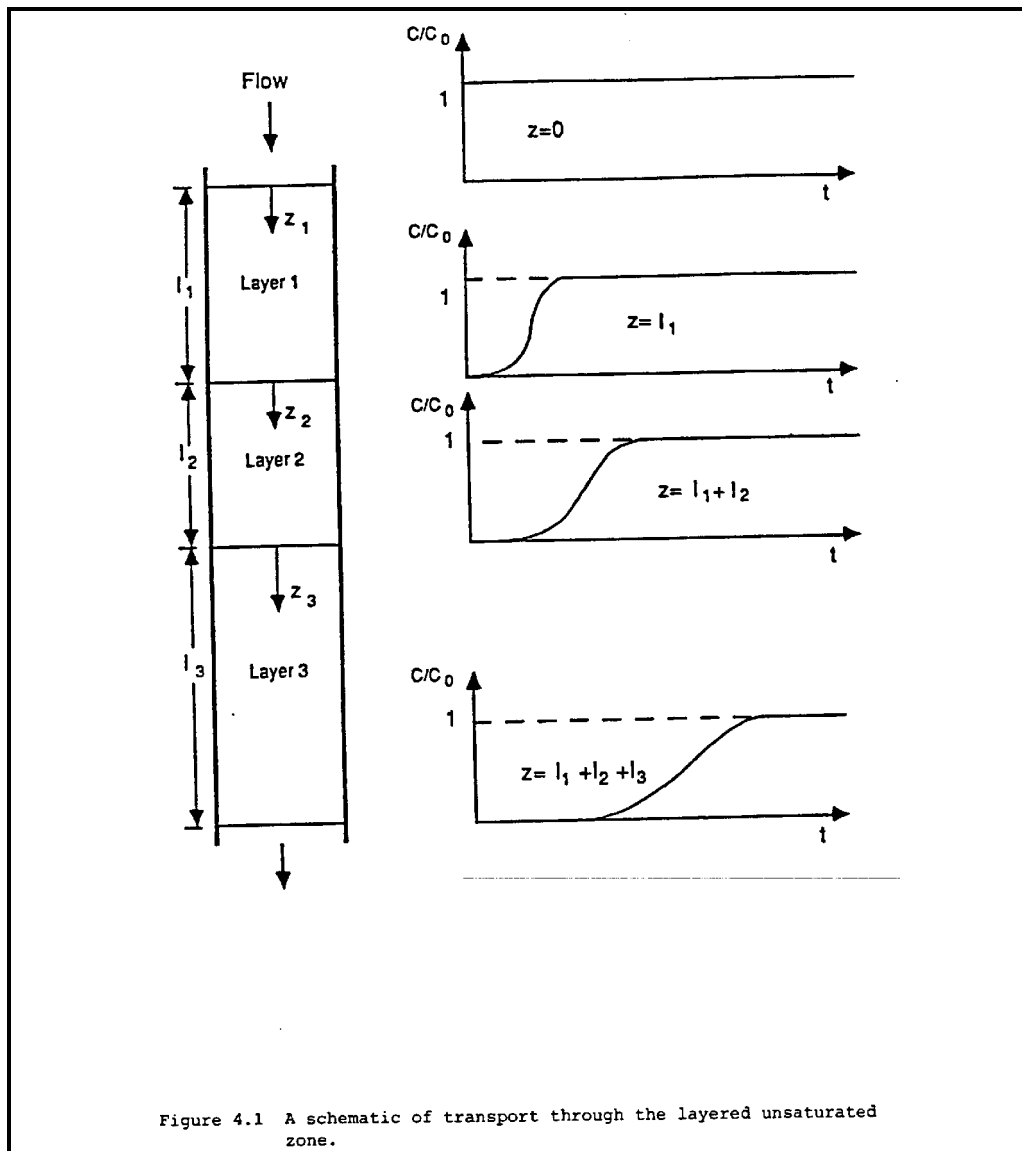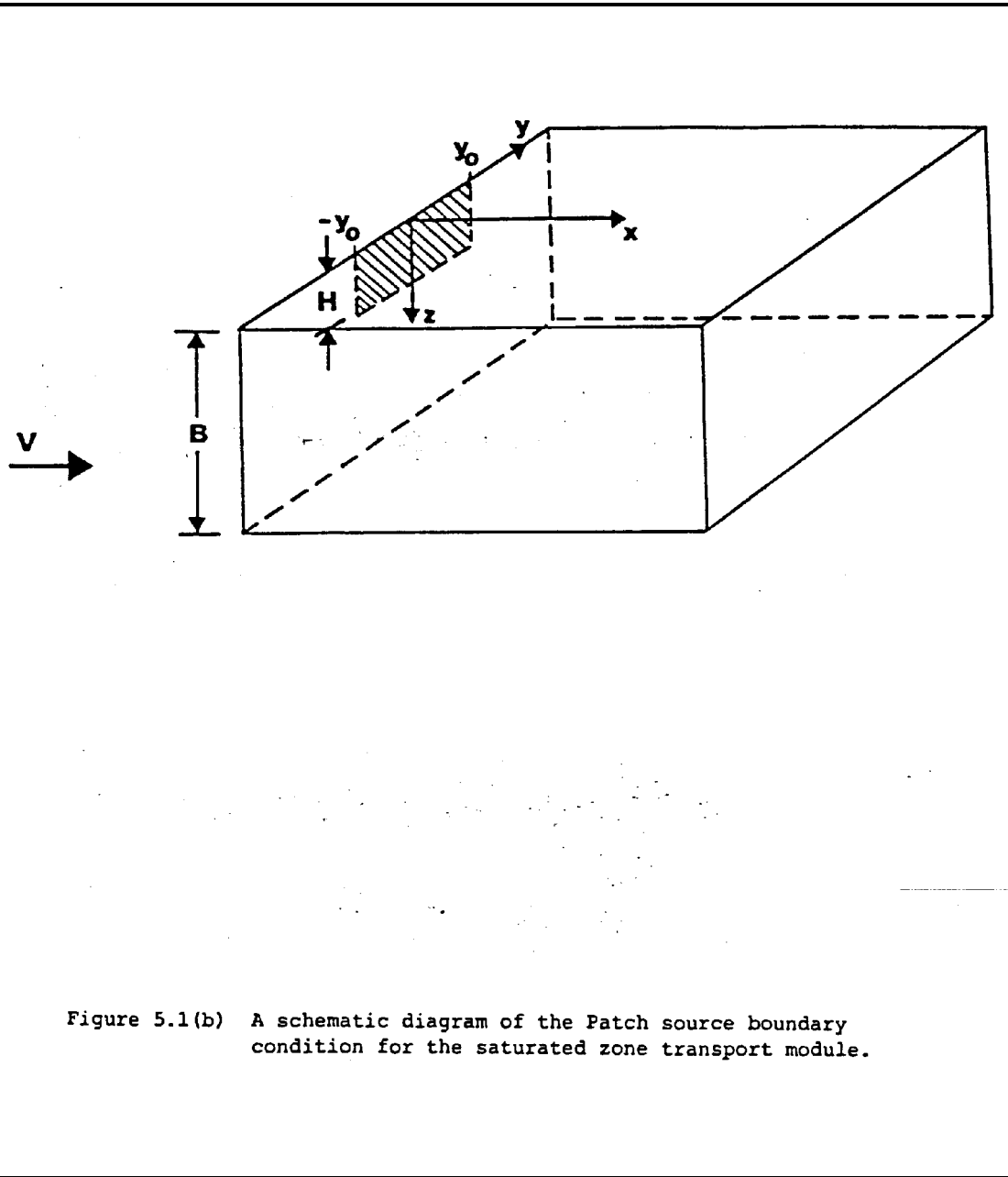
Figure 5.1(b)   A schematic diagram of the Patch source boundary
condition for the saturated zone transport module.
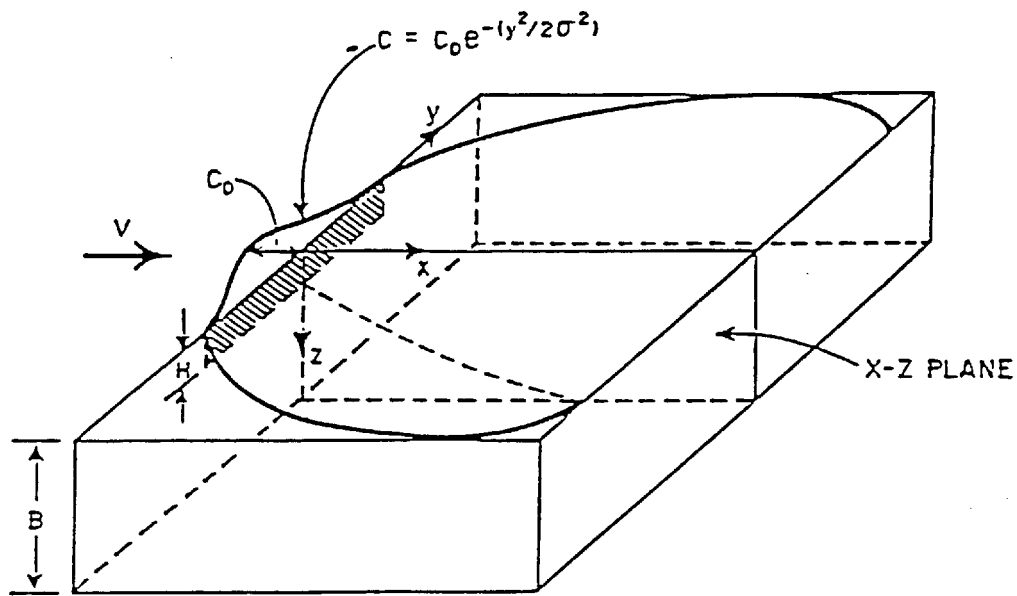
Figure 5.1(a)   A schematic diagram of the Gaussian source boundary
condition for the saturated zone transport module.
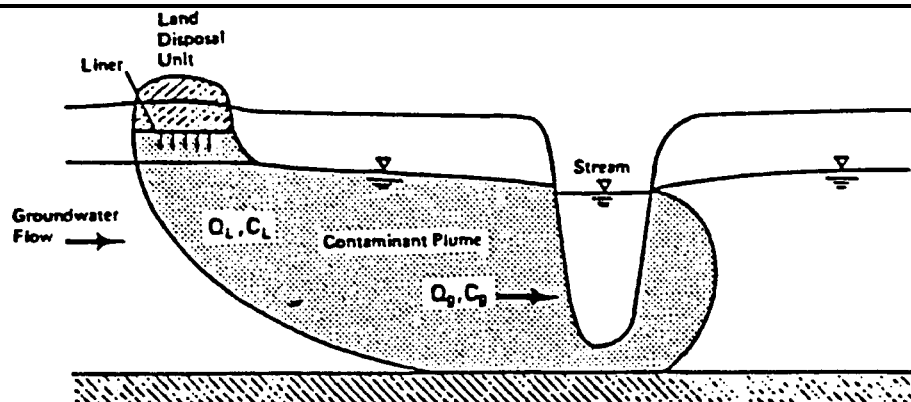
Figure 6.1(a)   Groundwater contaminant plume
                 interception by the surface stream.
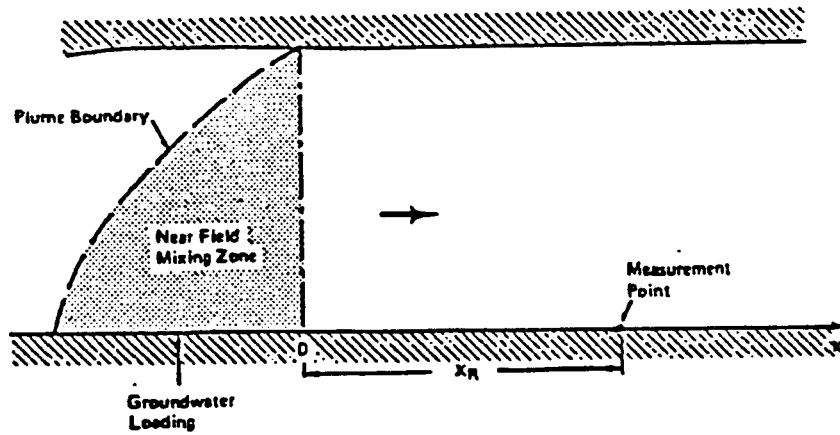
Figure 6.1(b)   Downstream contaminant transport from
                 the edge of the initial mixing zone.
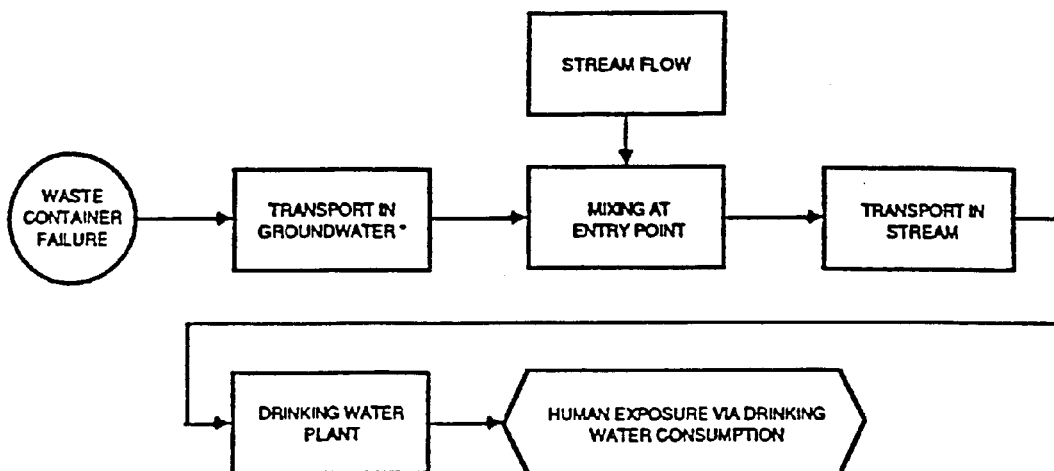
Figure 6.2(a)   Stages between failure of the waste containmant facility
and human exposure due to drinking water.
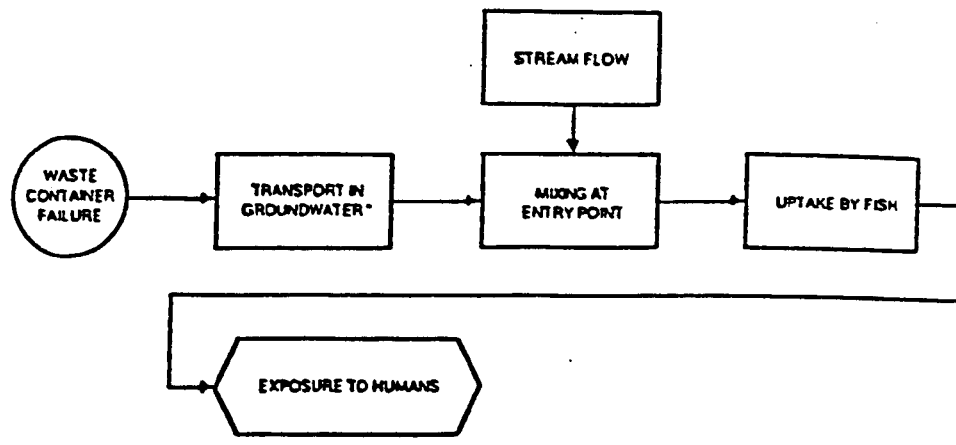
Figure 6.2(b)   Stages between failure of the waste containment
                 facility and human exposure due to fish consumption.
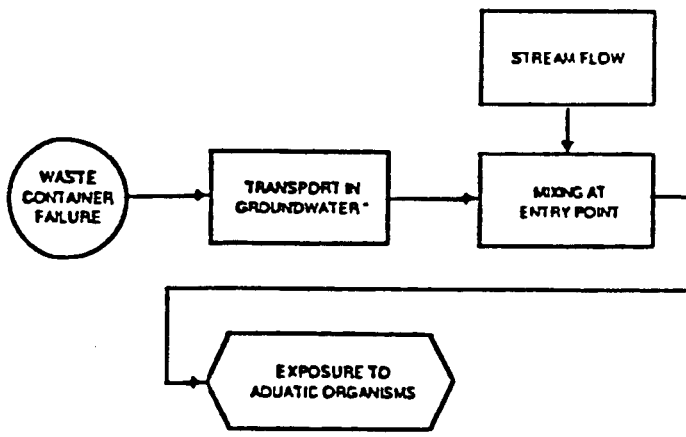
Figure 6.2(c)   Stages between failure of the waste containment
                 facility and exposure to Aquatic Organisms.
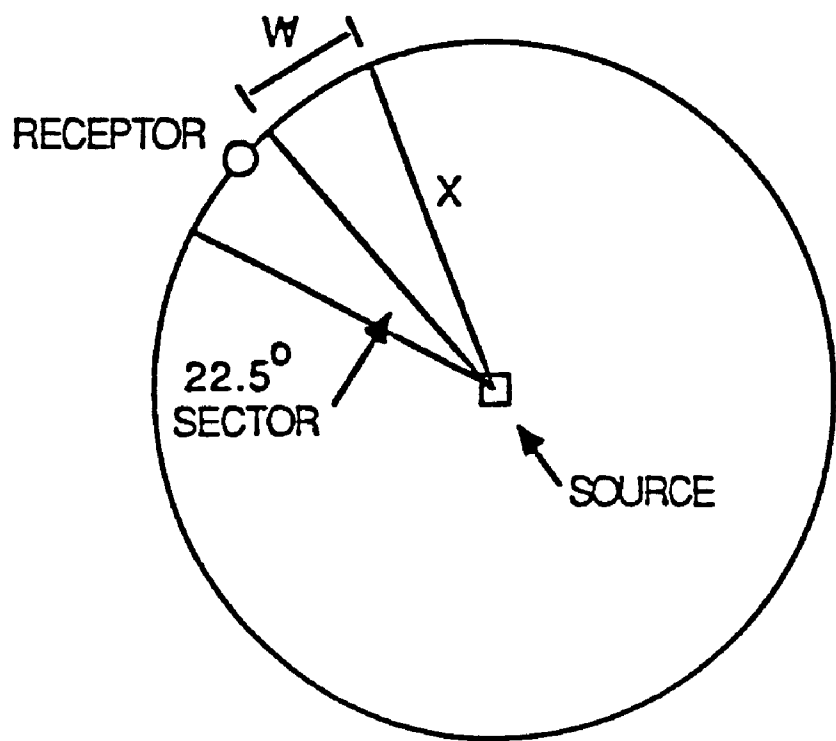
Figure 8.1   Wind direction sectors for Gaussian models.
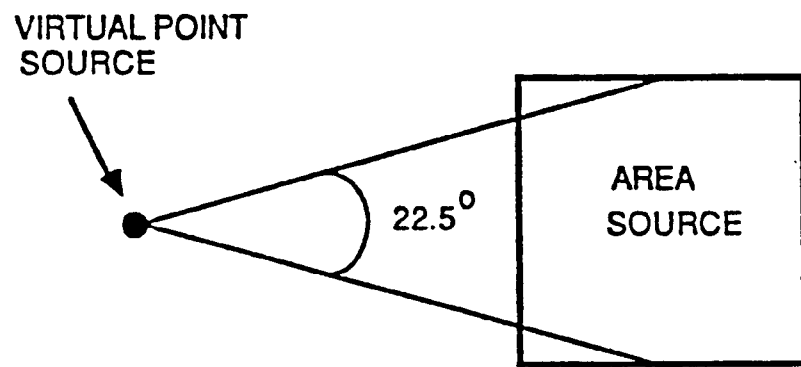
Figure 8.2 Virtual source approximation for long-term Gaussian models.

EFFECTIVE
SOURCE
AREA

22.5^o

SECTOR
CENTERLINE

RECEPTOR
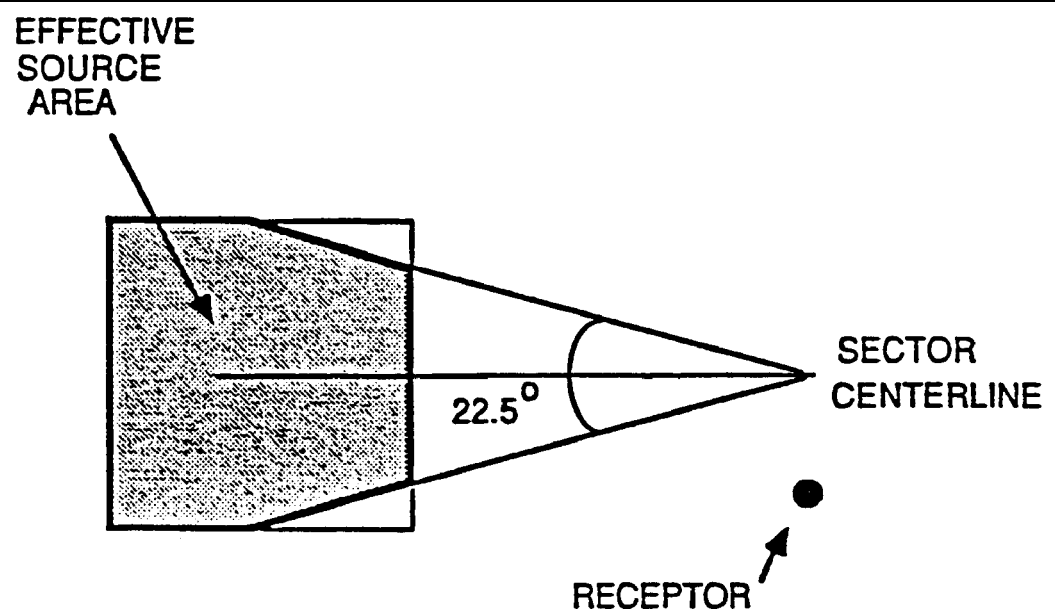
Figure 8.3 Effective source area used by VALLEY.
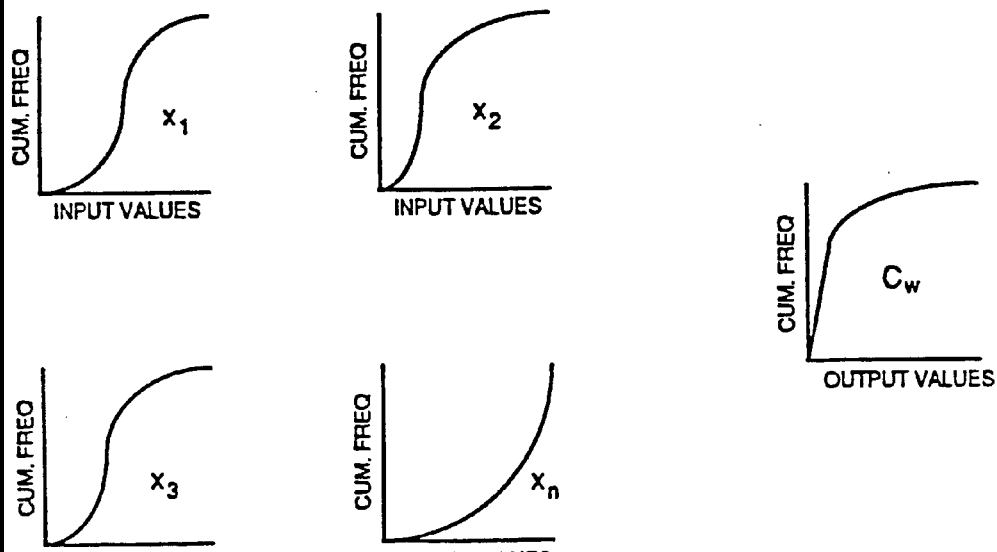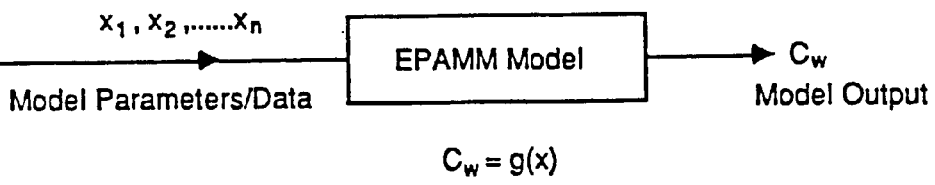
Figure 9.1   A schematic description of the Monte Carlo method of
uncertainty analysis.
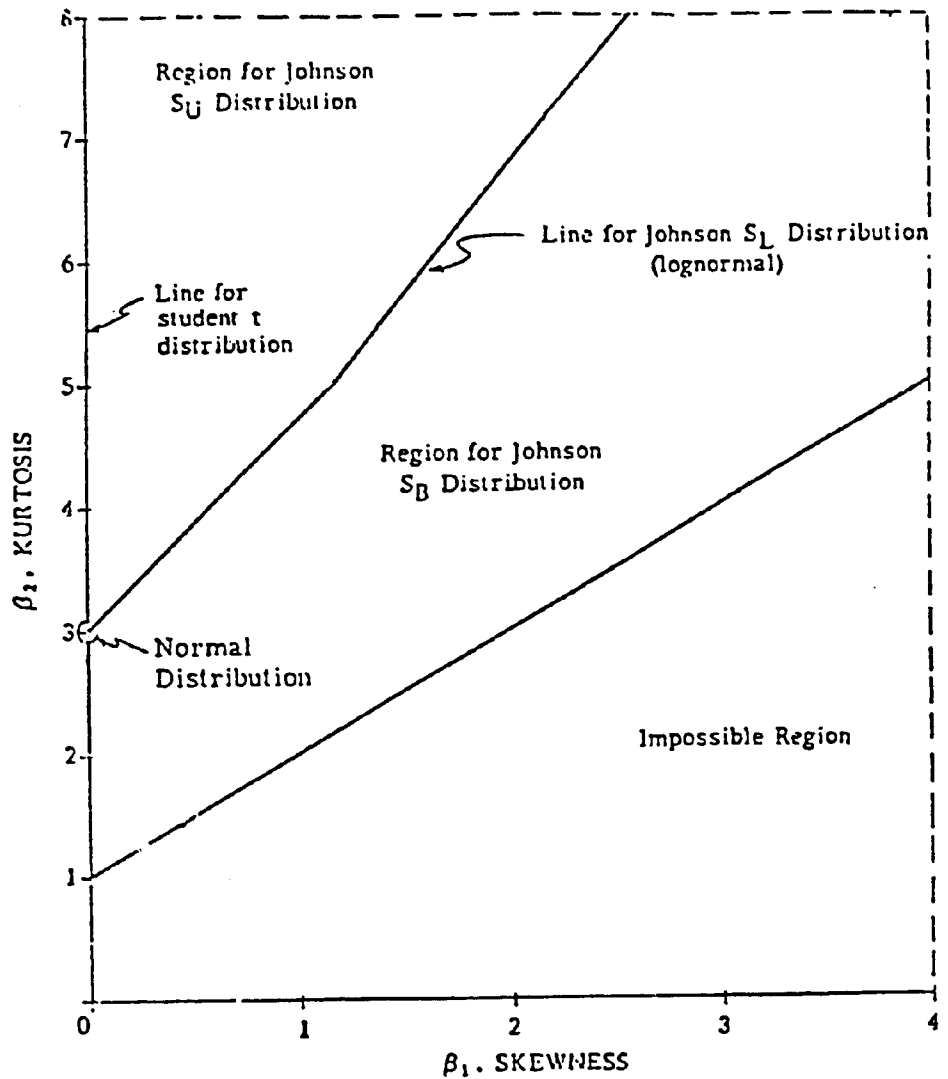
Figure 9.2   Selecting a Johnson distribution from skewness and kurtosis.
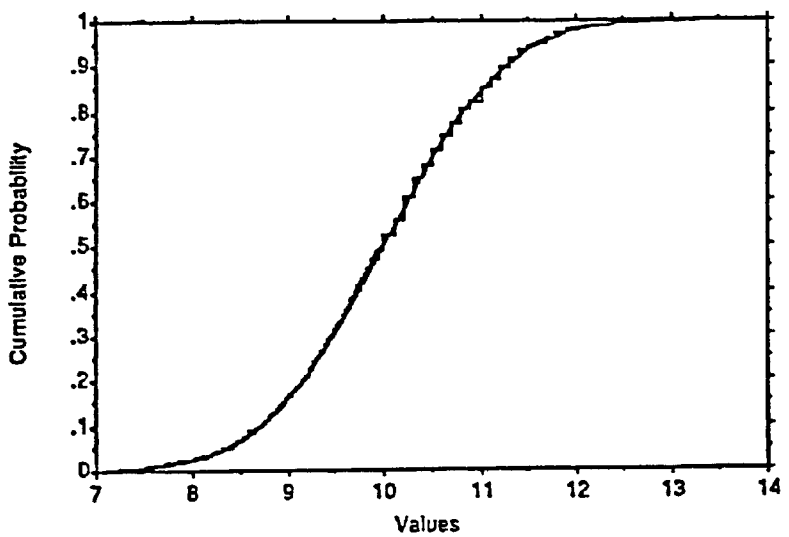
Figure 9.3 Comparison of the exact and the generated cumulative frequency
distribution for a normally distributed variable.
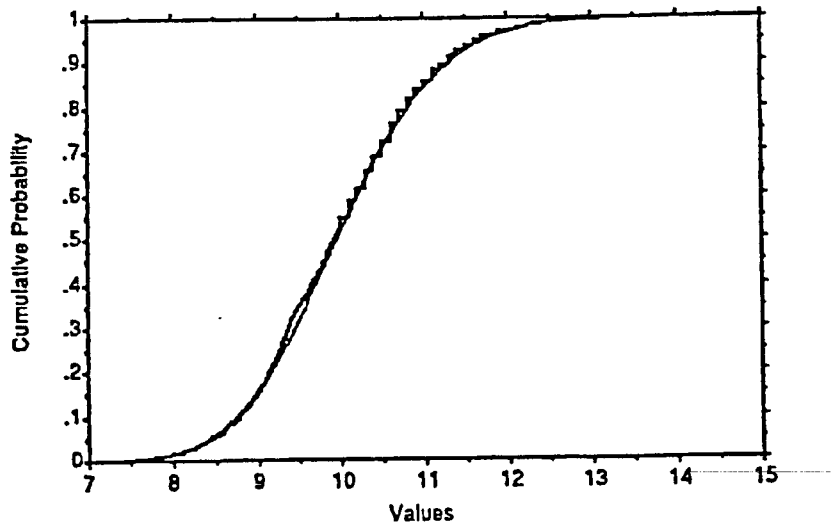
Figure 9.4 Comparison of the exact and the generated cumulative frequency
distribution for a log-normally distributed variable.
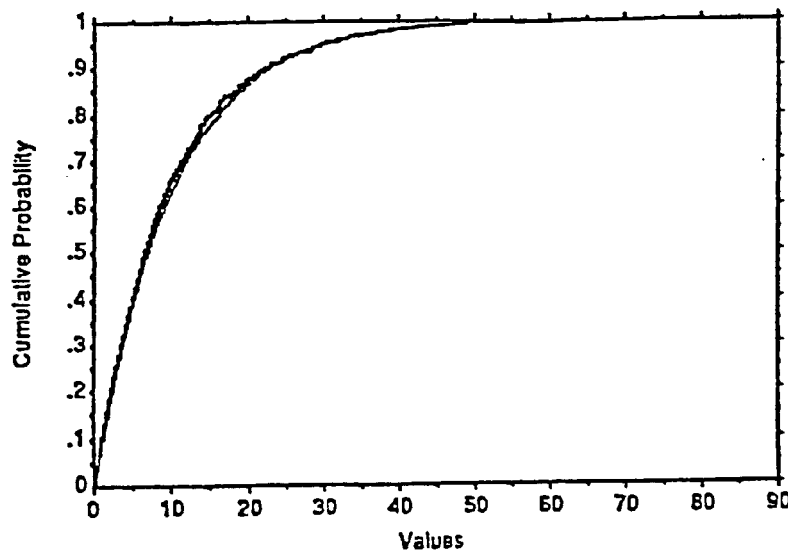
Figure 9.5   Comparison of the exact and the generated cumulative frequency
distribution for an exponentially distributed variable.
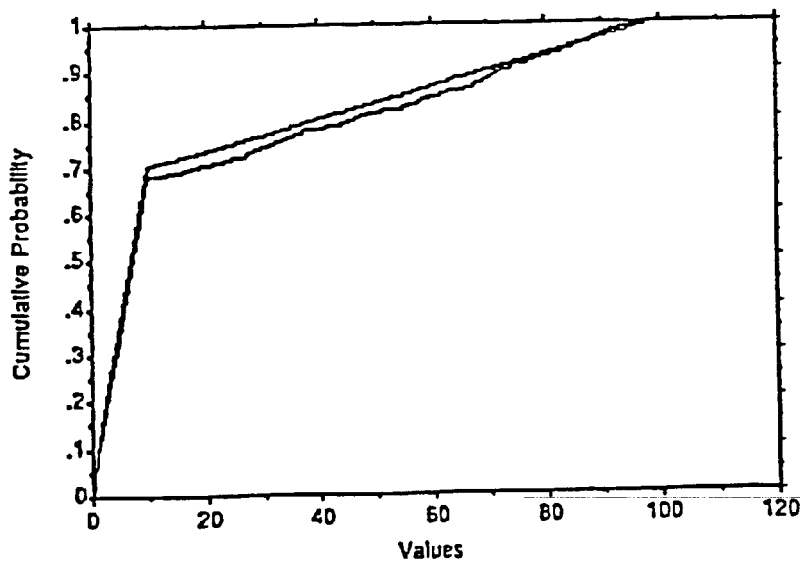
Figure 9.6   Comparison of the exact and the generated cumulative frequency
distribution for an empirically distributed variable.
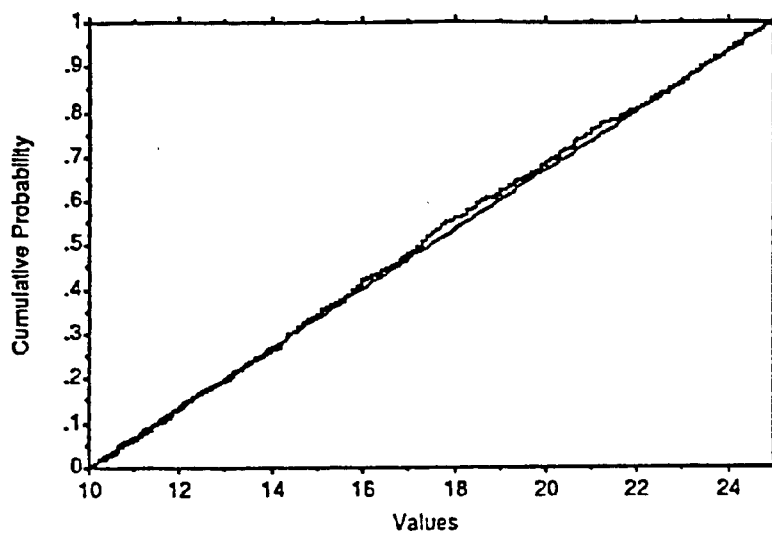
Figure 9.7 Comparison of the exact and the generated cumulative frequency
distribution for a uniformly distributed variable.
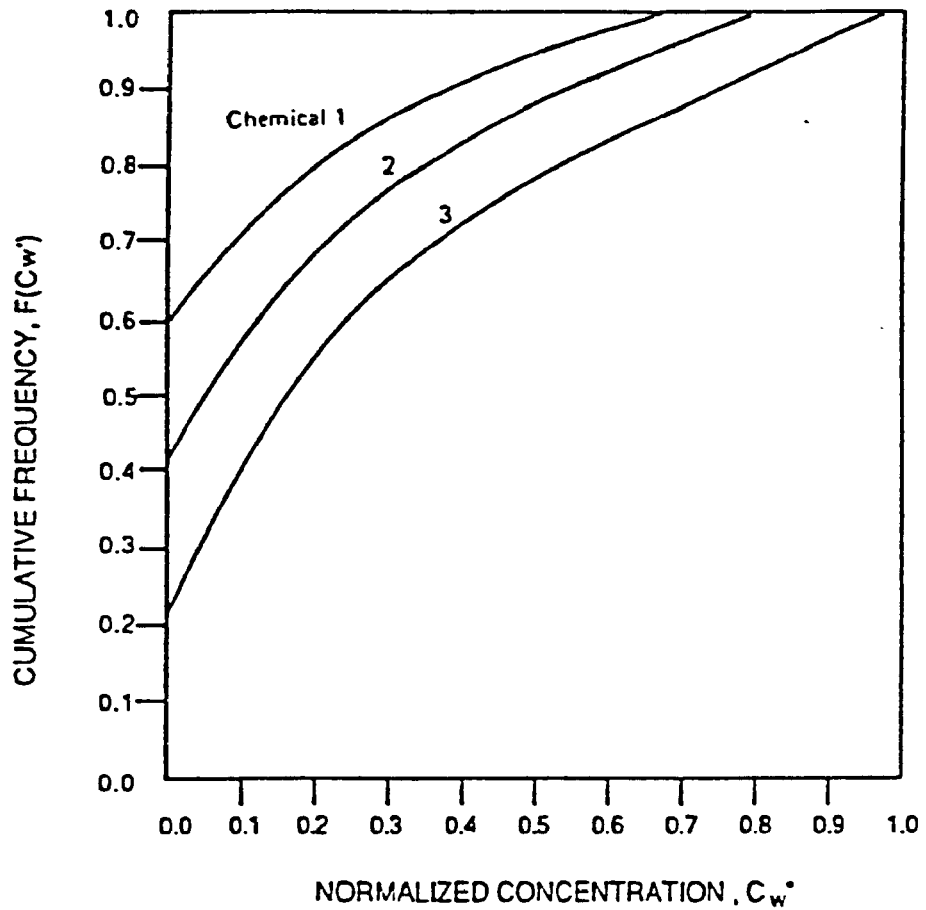
Figure 9.8   Typical results obtained using MULTIMED in the
             Monte Carlo mode.

TABLE 9-2(b). RESULTS OF RANDOM NUMBER GENERATOR TEST FOR 1000 VALUES

	Input Statistics		Observed Output Statistics			
	mean	std. dev.	mean	std. dev.	max	min
Normal	10.00	1.00	10.10	0.95	12.90	7.40
LogNormal	10.00	1.00	10.03	1.00	13.40	7.50
Exponential	10.00	10.00	10.00	9.66	81.20	0.00
Empirical*	18.855	-	19.73	27.33	99.90	0.10
Uniform	10**	25***	17.38	-	25.00	10.10

```
  *Cumulative Probability   0.0      0.1       0.7          1.0
       Values               0.1      1.0      10.0        100.0
    Expected Mean                         18.855

 **Minimum Value

***Maximum Value
```

TABLE 9-2(a).   RESULTS OF RANDOM NUMBER GENERATOR TEST FOR 500 VALUES

	Input Statistics		Observed Output Statistics			
	mean	std. dev.	mean	std. dev.	max	min
Normal	10.00	1.00	10.00	1.05	13.40	6.90
LogNormal	10.00	1.00	9.97	0.98	13.20	7.60
Exponential	10.00	10.00	9.80	9.67	53.70	0.00
Empirical*	18.855	-	18.54	25.54	99.20	0.10
Uniform	10**	25***	17.4	-	24.9	10.1

```
 *Cumulative Probability   0.0      0.1       0.7        1.0
      Values               0.1      1.0      10.0      100.0
   Expected Mean                         18.855
```

 **Minimum Value

***Maximum Value